Project approved for funding
as part of the ERA-NET
GeoERA

Authors and affiliation:
Nina Rman, GeoZS
Éva Kun, MBFSZ
Natalija Samardžić, FZZG
Dejan Šram, GeoZS
Jure Atanackov, GeoZS
Miloš Markič, GeoZS
Andrej Lapanje, GeoZS
Dušan Rajver, GeoZS
Ildikó Sarolta Selmeczi, MBFSZ
Gyula Maros, MBFSZ
Tamara Marković, CGS-HGI
Tamás Budai, MBFSZ
Edit Babinszki, MBFSZ

Deliverable 4.2

A joint report on geomanifestations in the Pannonian basin

E-mail of contact person:
nina.rman@geo-zs.si

Version: 21.05.2021

This report is part of a project that has received funding by the European Union's Horizon 2020 research and innovation programme under grant agreement number 731166.

Deliverable Data		
Deliverable number	D4.2	
Dissemination level	Public	
Deliverable name	A joint report on geomanifestations in the Pannonian basin	
Work package	WP4, T4.2 Geomanifestations	
Lead WP/Deliverable beneficiary	MBFSZ/GeoZS and MBFSZ	
Deliverable status		
Submitted (Author(s))	21/05/2021	Rman Nina et al.
Verified (WP leader)	24/05/2021	Gyula Maros
Approved (Coordinator)	25/05/2021	Renata Barros

TABLE OF CONTENTS

1 INTRODUCTION

This report is a part of T4.2 where we analysed occurrence and properties of selected geomanifestations. We tested whether they confirm the evolved structural-geological model in task 4.1. Datasets are based on approach as listed in Milestone M7a Inventory of available geomanifestations for the Pannonian basin case study. Point data, photos and fact sheets are stored separately, in EGDI, while description of geomanifestations is given in this report.

The Pannonian Basin is a young, Neogene basin system on the top of a complex Paleo-Mesozoic crystalline and sedimentary sequences. It is built up of numerous subbasins of slightly different age, and core complexes and emerged island mountains. The following chapters focus on geomanifestations, geological and hydrodynamic models of the pilot areas, similar geotectonically.

What is a geomanifestation? This term was initiated by Barros & Pissens (2020). They introduced the concept of geomanifestations “to define any distinct local expression of ongoing or past geological processes. These manifestations, or anomalies, often point to specific geologic conditions and, therefore, can be important sources of information to improve geological understanding of an area.”

The investigation of geomanifestations in the Mura-Zala basin (Slovenia, Croatia, Hungary), Battonya High (Hungary, Romania) and the Northern Bosnia & Herzegovina territory (Figure 1) were prevailed by a stratigraphic harmonization and model-building process, which laid the foundation of the pilot area workflows. In the followings we added a geotectonic summary about the evolution of the Pannonian Basin, which is based on Budai & Maros (2018), and a short stratigraphic harmonization of the infilling sedimentary sequences of the basin.

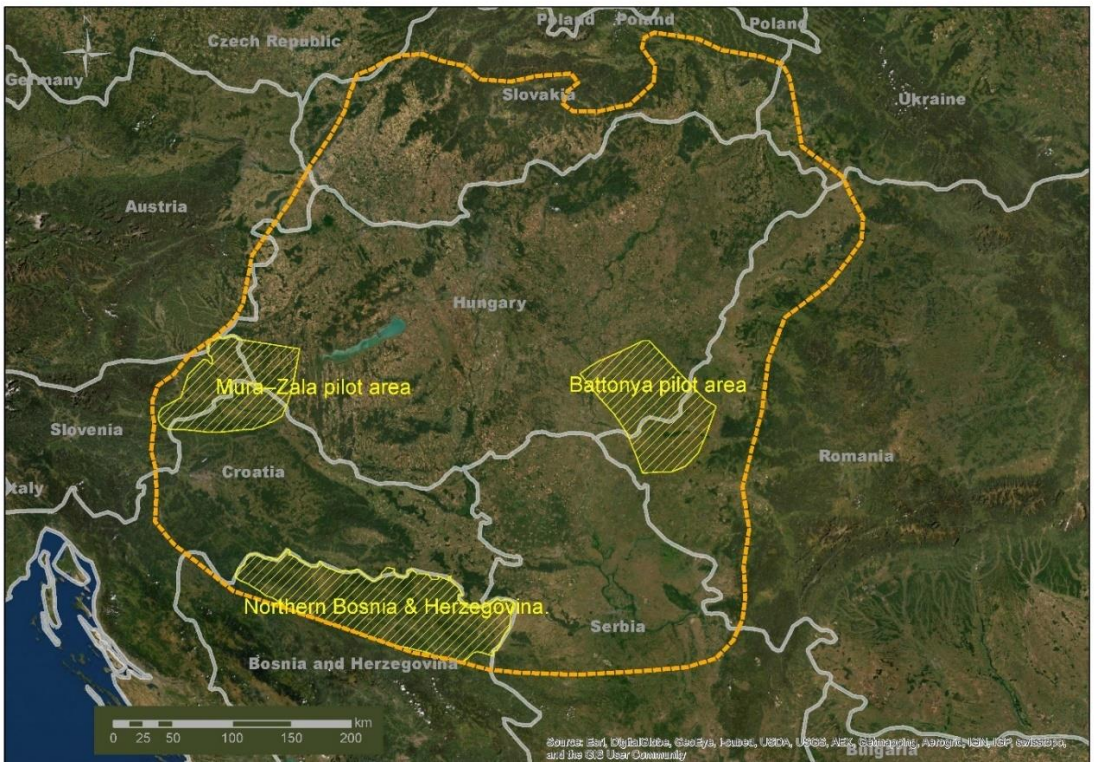

Figure 1: Pilot territories of the project AOI relevant for distribution of geomanifestations

2 STRUCTURAL FRAMEWORK OF THE PANNONIAN BASIN

The Pannonian Basin is a young, Neogene aged basin system on the top of a complex Paleo-Mesozoic crystalline and sedimentary sequences. The whole basin is built up from numerous subbasins of slightly different age, and besides core complexes and emerged island mountains can be found within it. However, the whole Pannonia Basin is a repository of geomanifestations the following chapters will focus on geomanifestations, geological and hydrodynamic models of the pilot areas in the basin, which are similar in geotectonic build-up, but could be remarkably different from the types of geomanifestations in the depth and on the surface. What does it mean geomanifestation? This term was initiated by Barros & Pissens (2020) in an internal methodology report of the GeoConnect³d project. They introduced the concept of geomanifestations "to define any distinct local expression of ongoing or past geological processes. These manifestations, or anomalies, often point to specific geologic conditions and, therefore, can be important sources of information to improve geological understanding of an area."

The investigation of geomanifestations in the Mura-Zala, Battonya and the Northern Bosnia & Herzegovina territory of the project area (Figure 1.) were prevailed by a stratigraphic harmonization and model-building process, which laid the foundation of the pilot area workflows. In the followings we add a geotectonic summary about the evolution of the Pannonian Basin, which is based on Budai & Maros (2018) and a short stratigraphic harmonization of the infilling sedimentary sequences of the basin.

2.1 The Pannonian Basin in the frame of the Alpine orogeny

The Alpine orogenic system (Figure 2) was formed by the collision of the stable European Platform and the Adriatic microplate of the African Plate (Argand, 1924, Channell & Horváth, 1976). The collision resulted complex suture zones of different ages, nappe systems of different vergency, numerous crustal blocks and several oceanic crust fragments during the formation of the Alpine-Carpathian-Dinaridic system. Microplates were broken off the continental plates, and their movements were characterized by different rotations and extrusions. The polarity of the nappe systems along the suture zones was turned from North to South in the Alpes, from Northwest to Southwest in the Western Carpathians and in the Dinarides, to the East and to the South in the Eastern and Southern Carpathians. The obducted continental crust slabs appear either in the lower crust or the upper crust position (Handy et al. 2014). Due to the upwelling of the asthenosphere, the initiation of lower crustal or upper mantle detachments (Handy et al. 2014) and (Horváth 2007), the subductioning slab roll-back motion caused pull force led to an extension in the crust and formed the Pannonian Basin as an intramountain basin.

The Pannonian basin infilling sediments and volcanic sequences situate on a complex geological setting (Figure 3). The Pannonian Basin itself, apart from the Vienna and Transylvanian Basins, is a geologically well-defined structure. Its sub-basins are the Kisalföld (Small Hungarian Plain or Danube Basin), the Steier Basin, the Drava Trench, the Eastern Slovakian Basin, and the Alföld (Great Hungarian Plain), together with the areas of Bácska, Bánát and Kárpátalja (Transcarpathia).

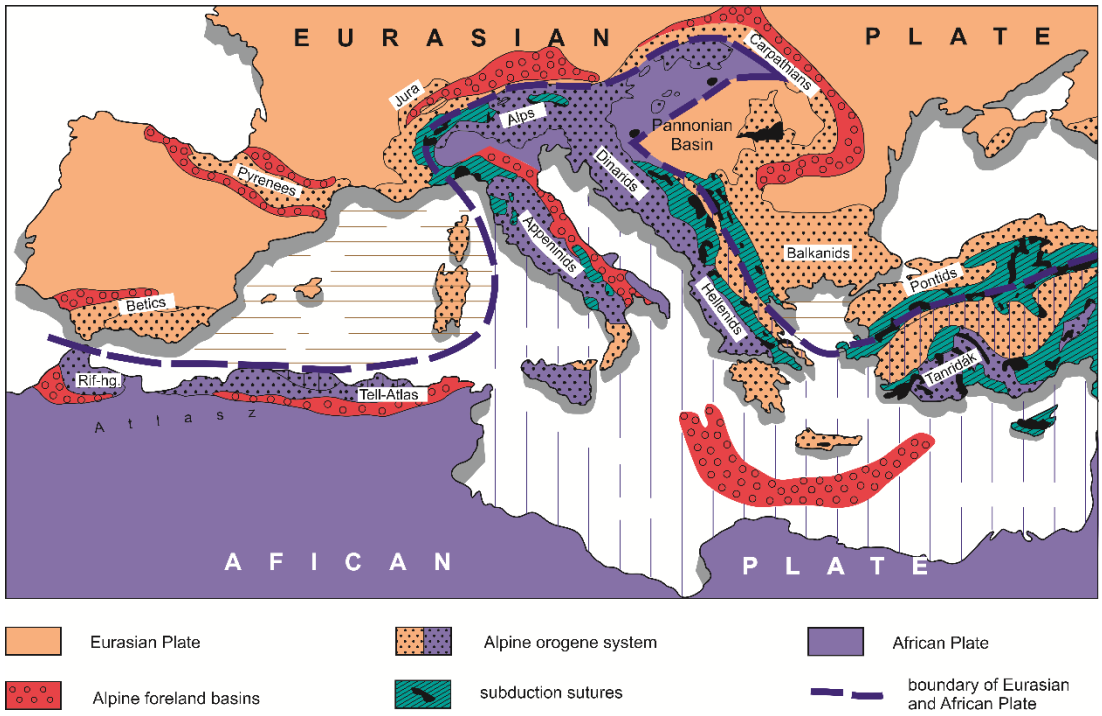

Figure 2: Geotectonic position of the Carpathian basin within the Alp-Carpathian-Dinaride system (after Haas et al. 2002)

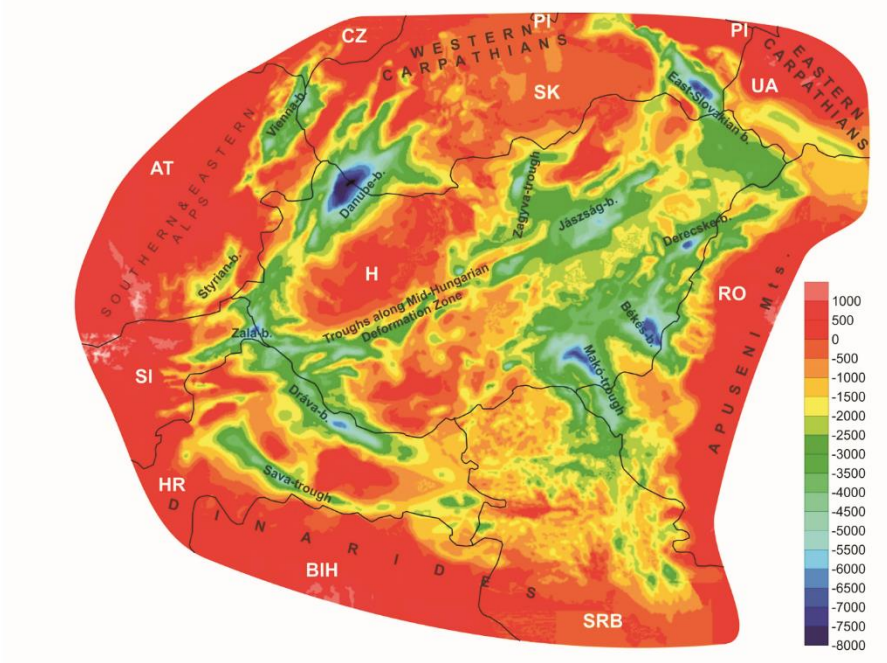

Figure 3: Main subbasins in the Pannonian Basin and their depth conditions (Budai & Maros 2020)

The geodynamic and plate tectonic evolution of the Pannonian Basin and the basement of it can be divided into two main phases. The first, longer period that built up the basin of the later formed Pannonian Basin evolved during the Alpine cycle. We call it here as Pre-Pannonian phase. It started in the middle Permian and ended in the Early Miocene. The second phase, let us call it Pannonian phase started somewhere in the early and middle Miocene, in slightly different times within the different sub-basins and lasted until recent times. About 5 million years ago a compressional inversion phase were initiated.

2.1.1 Pre-Pannonian phase

By the end of the Carboniferous, a vast ocean called the Paleotethys penetrated the Pangea supercontinent from the east. At its southern margin, a new ocean called the Neotethys opened up (Ricou, 1994), from the middle Permian. This resulted in the closure of the Paleotethys Ocean and the start of the so-called Cimmerian orogeny in the Late Jurassic. A sub-branch of this Neotethys Ocean was Meliata-Vardar oceanic branch was situated in the northern part of it, where sequences of the Alcapa and Vardar Mega-units were deposited during the Triassic.

From the west the rifting of the Central Atlantic Ocean was started in the Late Triassic as a crucial point of the Alpine orogeny. During this process oceanic sub-basins were opened up and developed as the Alpine Tethys (Stampfli & Borel 2002). The Tisza Mega-unit was isolated from the European Plate during this process in the Middle Jurassic (Csontos, Vörös 2004), and it was surrounded by the Meliata Ocean from the south and the Alpine Tethys from the north. The subsequent Codru, Villány-Bihor and Mecse units situated neighbouring along the edge of the Tisza Mega-unit. In the early middle Jurassic, the West Vardar oceanic branch isolated the latter Dinaric crust, and the new spreading centre caused obduction and initiation of accretional prism in the West Vardar and Dinaridic realm (Schmid et al. 2008).

The Alpine orogeny itself was started with the closure of the Alpine Tethys in the Early Cretaceous (Figure 4). This time originated the Austroalpine nappe systems in the Alcapa Mega-unit (Ratschbacher et al. 1991), and the Mecsek, Villány-Bihor and Békés-Codru nappes were thrusted in the Tisza Mega-unit more or less at the same time. With the closure of the Ceahlau-Severin oceanic branch the East Vardar units were trusted onto the Dacia Mega-unit and nappe origination were took place within it as well.

The deeply buried nappes were highly metamorphosed and suffered plastic deformations. While the upper crust units suffered only light flexural structures or more intensive fold tectonics (Kovács et al. 2000), during these processes. The basement Variscan crystalline rocks suffered retrograde Alpine metamorphism (Haas ed. 2001).

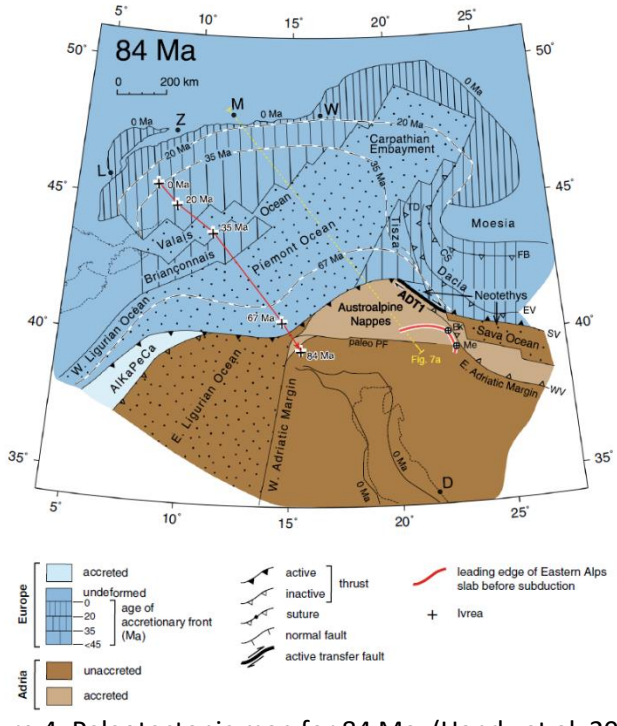

Figure 4: Paleotectonic map for 84 Ma. (Handy et al. 2014)

In the late Cretaceous the collision was continued in the Dinarides, in the Alcapa and Tisza Mega-units, the Dacia Mega-Unit thrusted on the European plate at Moesia. Collisional magmatic events originated like banatites in the Tisza Mega-unit and the suture zones like the Pieniny and Sava zone were initiated (Schmid et al. 2008). A short orogenic event occurred in the East and South Carpathians (Laramide phase) affecting the Transylvanian Basin too (Schmid et al. 2008).

The compressional phase was followed by quite rapid emergence and gravitational collapse starting in the Late Cretaceous. This was the so-called "Gosau event," which resulted in a deposition of terrestrial, terrigenous, reef, and later a continuously deepening marine sequence above the folded and erosionally truncated surface of pre-Gosau formations. The chain of Gosau basins was surrounded by normal and strike-slip faults. Due to the north-south compression, the emerging nappe systems were deformed by transpressional stress fields (Froizheim et al.2008).

During the Paleogene the nappe stacking continued in the Dinarides (Mioč, 2003), and the Hungarian Paleogene Basin was formed (Báldi, 1986) and stretched from Slovenia to the present Northern Hungary. From the plate tectonic point of view, this basin was a foreland, flexural-type basin (Tari et al. 1993), subsidence of which was provoked by the load of the nappe stacks buckling the continental crust.

The Alcapa Mega-unit, contemporaneously with the formation of the Paleogene Basin, was moving towards the ENE along the Periadriatic Lineament and the Balaton Line of the Mid-Hungarian Shear Zone (Kázmér & Kovács S. 1985). The Alcapa Mega-unit has a highly complex geologic setup and originated from the African Plate, while the nowadays south-situated Tisza Mega-unit has a European Plate origin. The two tectonic mega-units are attached to each other along the Mid-Hungarian Shear Zone which stretches SW to NE. The Mid-Transdanubian (Sava) unit, situated south of the Mid-Hungarian Line (or Lineament), has two definitions in the most recent literature: according to Haas et al. (2000), it is defined as a highly deformed geologic unit with Southern Alpine origin, but excluding the Szolnok-Máramaros flysch belt (Figure 5). Schmid et al. (2008) and Ustaszewsky et al. (2008) have a different opinion, as they include the Szolnok-Máramaros flysch belt in the Sava unit.

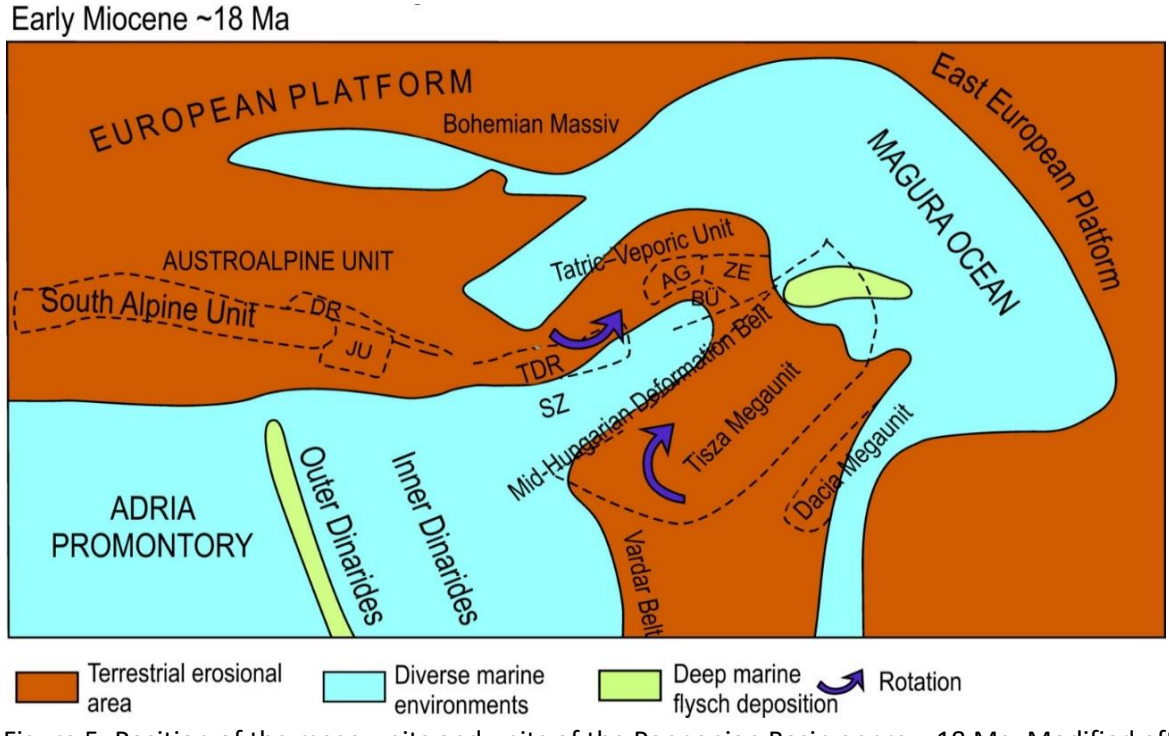

Figure 5: Position of the mega-units and units of the Pannonian Basin approx. 18 Ma. Modified after Haas [ed.] et al. (2002).

The geodynamic model of this movement can be explained as an escaping orogenic wedge, or as a gravitational collapse along with a dragging effect associated with the initial subduction beneath the Eastern Carpathians. Most likely, both effects were involved. The southern boundary of the Alcapa Mega-unit is well defined with steep shear zones and bunches of strike-slip structures in the upper crust, along the Mid-Hungarian Shear Zone (Csontos & Nagymarosy 1988). These strike-slip faults truncated the sedimentary sequences in the Paleogene sub-basins. These times the Mid-Hungarian Shear Zone and the Periadriatic lineament were in an effective continuation and acted as a dextral strike slip (Fodor et al. 1999) with transpressional revers faults (Palotai, 2013). The whole unit either in sense of Haas et al. (2000) or Schmid et al. (2008) can be interpreted as a suture zone of geodynamic mega-melange of mainly South Alpine originated fragments and subunits with remarkable magmatic signal of tonalities with subordinate granodiorites. In our territory the Karavanke-Pohorje plutons are part of these intrusions. The Paleogene magmatic event may directly link to the shear zone, and can be followed in the Southern Alps to Slovenia and observed in the Hungarian Paleogene Basin as well.

Cretaceous-Paleogene sedimentary units of the Szolnok-Máramaros flysch belt were deposited in the Magura Ocean, while the oceanic crust progressively subducted between the continuously north-eastward moving Alcapa Mega-unit, the Tisza Mega-unit and the stable European Platform. This flysch belt is the pinched, sheared remnant of the oceanic crust between the Alcapa and Tisza Mega-units (Schmid et al. 2004).

The formation and the main deformation phase along the Mid-Hungarian Zone occurred also in the Paleogene-early Miocene. During this process the Alcapa Mega-unit moved east-northeastward along this zone and rotated clockwise (Márton 2001). The Alcapa Mega-unit rotated the Tisza Mega-unit into the Magura Ocean, while deforming between them the pinched, sheared blocks of South alpine relation and sediments of the flysch ocean. (Balla 1984, Balla 1986, Balla 1988, Csontos et al. 1992, Fodor et al. 1998) (Figure 5).

By the Middle Miocene, mega-units in the basement of the Pannonian Basin had settled into their current position. In the Dinarides the dextral transpression re-occurred in the middle Miocene, the shortening in the external Miocene thrust belts along the arc of the Carpathians were active and contemporaneously, basin evolution processes started in the central part of the Alp-Carpathian-Dinaric orogene, which led to the formation of the Pannonian Basin.

2.1.2 Pannonian Basin evolution phase

Budai & Maros (2018) The history of the Pannonian Basin is in strong connection with a basin system which had been separated from the Alpine Tethys in the Paleogene and was named Paratethys. The initial real sea circumstances changed later in the Late Miocene into an endemic lake and completely filled up with sediments by the Pliocene.

The shortening, caused by plate convergence of Adria and Europe gradually was overspeeded by the extension caused by the roll-back effect of the subducting slab (Dewey 1980) in the territory of the Pannonian basin. In other parts of the orogenic system, as in the foredeep basins of the Carpathian arc, contemporaneous thrust faults were active. In the territory of the back-arc type Pannonian Basin the main structural phases of the basin evolution can be explained by a thermo-mechanical and isostatic compensational model of Mckenzie (1978). The roll-back mechanism was accompanied by attenuation of the crust, which resulted in an asthenosphere upwelling (Royden & Horváth, 1988). This was strengthened by the asthenosphere flows (Kovács I. et al. 2012). In practical terms, the subsidence was due to the isostatic movement of the attenuated and low-density crust (i.e. Royden & Keen, 1980). In summary, the thermal flux of the crust increased.

The extensional tectonic regime was characterized by probably rotating extensional forces as the subduction processes propagated from Eastern Carpathians to Vrancea Zone and below the Dinarides (Matenco & Radivojević, 2012). It was complicated by the rotation of mega-units as well, the axis of the main extensional force was probably rotated counterclockwise (Matenco & Radivojević, 2012). In general the extension activated the fault planes of nappe systems, with emerging previously buried basement core complexes and went along listric and steep normal faults (Figure 6), originating grabens and half-grabens (Horváth et al. 2006). The highly complex structure of the basement, its original complexity and the rotation linked to extensional tectonics originated a very complex trench system. Characteristics of some sub-basins are linked partly to strike-slip shearing.

In grabens and basins there are direct quantitative connections between sediment sequences, rotation and the tectonic event history (Balázs et al. 2016).

The amplitude of extension was several hundreds of kilometres, with a rate of approximately 1.4–1.6% for the whole territory and lithosphere (Lenkey, 1999). This rate may vary from 1.1% to 1.4% (Bereczki et al. 2017) in the individual sub-basins and for the rigid lithosphere, depending on the extensional fault pattern. Lithospheric extension rate of the mantle lithosphere may have been significantly higher than this.

We divide the basin forming process into two significant part: the so called Synrift phase and the Postrift phase. The Synrift can be characterized by the maximum extension, lasted from Eggenburgian to middle Badenian. Coevally the Alcapa and Tisza Mega-units were rotated oppositely in several phases: 80º CCW and 100º CW respectively (Márton & Fodor, 2003, Márton et al. 2007, Fodor, 2010). Siliciclastic sequences were deposited in the inner basin in considerable thickness, while only in limited extension at the shorelines.

The isostasy induced sinking reached balance in the Late Miocene, the start of a thermal balance may also have been achieved, which resulted in a cooling of the crust, which led to a thermal induced subsidence phase. This period is defined as a Postrift phase in the geologic literature (Horváth, 2007). The beginning of this Postrift phase is not contemporaneous in the Pannonian Basin, but generally started from the end of Sarmatian. The docking and collision of main units in the basement which had by then occurred in the Eastern Carpathian area then resulted in the fall of extensional forces and a quick basin inversion (Horváth, 1995). This post-Sarmatian inversion resulted in the folding of synrift deposits and erosion at certain part of the basin, in contrast to the very thick sediment accumulation in other parts of the basin. In summary, approximately 5000–7000 metres thick sedimentary sequences were deposited during the Postrift phase (Figure 3). This was the time of Lake Pannon, which became totally isolated due to the contemporaneous emergence of the Carpathians and gradually filled with the terrestric sediments. At this stage the deformation regime was characterized by low amplitude strike-slip and normal faults, and with atectonic compaction.

At the beginning of the Pliocene, subduction was practically terminated due to the gradual rise of the subduction dip angle, a northern compression of the Adria microplate that rotated counterclockwise, and started to dominate the stress field of the realm (Bada et al. 2007). Relative to all these processes, a compressional stress field came about within the Carpathian Basin. The subsidence had been changed to inversion in the mountainous area, while subsidence of deep sub-basins still continued (Horváth, Cloetingh, 1996). According to in situ stress measurements (Gerner et al. 1999), space geodesy methods (Grenerczy et al. 2005) and model calculations (Bada et al. 2007) this stress field is still active in the recent times.

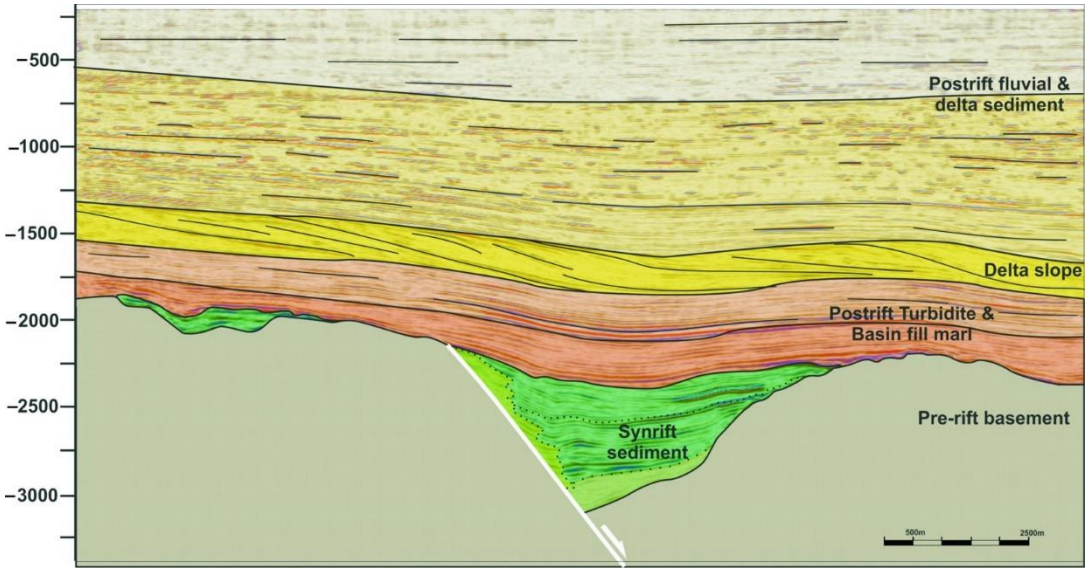

Figure 6: Typical synrift halfgraben structure with its postrift cover (interpreted seismic profile).

2.2 Stratigraphic harmonization

The stratigraphic harmonization prevailed the 3D model building of the Pannonian Basin in the frame of the GeoConnect3d project. In this introduction we provide a short summary about the geohistory of the infilling sedimentary sequences in the Pannonian Basin and the results of the huge work of harmonization of the sedimentary and volcanic unit stratigraphy and synonym harmonization of the formation names. This chapter is based on Budai & Maros (2018) with extensions.

Considering Early and Middle Miocene lithostratigraphic units, in case of some partner countries do not have already accepted, official names for the units, we temporarily used Hungarian names (e.g. in Serbia and provisionally Bosnia and Herzegovina, as well as in the areas along the border in Romania). Considering the Late Miocene units there is more or less a consensus using the Hungarian names; nevertheless, Slovakia has own names for its Pannonian lithostratigraphic units. The philosophy of displaying the harmonization was pointed out from Hungary occupying a central place in the Pannonian Basin. So almost all the charts (Figure 8-13.) contains a Hungarian column as a common point. The order of the charts is clockwise from south.

The Hungarian Neogene is characterized by the formation, evolution and infilling of the Pannonian basin, which was a sub-basin of the former Paratethys over the last 24 million years. During this time, within the Intra-Carpathian region, 6000-7000-metre-deep sub-basins and ridges were formed. These were infilled with fine grained siliciclastic sediments that were transported from the continuously emerging areas of Alps and Carpathians.

Early Miocene

At the beginning of the Miocene, marine sedimentation was limited to the northern sub-basins of the Paleogene basin. The fine grained open marine sedimentation (Szécsény Schlier Formation) was characteristic mainly of the Late Oligocene, but this situation changed with the deposition of coarser grained material (Budafok Sandstone and Pétervására Sandstone Formations) in the Early Miocene, supplied by newly formed huge delta systems. The Eggenburgian sedimentary basin became filled up with the fluvial-alluvial succession (Zagyvapálfalva Formation) which was covered with the material of the “Lower Rhyolite Tuff”. This allowed the particular preservation of the “footprint sandstone” in Ipolytarnóc Fossils Nature Conservation Area. In the South Slovakian Basins the Eggenburgian open marine sedimentation was manifested in the formation of the Filakovo Formation, and the marine

regression resulted in the deposition of the Bukovina Formation comprising continental deposits with rhyodacite tuffs. The Early Miocene of the Danube Basin in Slovakia represents a different sedimentation realm.

From the Ottnangian onwards, coal deposition occurred in many areas of the evolving lacustrine and swamp environments (Salgótarján Formation – both in Hungary and Slovakia).

Simultaneously, in the early Miocene thick deposits of fluvial–alluvial sediments of the Szászvár Formation were deposited in the Tisza Mega-unit, and in the freshwater marshes on the alluvial plains. The intense andesite volcanism during the Early Miocene was related to the beginning of the subduction of the Magura Ocean (Mecsek Andesite, Peripannon Pluton Formation in Slovenia). Similar continental sediments can be found in the Transdanubian Range Unit, in western forelands of the Transdanubian Range (Somlóvásárhely Fm).

In the Hravatsko Zagorje Basin (Croatia) the late Oligocene – early Miocene was predominated by shelf prodelta sediments (Meljani Formation), marine-brackish shoreface, delta and prodelta deposits (Golubovec Formation) and the prevailingly shoreface Macelj Formation, the Čemernica Member of which shows shoreface-offshore transition. The Ottnangian Bednja and the Karpatian Crkovec Formations also represent shoreface–offshore transition. The offshore character of the Crkovec Formation becomes more pronounced towards the corresponding Slovenian Haloze Formation.Extensional tectonics related to the late-stage evolution of the Dinarides and the opening of the Pannonian Basin allowed the formation of freshwater sedimentary basins in the Dinarides (Dinaric and Serbian Lake Systems) and in the southern margin of the Pannonian Basin (Kiskunhalas Formation). In the Mecsek Mts. (S Hungary) syn-rift age sediments crop out to the surface. These freshwater (at most slightly brackish-water) deposits are supposed to be coeval with the initiation of extension (Sebe et al. 2018).

The early Miocene succession of the North Croatian Basin more or less corresponds with the Zala-Dráva-Mecsek area in S Hungary. The alluvial Daranovci Formation can be correlated with the Szászvár Formation and the lacustrine members of the Glavnica Formation can be correlated with the Kiskunhalas Formation which has only been clarified somewhat by recent research.

In the charts showing the lower Miocene units of Serbia and the Samac-Orasje Depression of Bosnia-Herzegovina the Vrdnik Series corresponds to the Hungarian Szászvár Formation. For the syn-rift lacustrine sediments the Kiskunhalas Formation has been used. The Tuzla Basin has its own succession with local names.

In N Hungary the Karpatian marine sedimentary cycle starts with coarse-grained clastic beds of the Egyházasgerge Formation. As the sea level rose, fine-grained siliciclastic sequences were deposited in the open basins (Garáb Schlier Formation). At the end of the Karpatian coarse-grained and carbonate sedimentation (Fót Formation) took place again due as the sea became shallower. In the South Slovakian Basins, the Salgotarjan Formation passes up into the Modry Kamen Formation with consists of mixed marine and brackish sandstones/siltstones, upwards passing into littoral and bathyal sediments, classified into 3 members.

The Eggenburgian open-marine deposits of the Presov Formation and Celovce Formation in the East Slovakian Basin correspond to the Burkalo Formation in the Trans-Carpathian Trough of Ukraine. Subsequently a hyatus in the Ottnangian, the Slovakian Teriakovce, Sol'na Bana and Kladzany Formations of Karpatian age can be correlated with the Tereshul Formation in Ukraine.

Middle Miocene

In the Badenian age of the Middle Miocene, pelagic basins were formed in the trenches opened up in the Karpatian and earliest Badenian. The first deposits – made up of breccia, conglomerate and sandstone comprising tuffaceous intercalations – belong to the Abony Formation in the Great Hungarian Plain. Transgression resulted in the deposition of fine-grained siliciclastic sediments (Baden Formation). In the early Badenian (~ Langhian) along the shores – with minimum or moderated terrigenous influx – the highly variable lithofacies of Leithakalk (Lajta Limestone Formation Pécsszabolcs Member= "Lower Leithakalk") were formed. In case of higher fluvial influx from the hinterland, shoreface conglomerates, pebbly sandstones, sandstones and sand were deposited [Budafa Formation (S Transdanubia), Pusztamiske Formation (NW Transdanubia)]. A temporary shallowing took place during the middle Badenian resulting in coal formation in the Mecsek (Hidas Formation) Indications of evaporites in well successions correlate with the Badenian Salinity Crisis (~13.8 Ma).

Badenian marine deposition started earlier in the Slovenian area. The Haloze Formation of Karpatian-early Badenian age comprises different lithofacies, such as conglomerate and breccia, as well as marl, siltstone and sandstone with tuff interbeddings. The Spilje Formation in Slovenia (comprising several members/lithofacies) is of Badenian and Sarmatian ages and represents shoreface to offshore-bathyal sedimentary environments. It corresponds to the Hungarian Baden Formation (including the former Tekeres Schlier and Szilágy Clay Marl as members) and Lajta Limestone Formation, as well as the Sarmatian Kozárd and Tinnye Formations. In the Hravatsko Zagorje Basin and the North Croatian Basin the Badenian Veljanica Formation and Sarmatian Dolje Formation – both of offshore facies – and the Vrapče Formation (Badenian) and the Pećinka Member of the Dolje Formation (Sarmatian) made up of shoreface carbonates, correspond to the members of the Spilje Formation in Slovenia and the Baden Formation and Lajta Formation, as well as the Kozárd and Tinnye Formations in Hungary (see later).

For Badenian and Sarmatian offshore and shoreface units, Hungarian names have been used in Serbia and Bosnia-Herzegovina (see HU–SRB–BIH chart). Abony Formation (coarse clastic succession underlying the Badenian marine sediments in the Great Hungarian Plain) and Budafa Formation (shoreface coarse clastics and sandstone of early Badenian age) have also been depicted in the chart.
In the Danube Basin the lower Badenian Bajtava Formation comprising transgressive marginal conglomerates, sandstones and volcanoclastics is overlain by a siliciclastic succession (siltstones, calcareous clays) called Spacince Formation. This is followed by the Pozba Formation consisting of calcareous clays, siltstones and sandstones and volcanoclastics. Biogenic limestones are also found in the marginal areas. The fine-grained Badenian siliciclastics correspond with the Baden Formation, whereas the Sarmatian Vrable Formation can be correlated with the Kozárd Formation in Hungary.

Due to the continuous subduction of the European Plate, an intensive, island arc-type andesite volcanism took place during the mid-Badenian, and a chain of great volcanoes were formed along the inner arc of the emerging Carpathians (N Hungary: Börzsöny-Visegrád and Mátra Volcanic Formation Groups).

In the East Slovakian Basin volcaniclastic deposits (Nizny Hrabovec Formation) of early Badenian age can be found. The Mirkovce Formation occurs in the western part of the basin and comprises monotonous grey claystones and siltstones originated from below the wave base. The Middle Badenian in the central basin part is represented by the Vranov Formation made up of siliciclastics (sandstone and pelites). The deep-marine environment changed into a shallow-marine one and later to a lagoonal one and evaporites of the Zbudza Formation were deposited. In the Ukrainian area the before mentioned evaporites correspond to the Novoselytska, Tereblianske Formation and Solotvino Formation formed due to a regression. [From the upper part of the Badenian onwards up to the

Pannonian lithostratigraphic units can be well correlated between E Slovakia and Ukraine (see the lithostratigraphic chart)].

During the sea-level rise in the late Badenian, carbonate sedimentation took place in shallow marine shelf environments (Lajta Limestone Formation Rákos Member =“Upper Leithakalk”), while sedimentation was characterized by fine-grained siliciclastic deposits in the open marine environments (Baden Formation Szilágy Clay Marl Member).

In the Middle Miocene, at the beginning of the Sarmatian, volcanic activity renewed with rhyolitic tuff falls, followed by carbonate sedimentation in shallow marine shelf environments. The volcanism, predominantly felsic, andesite, rhyolite and dacite, moved eastward along the inner arc of the Carpathians, to the Tokaj-Nyírség area. There it formed huge stratovolcanoes. In the South Slovakian Basins the Halic, Vinica, Opava, Lysec and Pokoradza Formations represent volcanic activity.

During the entire Sarmatian, in shoreface environments biogenic calcarenite, coarse, porous limestone, oolithic-bioclastic limestone, pebbly calcareous sandstone and locally pea gravel belonging to the Tinnye Limestone Formation deposited. Towards the open sea there is a transition from the Tinnye Limestone into the offshore clay marl, marl and siltstone (Kozárd Formation).

Late Miocene

Evolution of the Carpathian Basin during the Late Miocene was determined by thermal subsidence, in contrast to the Middle Miocene extensional tectonics. In accordance with the changing tectonic regimes, sedimentation patterns also changed. By the beginning of the Middle Miocene the central basin of the former Paratethys had closed completely, forming a lake with no runoff. This was Lake Pannon, which gradually became a freshwater lake due to continuous river inflow.

The evolution of the Lake Pannon can be divided into three main phases. At the end of the Sarmatian, the Carpathian Basin was separated from the Paratethys, erosion started on the emerging areas near shore, and freshwater input increased. The second phase occurred during the continuous rise of the sea-level, when the lake filled the whole Carpathian Basin. The third phase occurred during a slow regression and infilling of the basin, which was terminated at the beginning of the Pliocene (Figure 7).

Continuous infilling of the Lake Pannon was accomplished by the sediment influx of rivers originating in the elevating areas of the Alps and Carpathians. The intense NW sediment input (from Sarmatian delta systems at the edge of the Danube Basin). Later, there was NE input from the Eastern Carpathians, as well as from the Dráva and Mura valleys. Delta systems started to develop on the coastal areas of the basin, then gradually prograded into its inner parts. The water might have been a thousand metres deep in the deep inner areas, due to continuous subsidence, e.g. in the Békés Trough. During the transgression, a calcareous marl with high organic content was deposited onto the top of the basement (Endrőd Formation); while in the deeper central areas of the basin the sedimentary environment was characterized by very thick turbidites (Szolnok Formation).

On the delta plain and at the delta front, there were various lithologies dominated by clay-silt sedimentation with sandstone interbeddings; on the delta slope, claymarl and silt was deposited (Algyő Formation).

In Slovakia (Danube Basin and Komarno-Sturovo area) the Endrőd, Szolnok and Algyő Formations correspond to the Ivanka Formation.

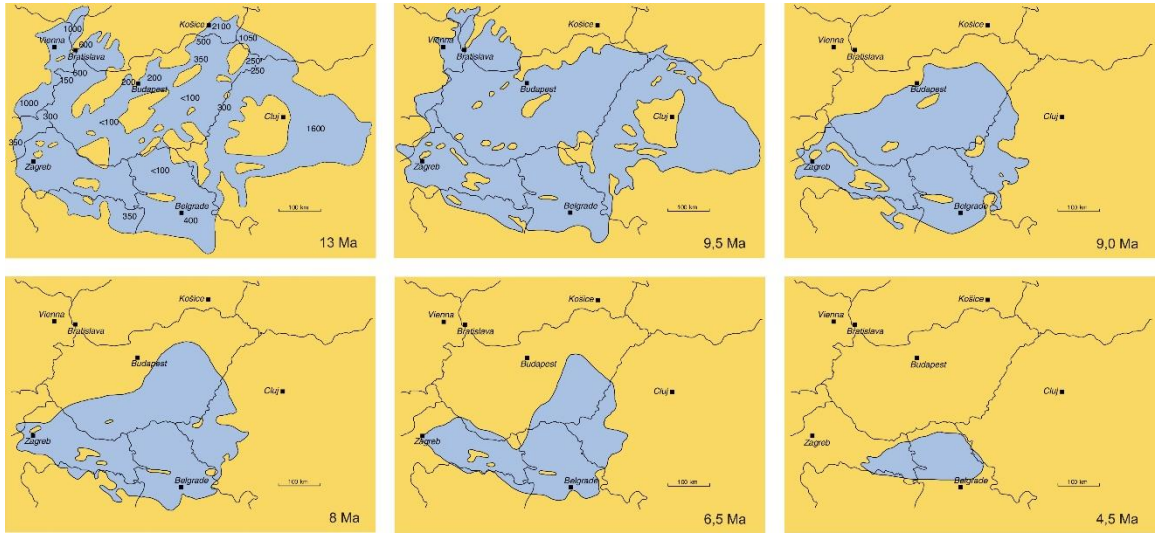

Figure 7: Evolution of the Lake Pannon (after Magyar et al. 1999)

Contemporaneously with the infilling of the deep basin (Újfalu Formation, see Beladice Formation in Slovakia (Danube Basin and Komarno-Sturovo area)), various depositional environments evolved in the shallow littoral areas. The southern forelands of the Transdanubian Range and the Alpokalja were characterized by shore swamps with lignite deposits. Sand and gravel deposited along the sea shore areas were characterized by strong wave activity, while still-water lagoons were characterized by the deposition of silt and clay, or by freshwater lime-mud. At the fronts of prograding deltas, sand was deposited, while the delta plain was characterized by fine grained sediment. Felsic rhyolite volcanism continued on the northern margin of Pannonian Basin during the Late Miocene, and the Nyírség area and Tokaj Mountains were involved in its post-volcanic activity. Meanwhile, basaltic volcanism was active in the SW part of the Transdanubian Range and the Danube Basin.

Pliocene

The Pannonian Basin was almost completely filled with sediments by the beginning of the Pliocene (Zagyva Formation, see Volkovce Formation in Slovakia (Danube Basin and Komarno-Sturovo area)), and a low dry-land emerged. In the subsiding areas, thick fluvial sedimentation occurred. At the shores of the basin mostly fine grained, fluvial-lacustrine siliciclastic sedimentation took place, while at the forelands of mountainous regions and hillsides coarser-grained sedimentation occurred. The Pliocene epoch was the main period of mafic basaltic volcanism, in the area from the Balaton Highland to the Danube Basin (Tapolca Basalt Formation). In the South Slovakian Basins, the Podrecany Formation represents basaltic volcanism.

Quaternary

In the basinal areas, several-hundred-metre-thick fluvial sequences were deposited during the Quaternary, containing upward fining cycles of pebble, sand and clay beds.

In the Pleistocene ice-age, the Carpathian Basin was a periglacial area. During glacial periods, wind erosion was strong. Sand was blown from deflational areas and flood plains of the paleo Danube and was deposited as blown sand. Thick loess was formed by deposition of wind-blown dust. In mountain areas the most widespread quaternary sediments are the slope deposits, while talus cones were formed at steeper hillsides.

River valleys were filled with alluvial deposits and accompanied by multi-levelled terraces on the sides. On the slopes of mountains that are built up of carbonates very thick travertine bodies were formed. Holocene sediments are relatively limited in thickness. Rivers deposited fine-grained sediments (silt, clay) on their flood plains and coarser grained sediments (gravel, sand) in their channels. Lacustrine environments were characterized by mud deposition, and swamps by peat accumulation.

It is important to mention that new descriptions of the lithostratigraphic units of Hungary are under preparation and lithostratigraphic charts will be compiled on the basis of the new descriptions. Volcanic units are especially affected, major changes are being made to them. Charts, made for GeoConnect3d reflect the names, age classifications and spatial distribution based on the so-far existing system.

Stratigraphic harmonization of Miocene lithostratigraphic units of the partner countries can be seen in Figure 8 to Figure 13.

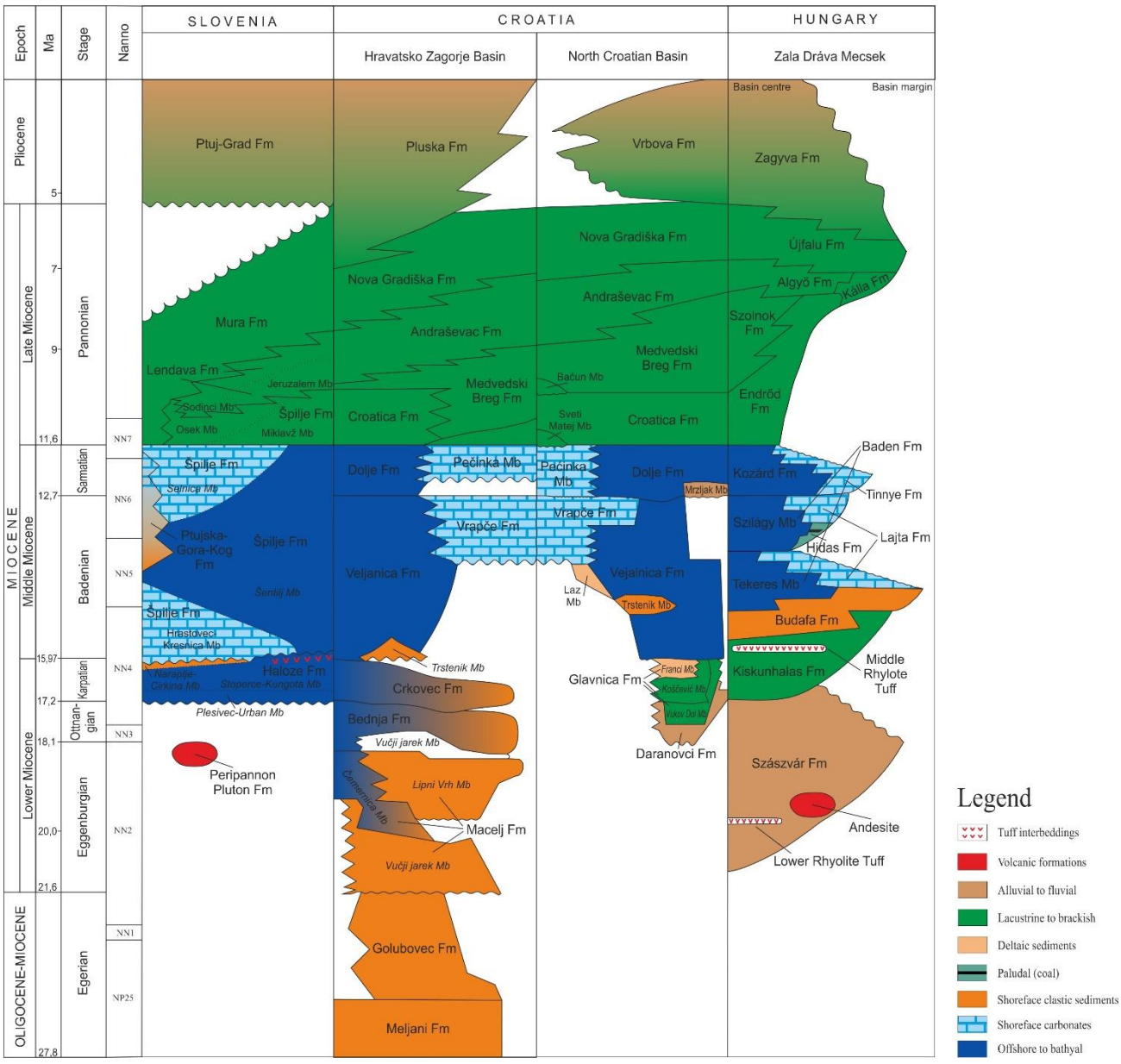

Figure 8: Harmonized stratigraphic chart between Slovenia, Croatia and Hungary

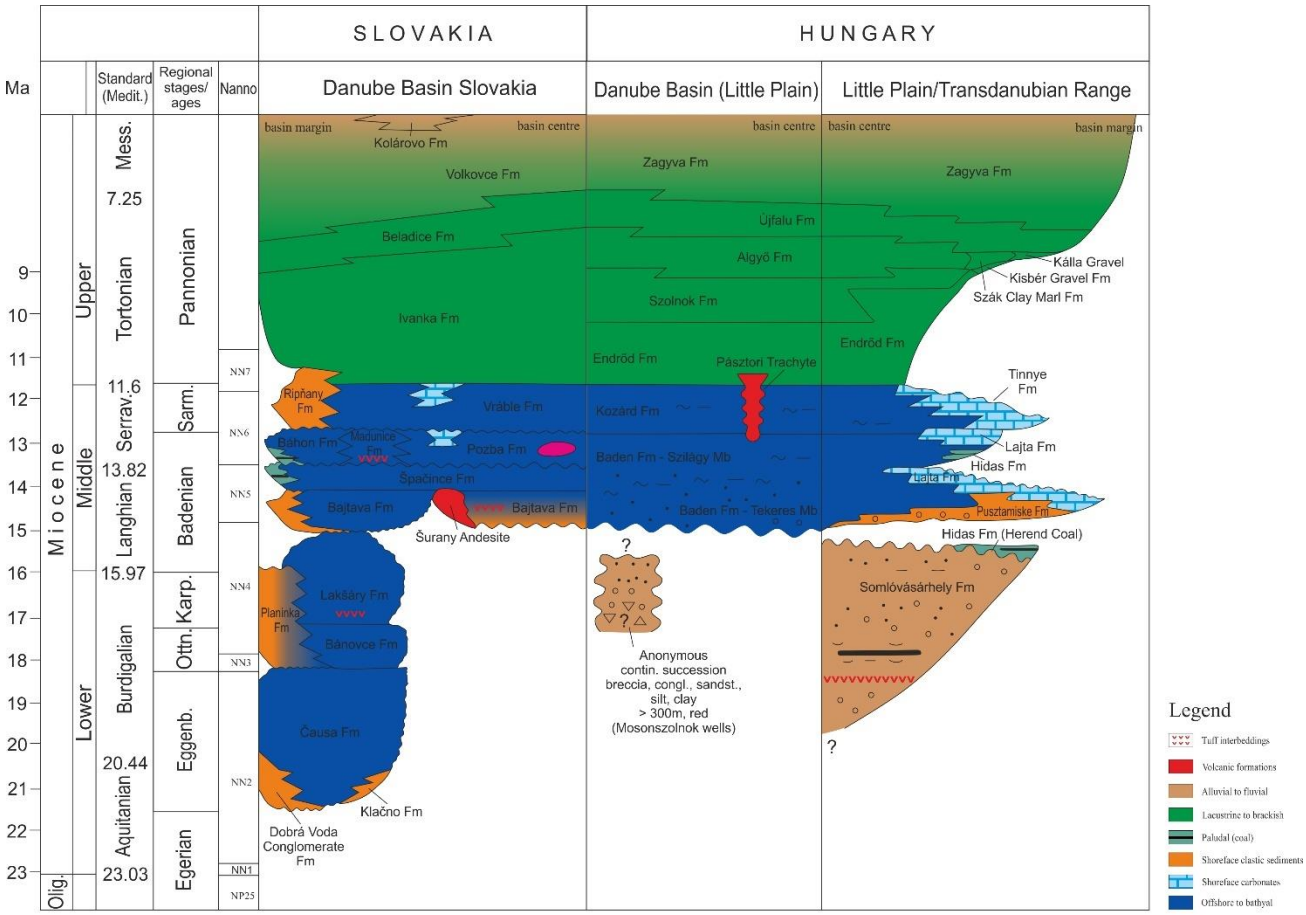

Figure 9: Harmonized stratigraphic chart between Western Slovakia and Hungary

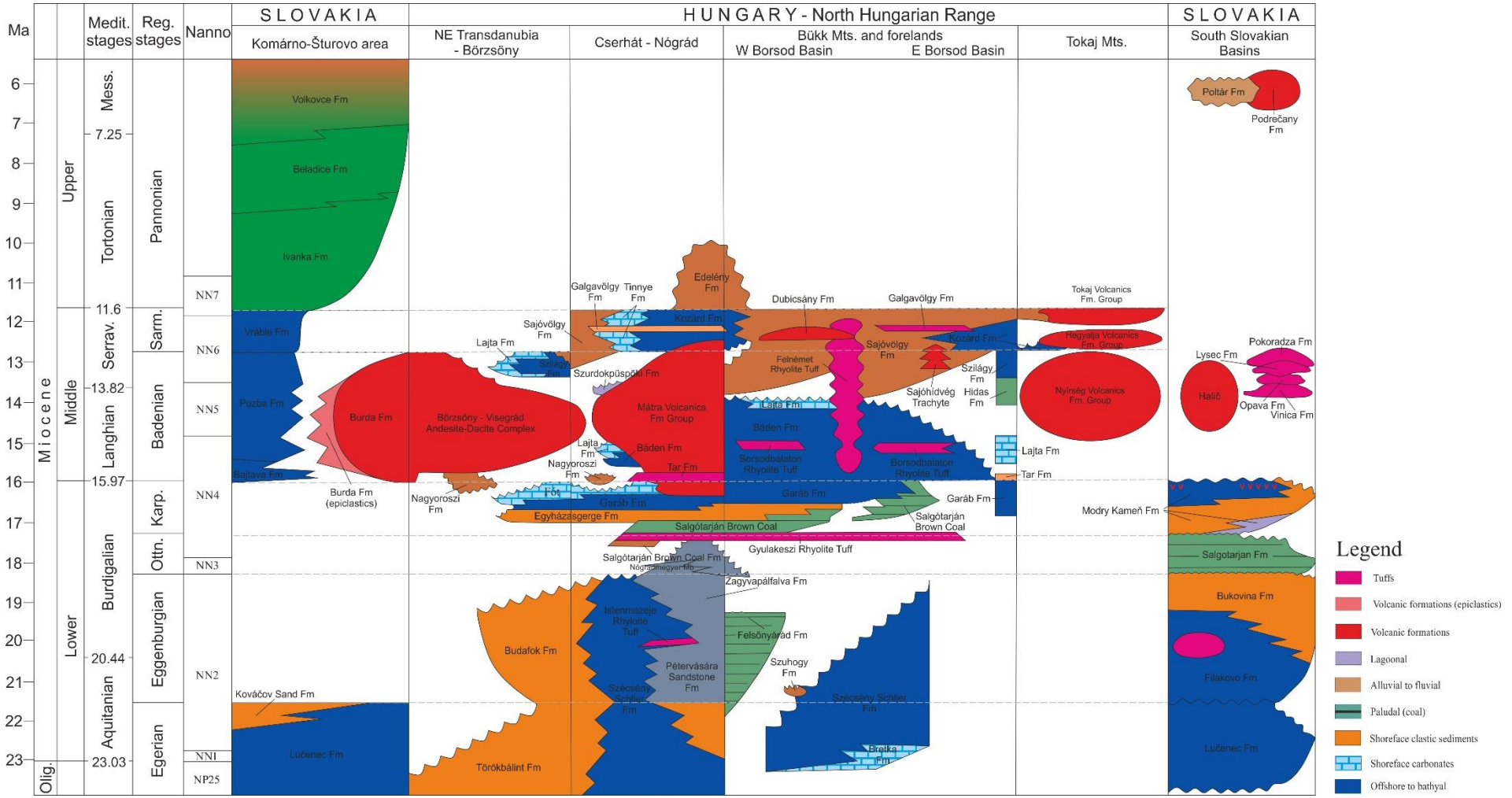

Figure 10: Harmonized stratigraphic chart between Eastern Slovakia and Hungary

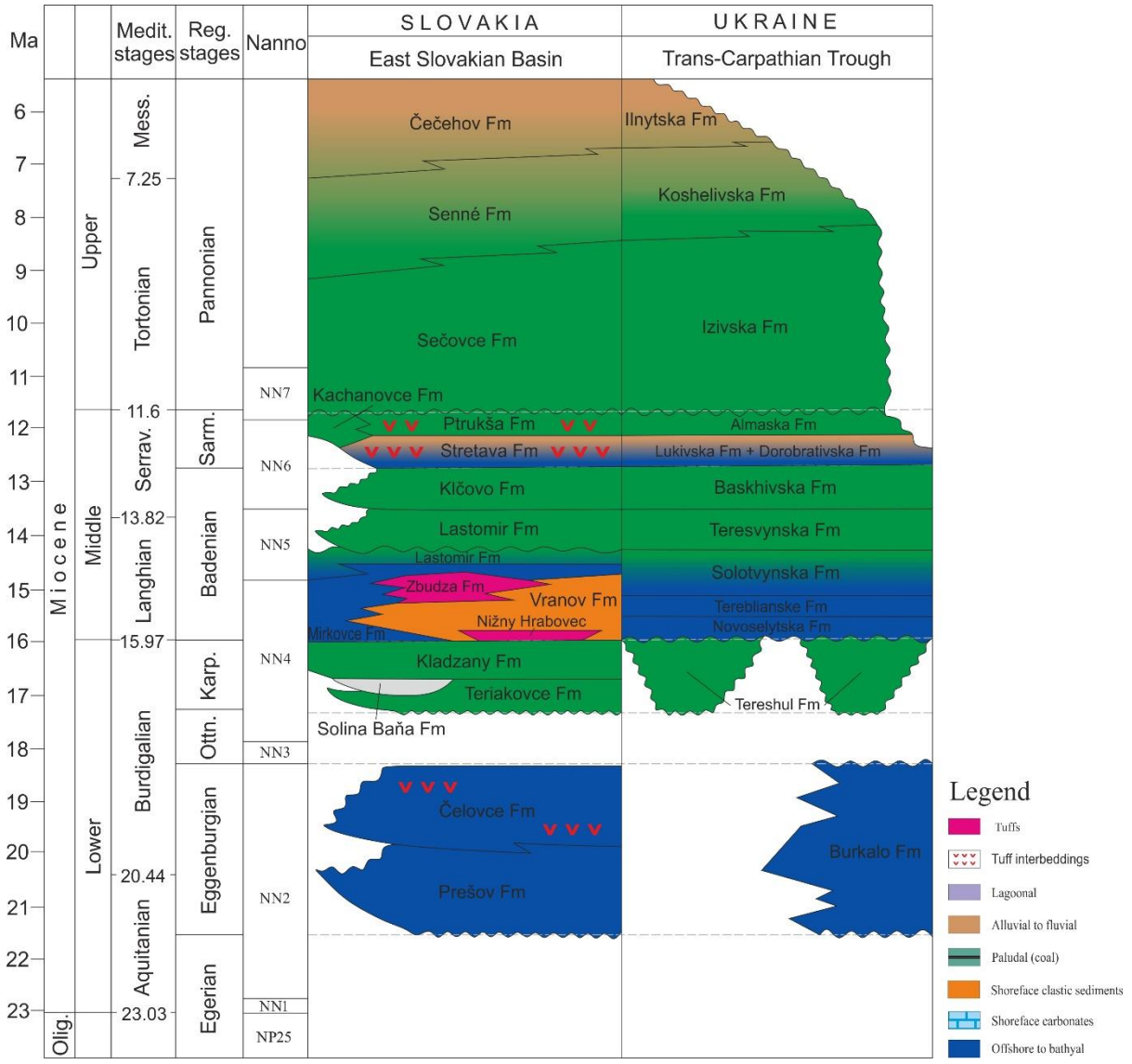

Figure 11: Harmonized stratigraphic chart between Slovakia and Ukraine

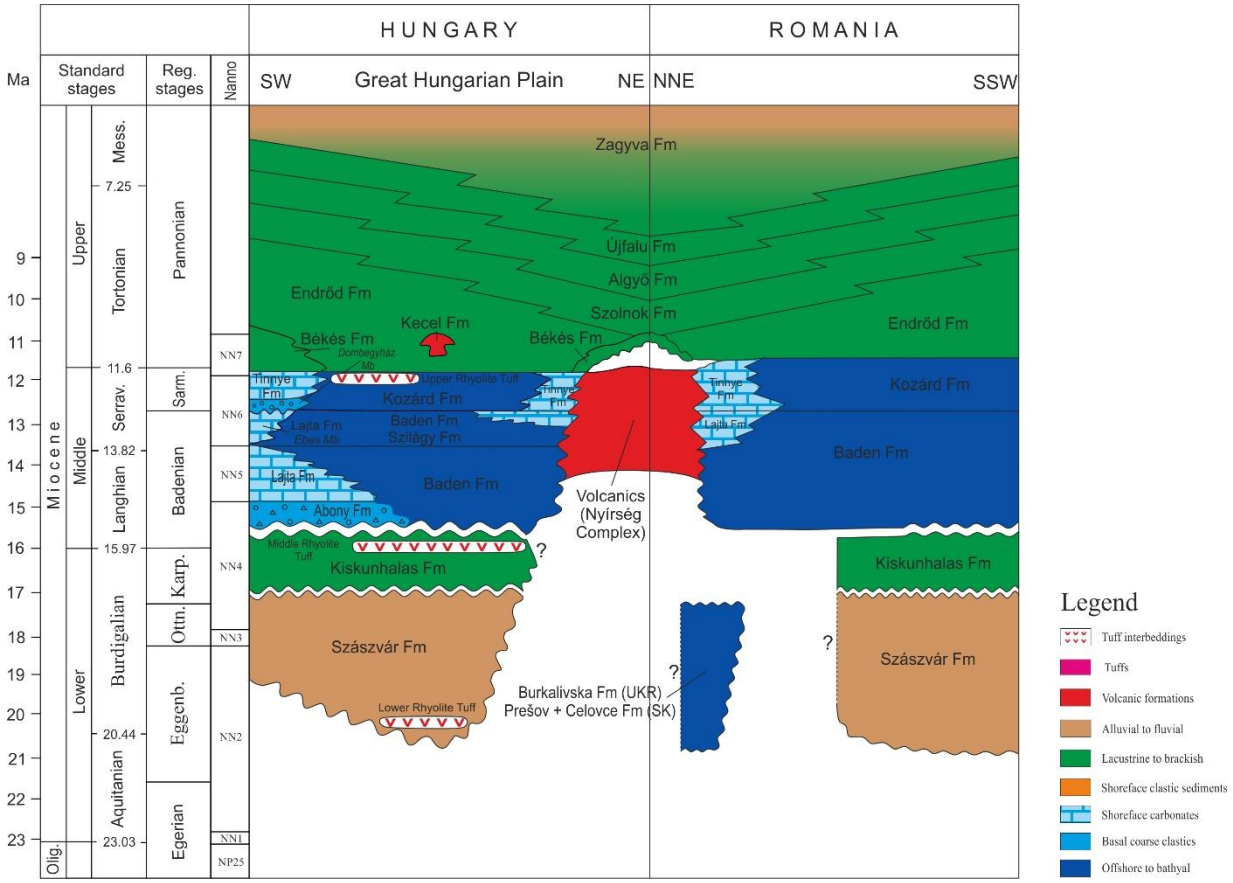

Figure 12: Harmonized stratigraphic chart between Romania and Hungary

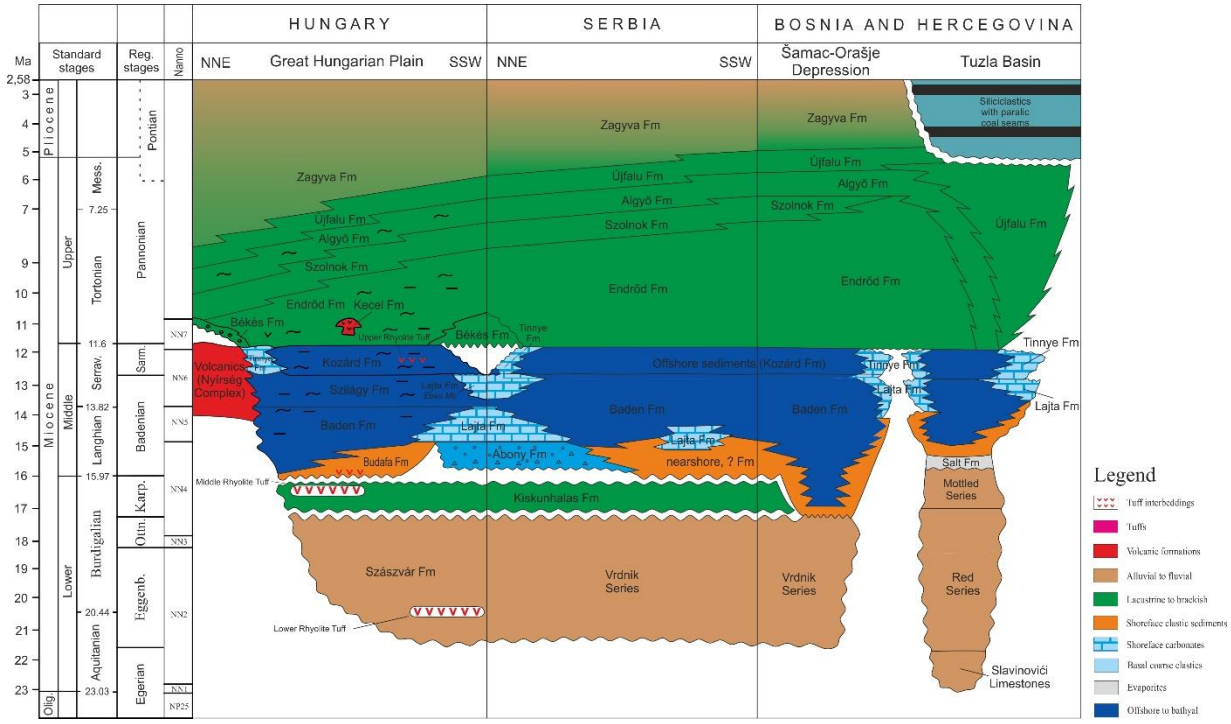

Figure 13: Harmonized stratigraphic chart between Serbia, Bosnia & Herzegovina and Hungary

3 GEOMANIFESTATIONS IN THE MURA-ZALA SUB-BASIN

The Mura-Zala sedimentary Basin is a Neogene basin with many competing geopotentials, spanning parts of Slovenia, Austria, Croatia and Hungary. Basin fil consists of Neogene sediments belonging to the Central Paratethys paleogeographic domain (Royden & Horváth, 1988). Regional stages (Figure 8) in use for the Central Paratethys are therefore used to describe the formations (Piller et al. 2007). Latest lithological formations and 3D geological model of the Slovenian part of the area are described in Šram et al. (2015 and references therein; Figure 14) so they will not be repeated here.

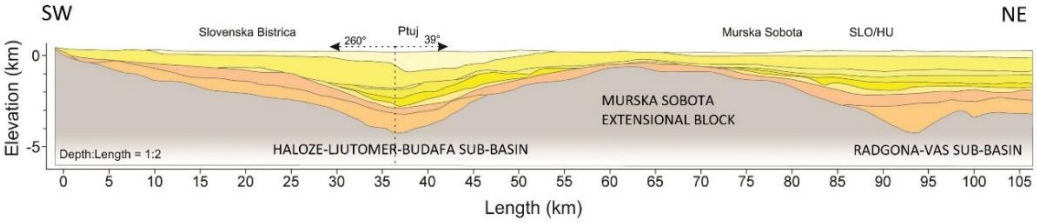

Figure 14: Geological cross-section with formations as modified after 3-3' of Fig. 7 in Šram et al. (2015). The sequence from the surface down is: Ptuj-Grad Fm., Mura Fm. (2 units), Lendava Fm. (2 units), Špilje Fm. (2 units), Haloze Fm. and basement rocks.

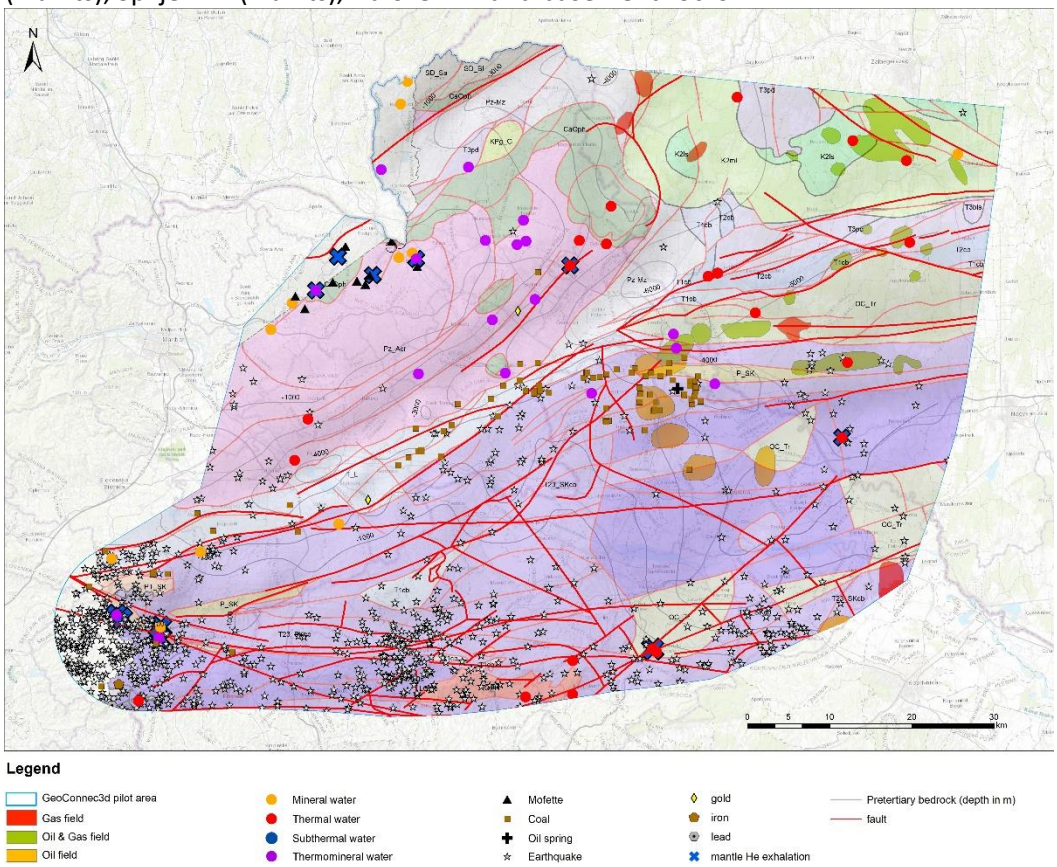

Figure 15: Presentation of all listed geomanifestations in the Mura-Zala pilot area. The area is limed by the SI-AT state border in the north, with the numerical model border in the NE and E, with the major fault zone in the south, and the rough extent of the most interesting geomanifestations in the west. Notice two different backgrounds. The coloured lithology is a

geological model of basement rocks and its structures according to DARLINGe project while bold red lines are newly interpreted faults within the GeoConnect3d project.

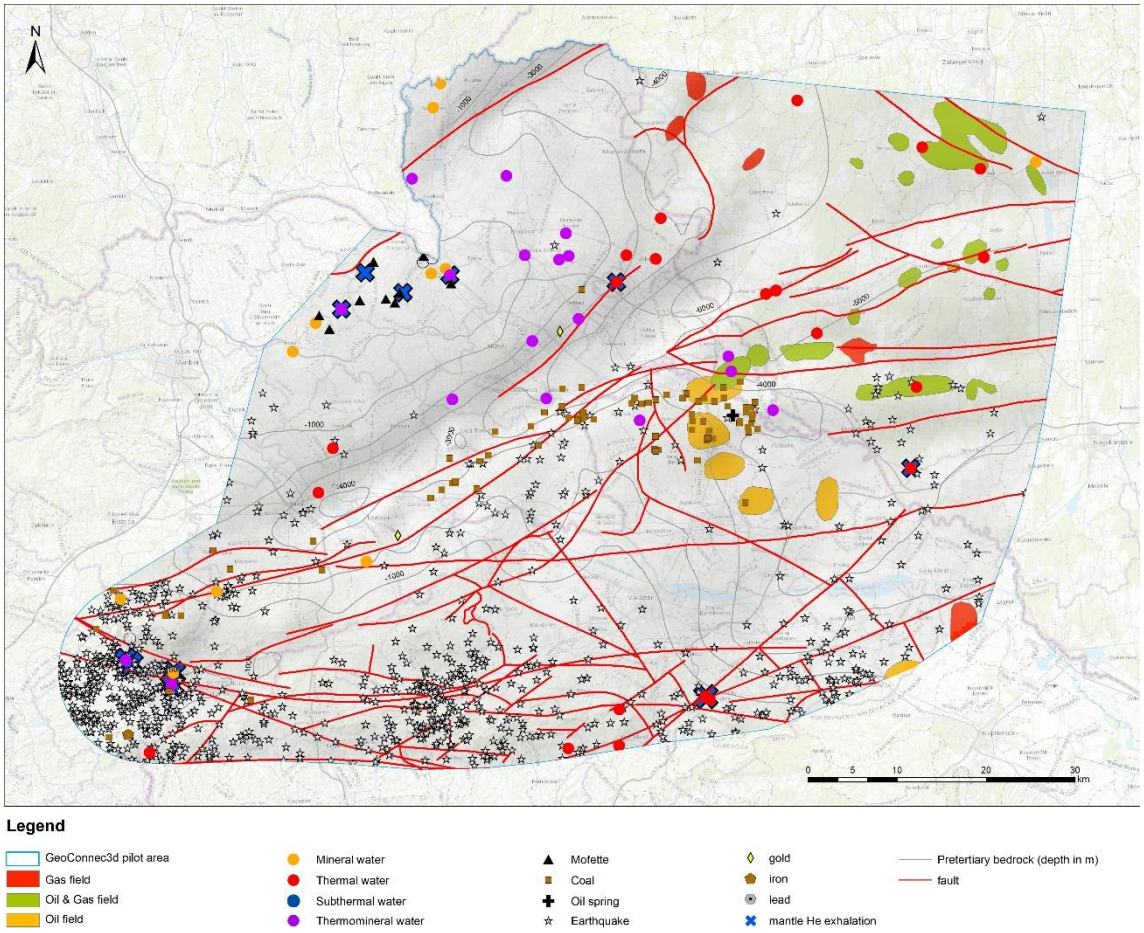

Figure 16: Presentation of all known geomanifestations in the Mura-Zala sub-basin area with newly delineated structural features (faults) within the GeoConnect3d project.

3.1 Geothermal anomalies

Heat in the Earth can be transmitted with conduction, convection, radiation and advection. In most of the Earth's crust conduction is a predominant mode of heat transfer, while convection is more pronounced in the active tectonic (fault-fracture) and volcanic zones with hydrothermal water and gas movements, while radiation is negligible. A new thermal model of Hungary, for example, assumes conduction as the main heat transfer mechanism (Békési et al. 2018), also known to be characteristic for Slovenia (Rajver & Ravnik, 2002).

3.1.1 Conductive heat flow due to thinner lithosphere

The Pannonian basin is well-known of its high geothermal potential (as summarized in Rotár-Szalkai et al. 2018, Goetzl & Zekiri, 2012). It is characterized by a positive geothermal anomaly, with heat flow density ranging from 50 to 130 mW/m2 with a mean value of 90-100 mW/m2 and geothermal gradient of about 45 °C/km. In the Mura-Zala basin, the values of 60-70 mW/m2 at Ptuj in the southwest increase towards the Slovenian-Hungarian border where they may reach 90-100 mW/m2 (Figure 17). This geothermal character is related to the Early-Middle

Miocene crustal extension when deep basins originated. As this is well known hypothesis and much was investigated in previous studies and EU projects, such as T-JAM, Transenergy, GeoMol and DARLINGe, within the GeoConnect3d project we focused on convection patterns and numerical modeling of the regional temperature distribution.

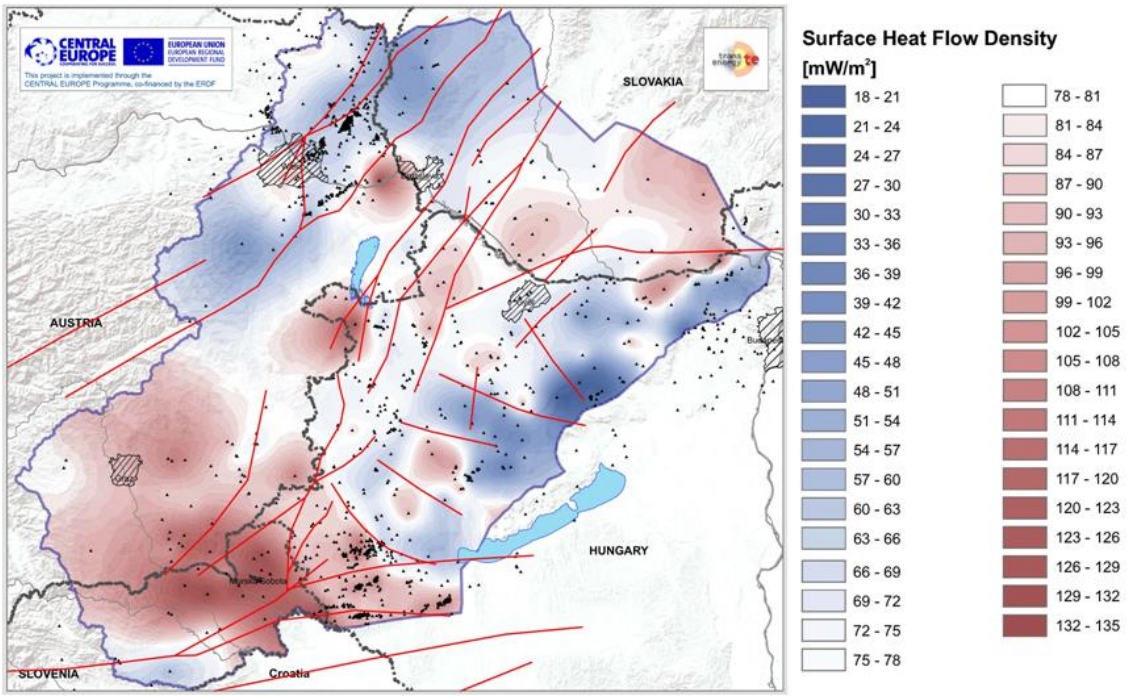

Figure 17: Map of surface heat flow density of the western part of the Pannonian basin was taken from Goetzl & Zekiri (2012). The Mura-Zala sub-basin comprises its SW part with highest HFD.

The observed heat-flow density may be disturbed by fast sedimentation, erosion and groundwater flow (Alföldi et al. 1985; Powell et al. 1988; Békési et al. 2018). Local variations in HFD (Figure 17) can be positive or negative and are a result of convection (see next chapter). Elevated HFD is attributed to convection zones in the relatively shallow lying Pre-Neogene basement which results in HFD of above 120 mW/m2 at the Murska Sobota high and near Lendava in Slovenia (Figure 14). In Hungary, in Nagylengyel-West and Zalaegerszeg-North area this is a consequences of the upwelling branch of the regional convection in the thermal karst. Lower values occur in the southwestern part of the Transdanubian Range (Keszthely Mountains) in Hungary, where the Mesozoic basement carbonates crop out and infiltrating cold karstic waters cool down the subsurface (Nador et al. 2012).

3.1.2 Locally elevated heat-flow density due to convection

The convection share in the temperature-depth profiles (thermograms) was determined in a visual manner with a help of calculated deeper temperatures in conductive regime for 33 boreholes in Slovenia, 3 of them outside the project pilot area, in the Čatež geothermal field. Also, HFD values were determined where reliable T-z profiles were available and thermal conductivity determined on cores (Table 1).

Table 1: The 33 boreholes in eastern Slovenia with calculated HFDs and visible convective part, determined at 11 of them (2 in the Čatež geothermal field). Red numbers have extra convective share.

borehole database №	borehole name	location name	borehole depth, m	q_total, mW/m^2	q_conductive share only	smaller uncertainty in calculation	extra convective share of q, mW/m^2	Legend for QGIS
1	SG-1/54	Hrastje Mota	435,4	106	106			0
2	Mt-2/61	Rimska čarda, Sebeborci	1462	120	120			1
4	BS-2/76	Benedikt	788	145	103		42	3
5	Pg-6/81	Petišovci	3200	112	112			1
8	Mt-6/83	Moravske Toplice	987	132	107		25	2
15	L-1/86	Mostec - Čatež	704	182	70		112	3
30	BŽ-3/87	Brežice-Grad	100	68	68	?		1
33	SOB-1/87	Murska Sobota	870	127	107		20	1
34	GB-1/87	Gabrnik	2196	79	79	?		0
39	T-4/87	Radenci	818	154	109	?	45	3
40	PDG-1/87	Podgorje	350	89	89			0
41	LJUT-1/88	Ljutomer	4048	116	116			0
42	SOB-2/88	Murska Sobota	887	108	108			0
51	Pg-7/88	Petišovci	2990	137	115	?	22	2
53	Mg-6/85	Murski gozd	3858	124	124			1
52	DOK-1/88	Dokležovje	1934	108	108	?		0
66	ŠOM-1/88	Plodršnica	1100	131	103		28	1
82	MB-0/90	Maribor	152	103	103			0
87	MB-1/90	Maribor - Stražun	1331	112	112			1
98	Peč-1/91	Pečarovci	2098	110	110			0
106	MB-2/91	Maribor - Stražun	1600	112	112			1
113	Dan-3/90	Dankovci	1400	150	110	?	40	2
128	Mt-7/93	Moravske Toplice	991	122	102		20	1
148	Mrt-1/93	Sv. Martin - Kobilji breg	3299	102	102	?		0
155	Sre-1/91	Središče	2708	107	107	?		0
205	Mot-1/76	Motvarjevci	3835	111	111			0
211	AFP-1/95	Dobova - Gabrje	700	187	72	?	115	3
212	Pan-1/76	Panovci	2744	98	98	?		0
444	Pg-9/89	Petišovci - Dolina	3011	154	114		40	3
515	Re-1g/11	Renkovci	1484,7	104	104			0
516	SOB-3g/12	Murska Sobota - Černelavci	1520,3	112	112			1
517	SOB-4g/13	Murska Sobota	1201,1	111	111			1
530	Niko-1/08	Nuskova	64	97	97			0
Legend:	boreholes in the Čatež geothermal field							

The difference in the surface HFDs for Slovenia was evaluated between the total surface HFD (Figure 18) and as decreased by convective component at most characteristic boreholes (Figure 19). There, only the conductive component is considered.

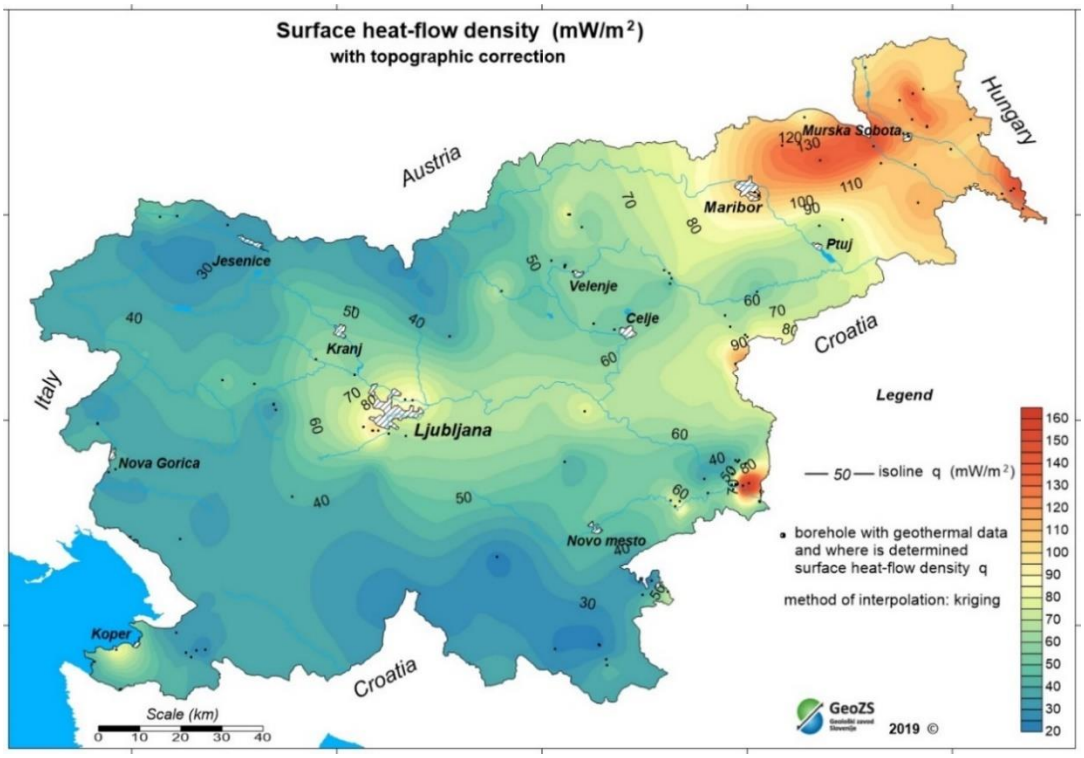

Figure 18: Surface HFD for Slovenia from the measured HFD values (total q).

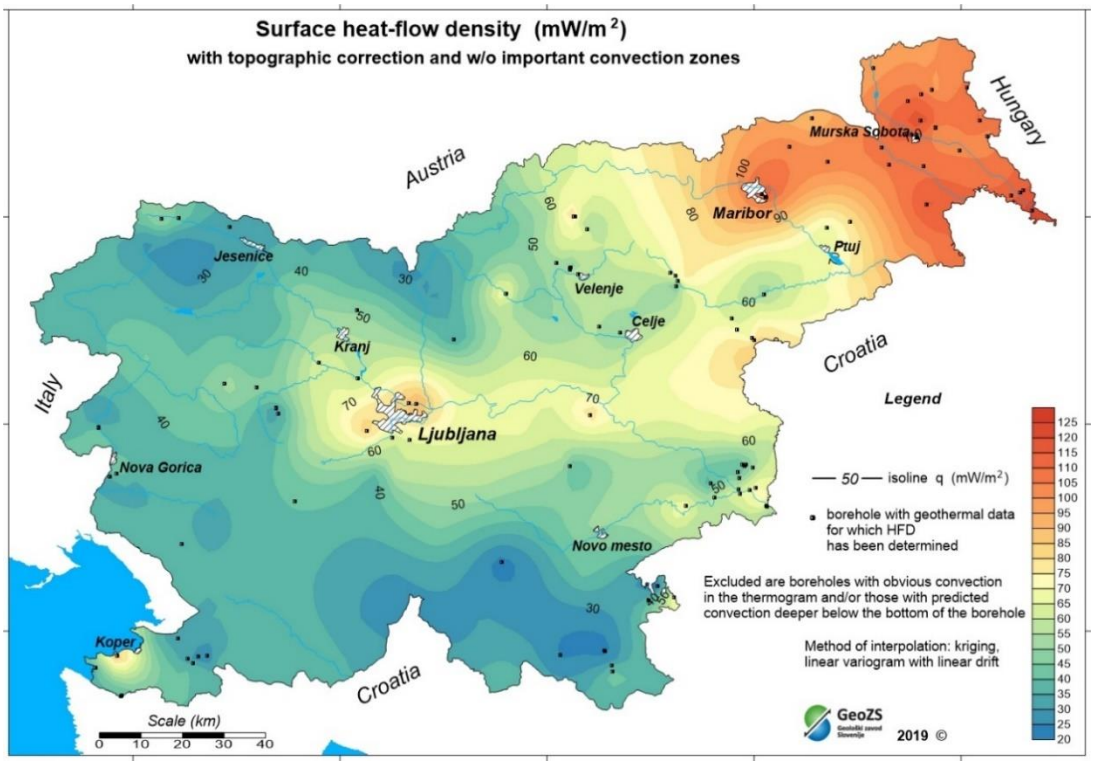

Figure 19: Surface HFD for Slovenia from the measured HFD values with convection component excluded and only conductive component considered.

Few years ago, in the TRANSENERGY project, the methodology for convective component of HFD determination was agreed to be in two ways: (a) with a Peclet number analysis, and (b) in a visual manner (Lenkey, pers. comm.). That is in a way where a deeper geotherm is drawn so that the convective part is not considered, but only the conductive component down to a deeper section. On the other hand, Lenkey et al. (2002) has calculated the convective heat flow component caused by groundwater flow in recharge areas from the ratio of the total energy output and the area of the mountains. Results show that the heat flow corrected for convective effects is close to the heat flow observed around the exposed carbonates. Anyway, our simple approach is in a rough agreement with the HFD values at the Mohorovičić (Moho) boundary for the Pannonian Basin (Békési et al. 2018), which attain ca 20-30 mW/m^2 in Hungary (as basal heat flow), for example. This is also the reason why it is so important to perform the heat-flow measurements (both T-z profiles and thermal conductivity determinations) in as much deep boreholes as possible (Chapman et al., 1984).

3.1.2.1 Determination of the convective HFD component in NE Slovenia

3.1.2.1.1. Be-2/04, Benedikt

From the measured temperatures in several attempts and different manner it has been predicted for this borehole that formation temperature at 2000 m depth could reach cca 84 °C (Figure 20), and that the convection cell could expand from some 800 m down to depth of cca 2000 m. While the temperature gradient in the Neogene section reaches 82 °C/km in the BS-2/76 borehole, it is 85 °C/km in this borehole. The HFD value has not been calculated because no thermal conductivity values are available from Be-2/04 (there has been no coring of rock samples).

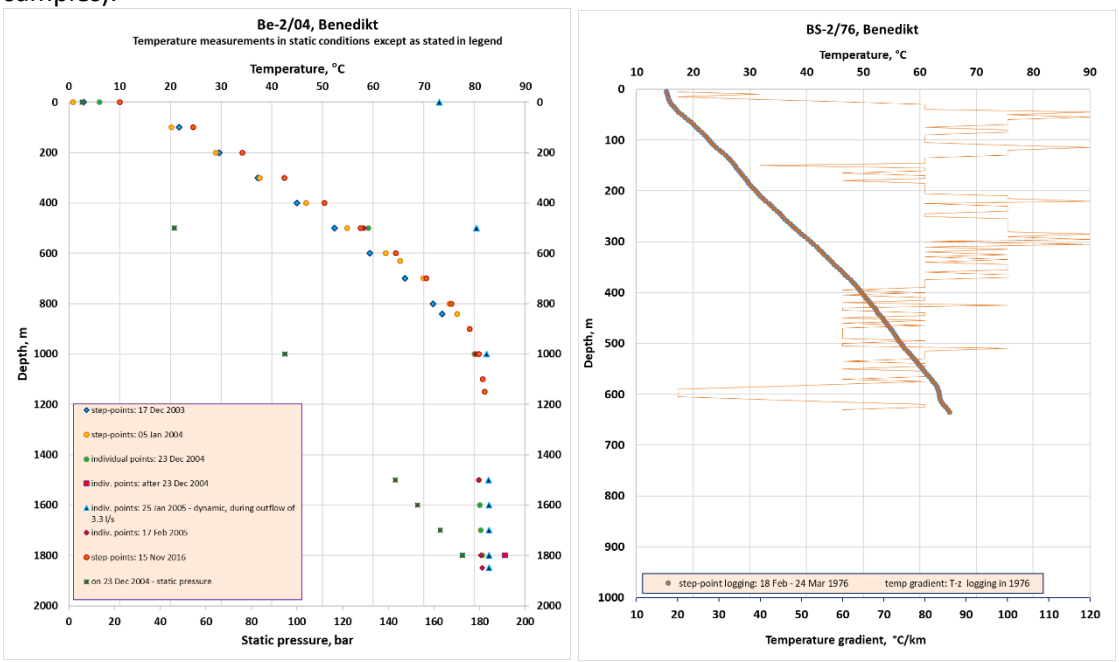

Figure 20: Thermograms of boreholes Be-2/04 (left) and BS-2/76 (right) at Benedikt.

3.1.2.1.2. BS-2/76, Benedikt

With a help of Be-2/04, the conductive HFD component was predicted to be ca q_{cond} = 103 mW/m^2. This value was calculated with regard to the expected temperature T=88 °C at a depth of 2 km (Figure 20) and the mean thermal conductivity for the entire sequence of 2 km, which is λ=2.65 W/(m·K). Temperature gradient is determined as $grad\ T = \frac{dT}{dz} = \frac{88-10.5}{2000} = 38.8\ °C/km$ and the conductive HFD is $q_{cond} = \lambda \cdot grad\ T = 2.65 \cdot 38.8 = 103$ mW/m^2
The measured HFD was 145 mW/m^2, therefore the convective HFD component is 42 mW/m^2.

3.1.2.1.3. Šom-1/88, Šomat – Plodršnica

Based on the measured T-z profiles, the formation temperature at 1200 m depth is predicted to be cca 70 °C (Figure 21). From the measured thermal conductivity on the cored rock samples, the mean value of thermal conductivity has been gained: λ = 2.61 +/- 0.41 W/(m·K).
However, it is assumed that below 1200 m there is a convection zone down to a depth of 1500 m. Then, the conductive HFD is: $grad\ T = \frac{70-10.5\ °C}{1500\ m} = 39.7\ °C/km$
Then the conductive HFD component is: $q_{cond} = \lambda \cdot grad\ T = 2.61 \cdot 39.7 = 103.5$ mW/m^2.
The measured HFD was 131 mW/m^2, therefore the convective HFD component is 28 mW/m^2.

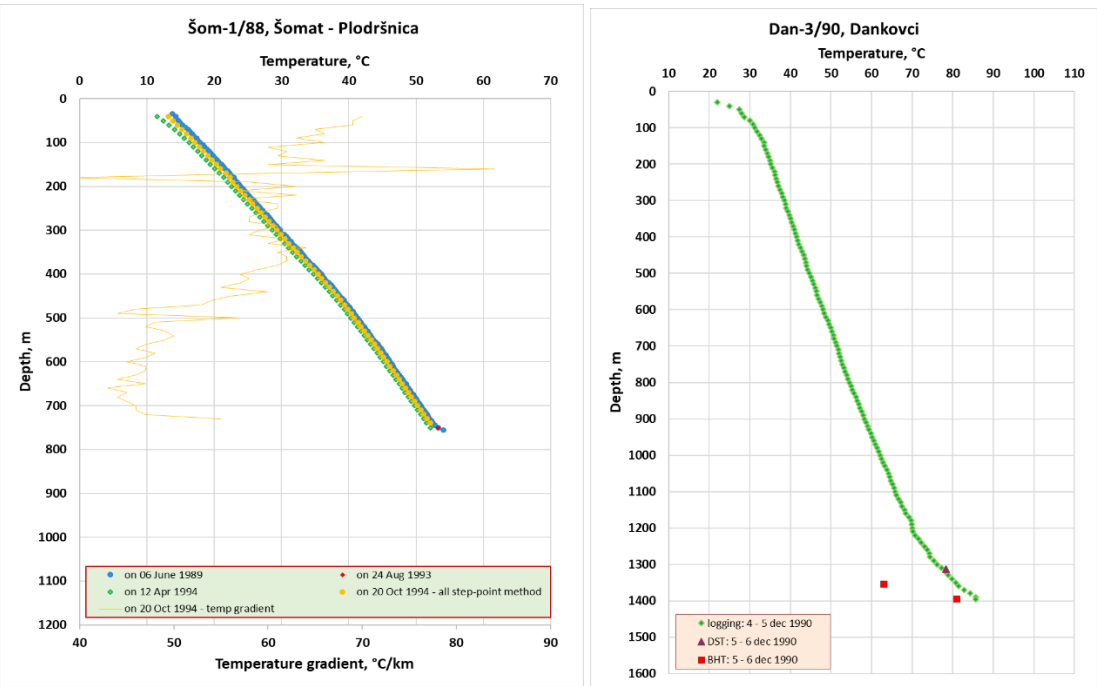

Figure 21: Thermograms of boreholes Šom-1/88 at Šomat (No. 66, left) and Dan-3/90 at Dankovci (No. 113, right)

Also some other boreholes in NE Slovenia show T-z profiles which represent apparent convective component or just hidden and implied convective component (Figure 21, Figure 22, Figure 23).

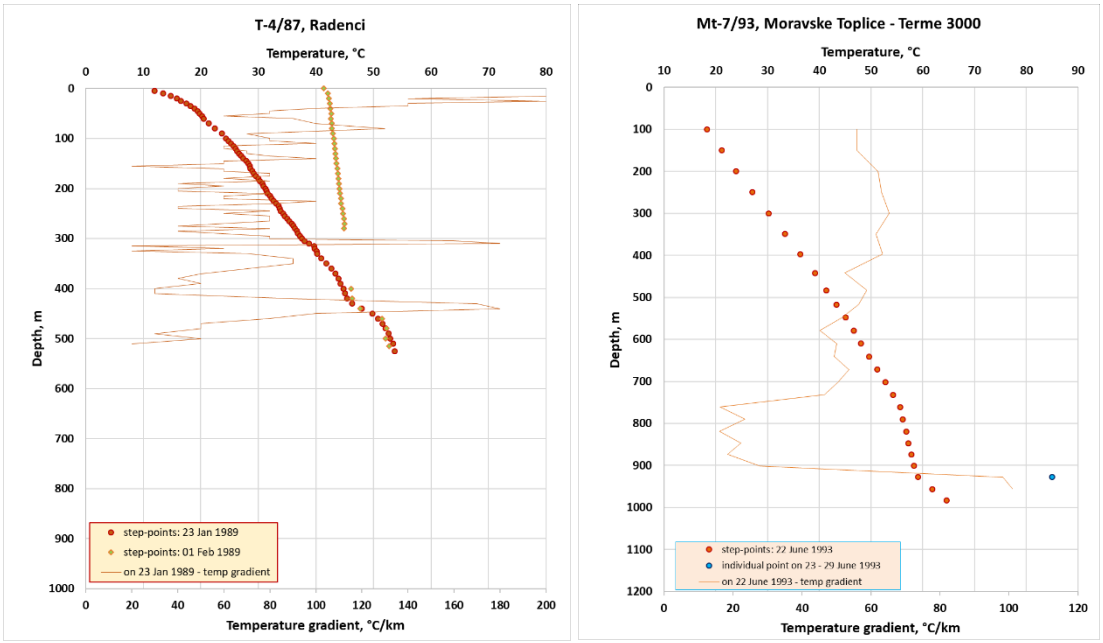

Figure 22: Thermograms of boreholes T-4/87 at Radenci (No. 39, left) and Mt-7/93 at Moravske Toplice (No. 128, right)

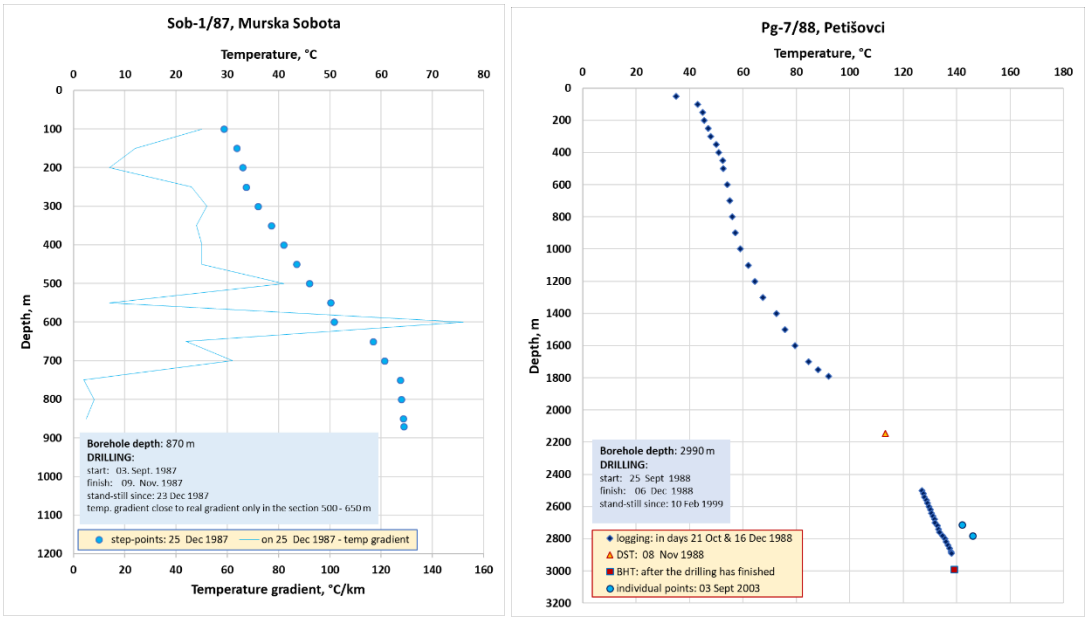

Figure 23: Thermograms of boreholes Sob-1/87 in Murska Sobota (No. 33, left) and Pg-7/88 at Petišovci (No. 51, right)

3.1.2.2 Determination of the convective HFD component in SE Slovenia

The Čatež geothermal field (Nosan, 1959; Ivanković & Nosan, 1973; Lapajne, 1975) is a typical example of a narrow (constrained) area where descending water penetrates deep into the Triassic-Jurassic basement carbonate rocks, is heated up and may return to the surface along faults at hot springs near the foot of the mountains (Andrews et al. 1982; Kilty et al. 1979). The pronounced positive surface HFD anomaly (Figure 18) may have several explanations. Griesser

and Rybach (1989) cited the following possible causes for a similar HFD anomaly in northern Switzerland: a) a strong local heat source in the Earth's mantle, b) cooling of shallow intrusions, c) high contrasts in petrophysical properties such as thermal conductivity and radiogenic heat production, d) rapid uplift and erosion of the territory, and e) rising deep groundwater.

After analysing all five causes, Rajver (2001) showed that the only remaining possibility in Čatež area is the existence of groundwater rising from greater depths. The main indicators of such groundwater circulation with a significant vertical component are: i) Natural thermal springs along the south and southwestern parts of the Krško basin, and ii) Generally decreasing geothermal gradient with depth, regardless of lithology and tectonics.

Typical T-z profile in the Čatež geothermal field shows very elevated temperature gradient in the Tertiary section with convection zone in the Mesozoic (carbonate) lithologic section (Figure 24). Very similar is the thermogram from the AFP-1 borehole at Dobova (Figure 12). This convection zone may extend down to a depth of at least 2 km if not 2.5 km.

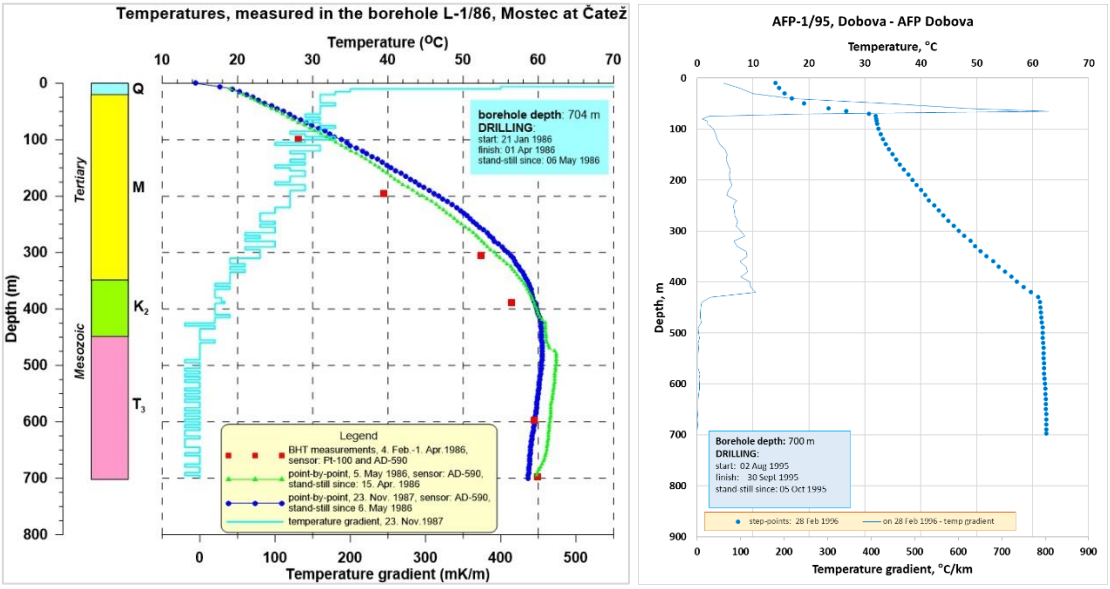

Figure 24: Thermograms of boreholes L-1/86 at Čatež (No. 15, left) and AFP-1/95 at Dobova (No. 211, right)

3.1.3 Numerical model of flow and heat transport to assess the effects of the Ljutomer Fault zone

A numerical hydrogeological and geothermal model was created to assess the possible permeabilities at the major, Ljutomer fault zone and its effects to the regional temperature field. The steady-state models were elaborated in the FEFLOW 7.3 software.

3.1.3.1 Conceptual model

We took simplified approach and modelled three main hydrogeological units of the system. The first, shallowest layer extends from the surface to the bottom of the delta plain of Mura Formation. It includes Quaternary sediments, Ptuj-Grad and Mura Formations, which represent

the regional and transboundary fresh and thermal groundwater aquifers. The middle layer expands from the top of Lendava Formation to the top of Pre-Neogene bedrock. It includes all Miocene sedimentary layers with Lendava, Haloze and Špilje formations, which represent local aquifers and may contain hydrocarbons. The bottommost layer represents basement rocks of various lithologies, of up to 6500 m asl depth, which usually do not contain significant geoenergy resources. As an additional structural feature, the Ljutomer fault zone was introduced into the model and it extends only within the Pre-Neogene, third layer (Figure 25).

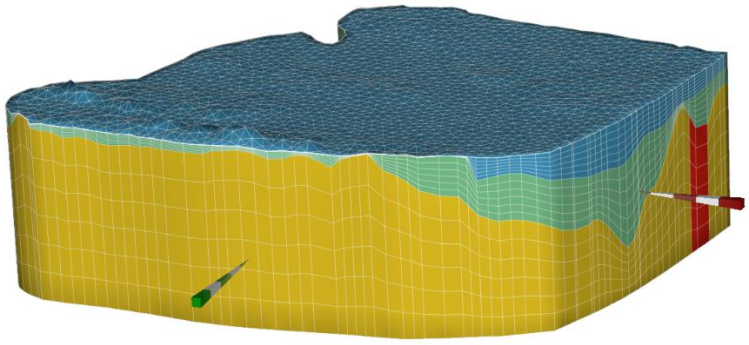

Figure 25: Geological (conceptual) model in the numerical model (Blue – Quaternary, Ptuj-Grad and Mura Formations; Green – Lendava, Špilje and Haloze Formations; Yellow – Pre-Neogene basement rocks; Red – Ljutomer fault zone).

3.1.3.2 Geometry and boundary conditions

Numerical model expands from the surface topography to 6500 m bsl depth. It covers an area of 115 x 85 km in EW and NS direction. It consists of 19 layers and 2017 nodes per slide (Figure 25 and Figure 26).

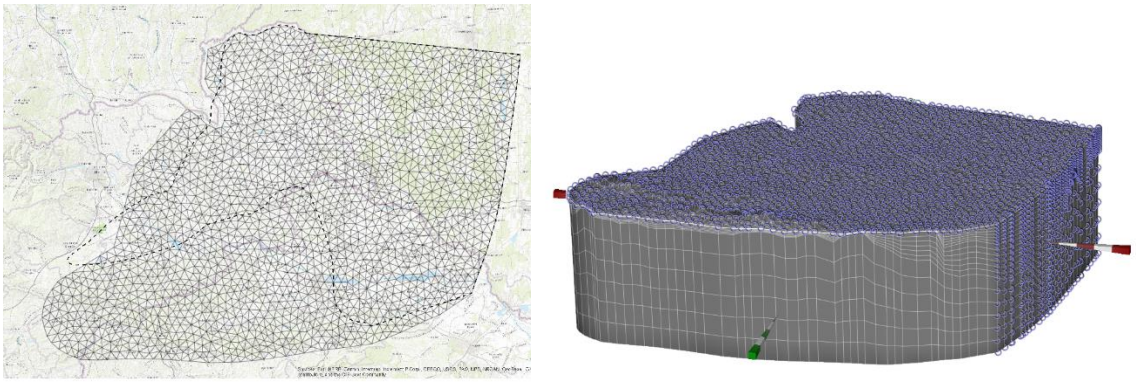

Figure 26: Expansion of the model and node density (left); Hydraulic head boundary condition (right)

Hydrological boundary conditions are set on top and E of the model. As the top boundary conditions the hydraulic heads from the T-JAM project model are assigned in Quaternary and surrounding hilly areas). On the east side constant head of 140 m is assigned as the regional flow mid-line is assumed here. In both cases, the 1st kind Dirichlet boundary condition is assigned (Figure 26).

Thermal boundary conditions for the thermal model are assigned as a constant temperature of 11 °C on top of the model and the heat flux on its bottom, from 32 mW/m^2 to 122 mW/m^2 (Figure 27).

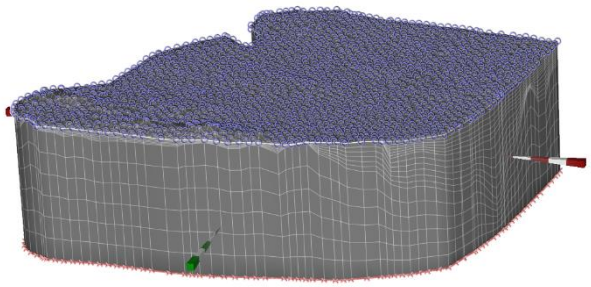

Figure 27: Thermal boundary conditions.

3.1.3.3 Calibration of the thermal model

We have used 23 boreholes with temperature logs from Slovenia for calibrating the thermal model. Depth of their last data varies from -359 m a. s. l. to -2317 m a. s. l. (Table 1) also the distribution in space varies (Figure 28).

Table 1: Borehole with last temperature log.

Borehole	Depth of last measurment (m a. s. l.)
Šom-1	-359
Dan-1	-394
Janezev-1	-555
Sob-2	-590
Mt-7	-797
Pt-74	-1034
Do-3	-1046
MS-3	-1052
Mt-2	-1152
Re-1g	-1301
Mo-2g	-1314
Mb- 3/91	-1334
P-2	-1364
Fi-3	-1370
Le-2g-3g	-1406
Mg-6	-1415
Do-1	-1610
Fi-14	-1673
Peč-3	-1767
Kor-1ga	-1810.2
Mt-6	-1814
Mot-1	-2118
DV-1	-2317

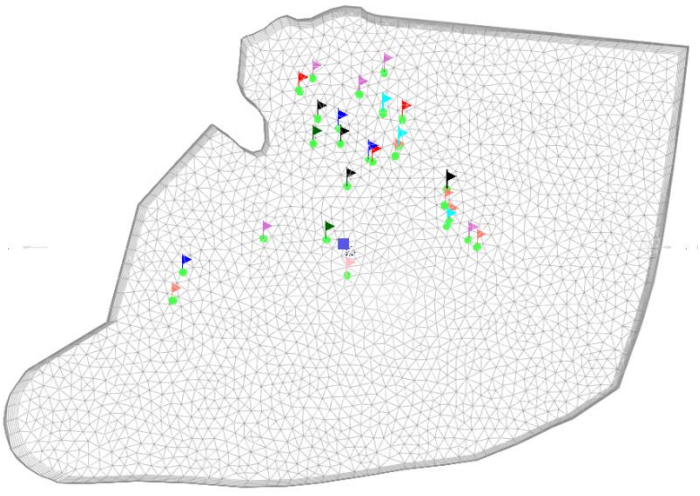

Figure 28: spatial distribution of boreholes with temperature logs.

3.1.3.4 Tested scenarios

Scenario 1 simulated anisotropy of hydraulic conductivity of Neogene basin filling (Kzz is 100-times smaller than Kxx=Kyy) and the basement rocks (Kzz is 10-times smaller than Kxx=Kyy). The Ljutomer Fault zone is isotropic (Kxx=Kyy=Kzz) (Figure 29). Kx, Ky and Kz values are homogeneous for each unit.

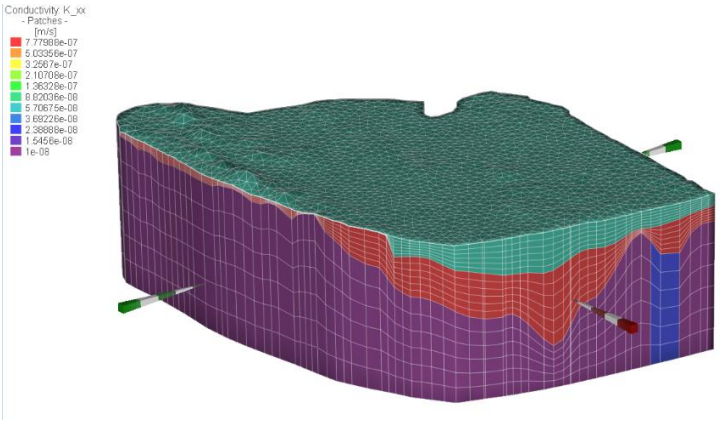

Figure 29: Hydraulic conductivities for Scenario 1.

Scenario 2 simulated anisotropy of hydraulic conductivity of Neogene basin filling and the basement rocks which is the same as in Scenario 1. However, the Ljutomer Fault zone is now anisotropic (Kzz is 100-times greater than Kxx=Kyy (Figure 30)). Kx, Ky and Kz values are homogeneous for each unit.

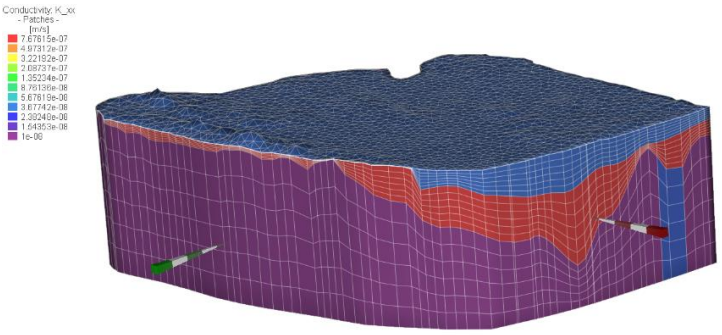

Figure 30: Hydraulic conductivities for Scenario 2.

Scenario 3 has simulated hydraulic conductivities the same as in Scenario 1, but now the Ljutomer Fault zone has the same values as the rest of the basement rocks. Kx, Ky and Kz values are homogeneous for each unit.

Scenario 4 simulated anisotropy of hydraulic and thermal conductivity of Neogene basin and Ljutomer fault zone using the pilot points. Kx, Ky and Kz values spatially vary in each unit based on pilot points (Figure 31).

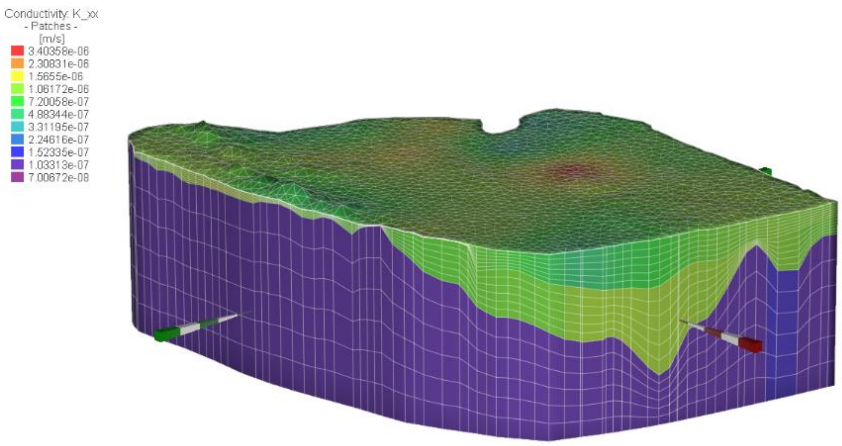

Figure 31: Hydraulic conductivity for Scenario 4.

3.1.3.5 Calibration with FePEST

Using FePEST, we calibrated Scenarios 1 – 3 and their hydraulic and thermal conductivities for the two Neogene layers, Ljutomer Fault zone and basement layer as homogeneous units.

Using FePEST in Scenario 4, we calibrated the hydraulic and thermal conductivities for the two Neogene layers and Ljutomer Fault zone as well but heterogeneously. For Neogene layers, we used 25 pilot points in each layer and for the Ljutomer Fault zone we used 13 pilot points. For thermal conductivity, we used 25 pilot points for Neogene layers in each layer. Pre-Neogene layer and the Ljutomer fault zone was calibrated to only one k_T value (Figure 32).

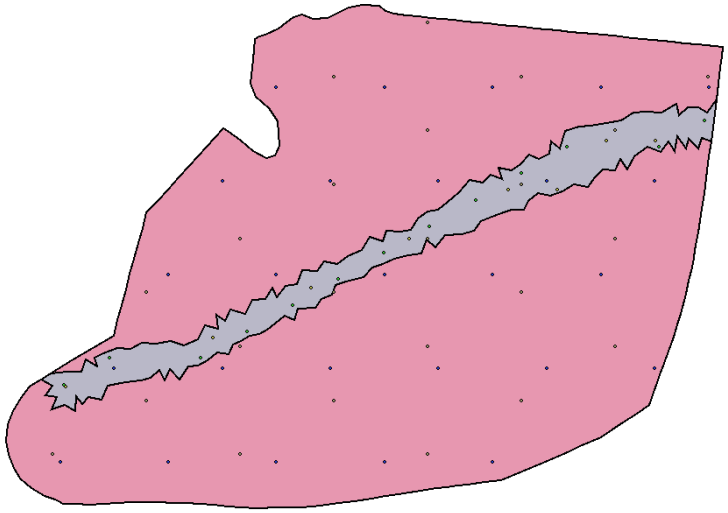

Figure 32: Pilot points that were used to calibrate the hydraulic and thermal conductivities

3.1.3.6 Results

3.1.3.6.1. Scenario 1

Temperature on the bottom of the Mura Fm. reaches up to 125 °C in the deepest parts (Figure 33). Temperatures at the top of the Pre-Neogene basement show similarities and up to 300 °C at 5 km (Figure 34). Observed vs. Modelled temperatures (Figure 35) show reasonable fit.

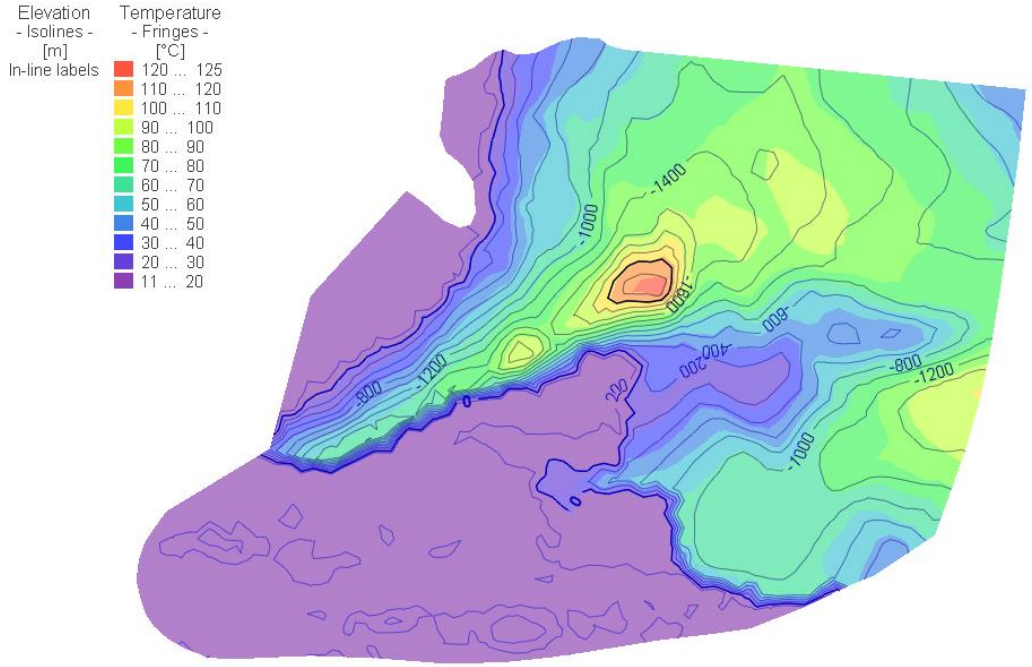

Figure 33: Temperature on the bottom of the regional geothermal aquifer Mura Formation (in coloured fringes) and elevation shown with isolines (m a. s. l.).

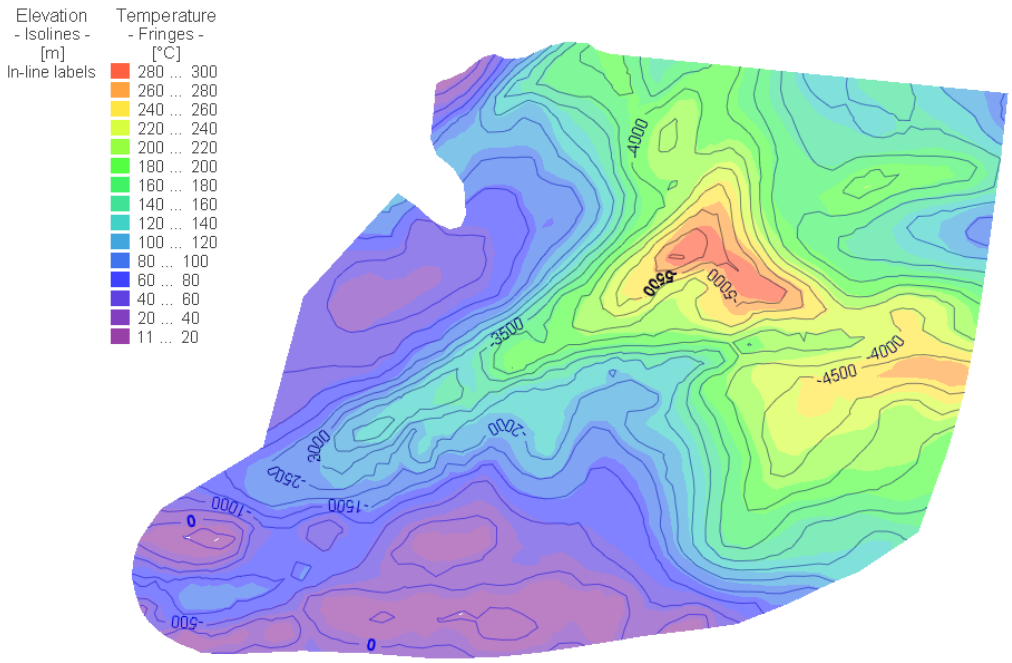

Figure 34: Temperature on the top of the Pre-Neogene (in coloured fringes) and elevation shown with isolines (m a. s. l.).

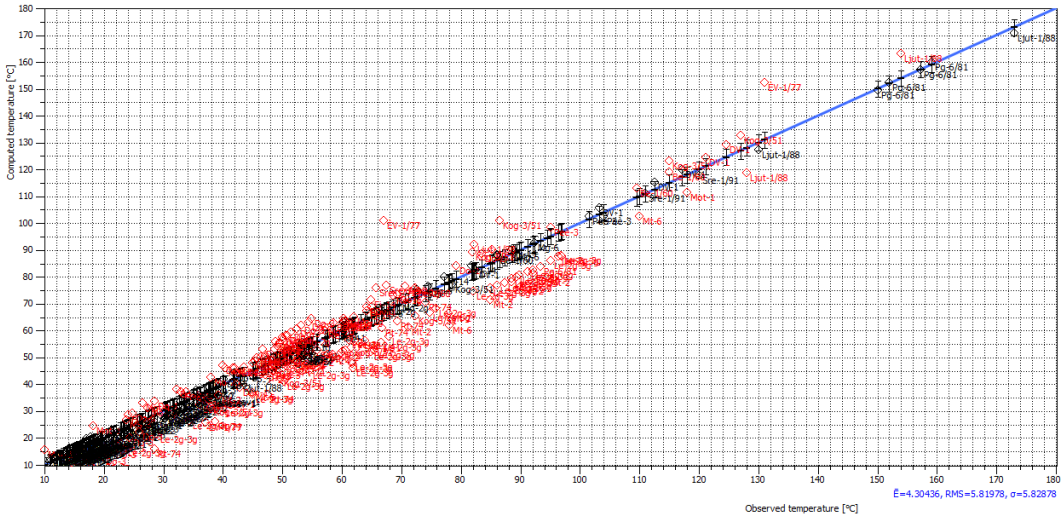

Figure 35: Scatter plot with observed and modelled temperatures with tolerance of 3 °C.

3.1.3.6.2. Scenario 2

Temperatures on the bottom of the Mura Formation (Figure 36) and the top of the Pre-Neogene rocks show very similar pattern as in Scenario 1 (Figure 37). Observed vs. Modelled temperatures do not show much difference from Scenario 1 (Figure 38).

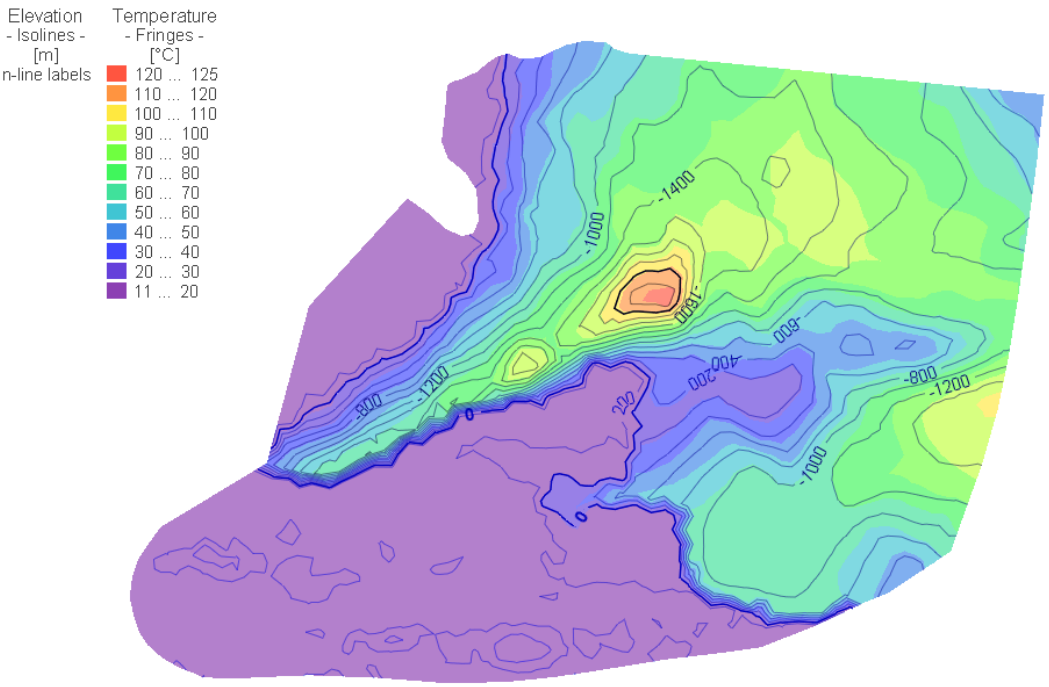

Figure 36: Temperature on the bottom of the Mura Formation (in coloured fringes) and elevation shown with isolines (m a. s. l.).

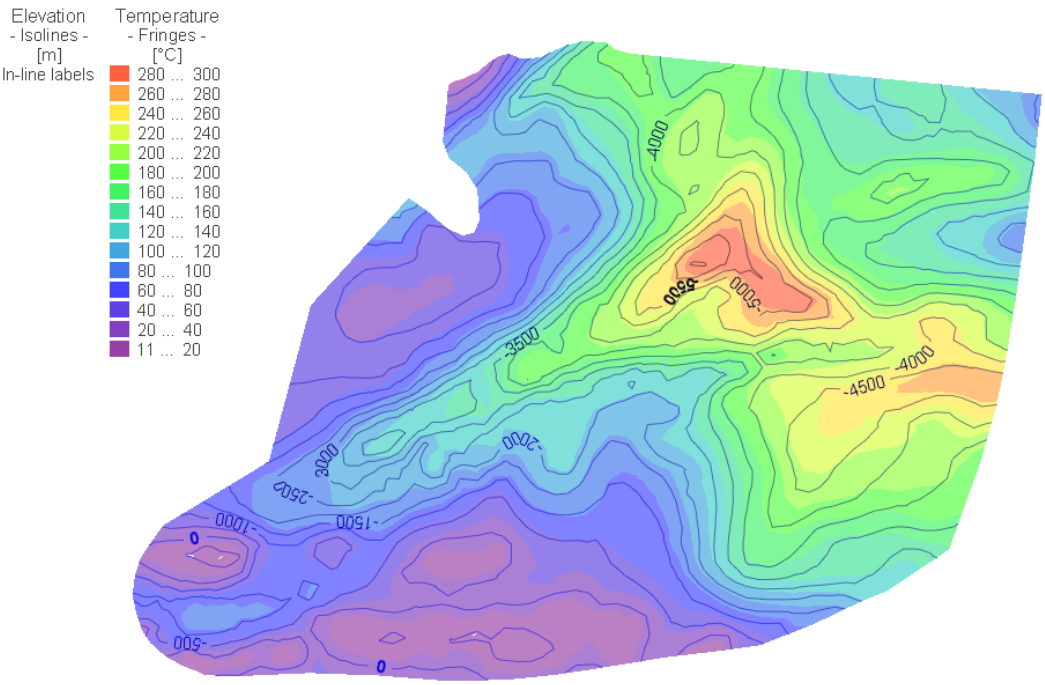

Figure 37: Temperature on the top of the Pre-Neogene (in coloured fringes) and elevation shown with isolines m (a. s. l.).

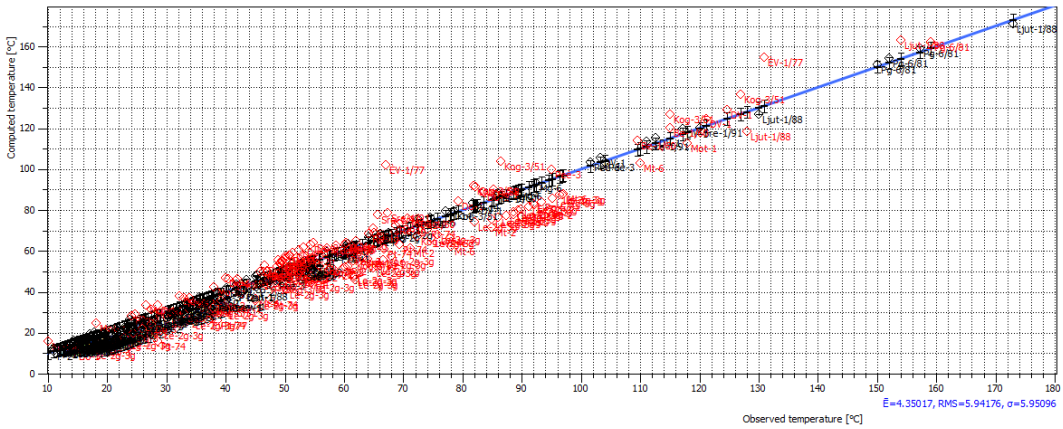

Figure 38: Scatter plot with observed and modelled temperatures with tolerance of 3 °C.

3.1.3.6.3. Scenario 3

As these results are very similar to Scenario 2, they are not presented here.

3.1.3.6.4. Scenario 4

Simulated temperatures (Figure 39, Figure 40) best fitted of all four scenarios (Figure 41). This is logical as most anisotropy and local adjustments could have been applied.

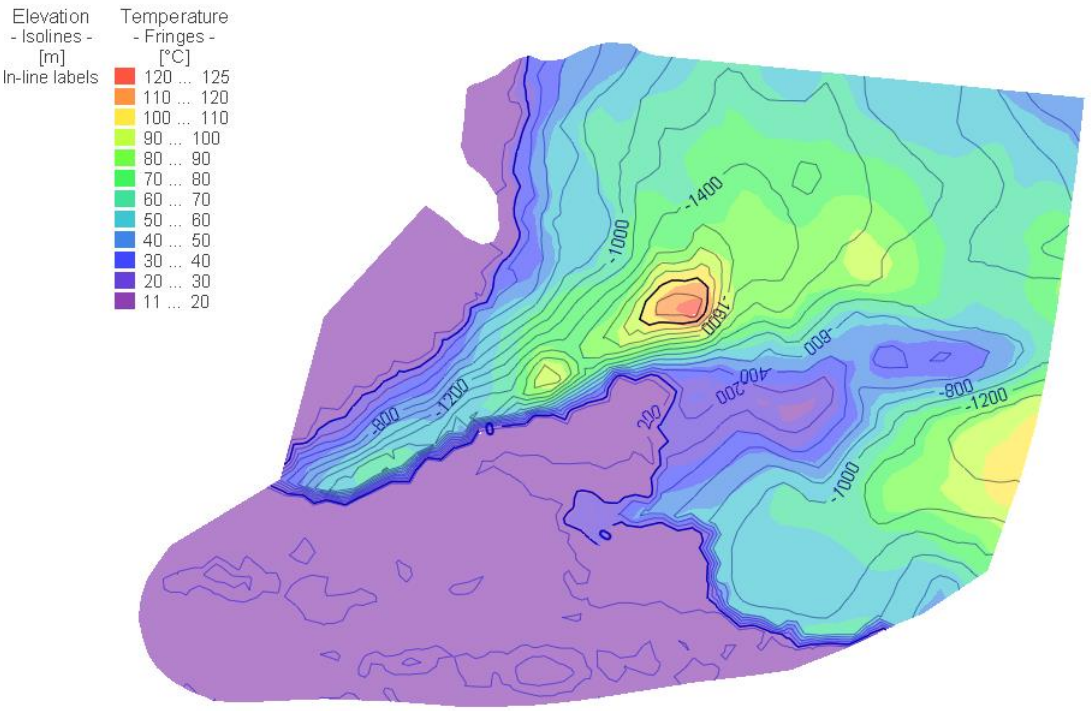

Figure 39: Temperature on the bottom of the Mura Formation (in coloured fringes) and elevation shown with isolines (m a. s. l.).

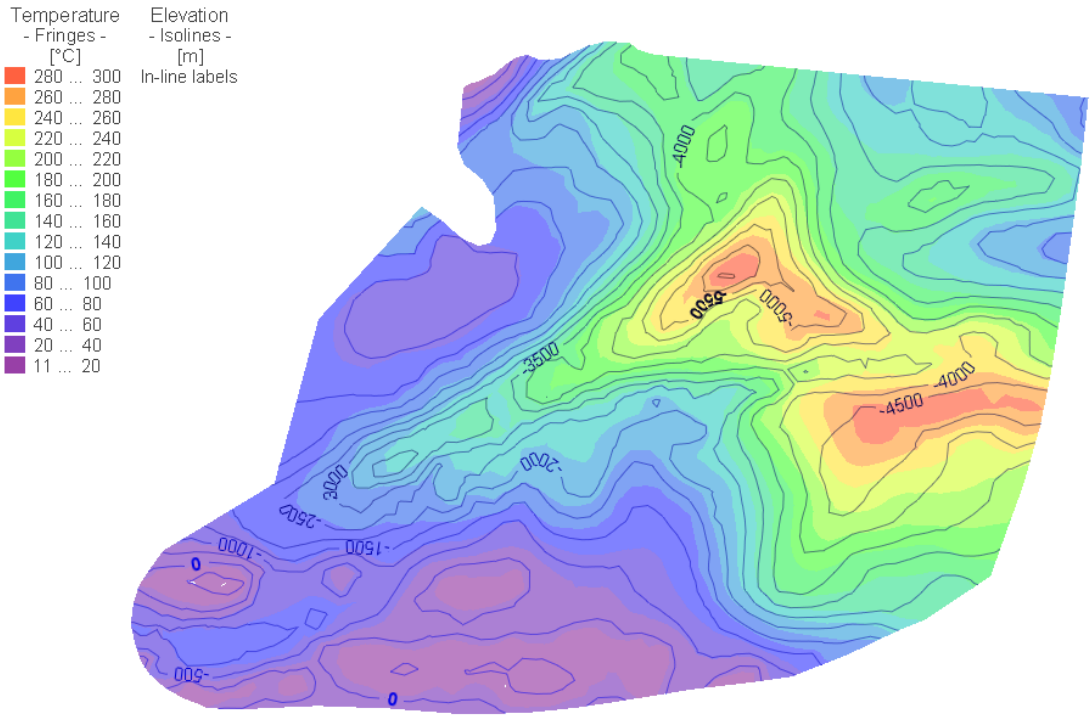

Figure 40: Temperature on the top of the Pre-Neogene (in coloured fringes) and elevation shown with isolines (m a. s. l.).

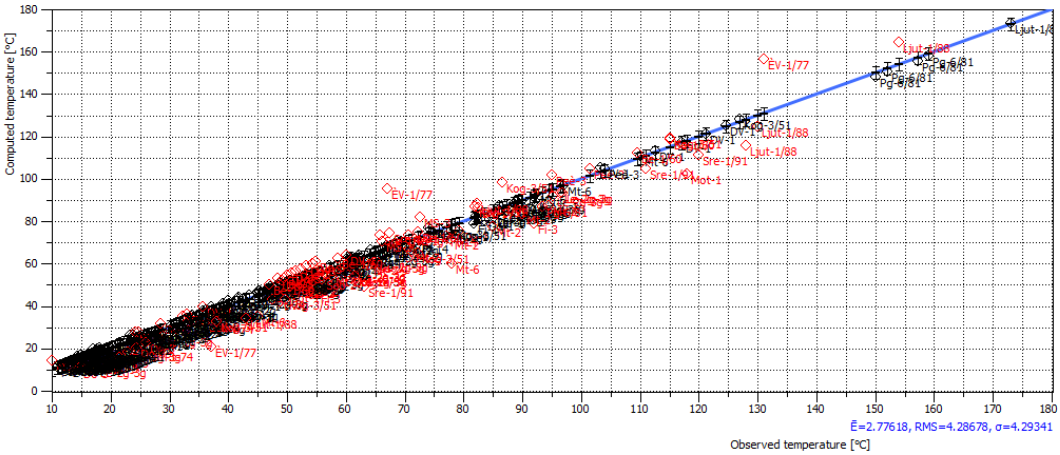

Figure 41: Scatter plot with observed and modelled temperatures with tolerance of 3 °C.

3.1.3.7 Differences between scenarios and interpreted effects of the Ljutomer Fault zone onto the temperature field

To observe the difference between the best fitted model (anisotropic Scenario 4) and others, we subtracted temperature values between Scenarios 1 and 2 (Figure 42) and them from Scenario 4 for bottom of Mura Formation (Figure 43, Figure 44) and top of the Pre-Neogene basement (Figure 45, Figure 46, Figure 47).

The following information should be accounted for when interpreting the results: i) Groundwater flow is in the general direction from Slovenia and Croatia to Hungary, so roughly W-E., ii) temperature distribution is also a result of topography of layers, so deeper parts are expected to be warmer, iii) the permeable Ljutomer Fault zone was simulated in basement rocks, so at deeper sub-basins this layer was rather thin, etc.

Scenarios 1 and 2 in the Mura Fm. differ for max. 7 degrees. The highest temperatures are given by Scenario 2, especially in the eastern boundary part of the model, where we did not used calibration data so the results should be used with caution – in Hungary and towards Croatia. There, the model is usable only for regional evaluation of the state and not for detailed analyses. Regarding this regional view, distribution of difference areas between scenarios is the same, so no huge difference in flow or thermal processes is expected. The coldest results are given by best fitted Scenario 4 but it is obvious that differences occur due to homogeneous layers (Sc. 1, 2) in the area where calibration data were available. The difference is both: inhomogeneous Sc.4 gives higher temperatures than homogenic Sc. 1 and 2 in Banovci, Lendava and Moravske Toplice while lower ones closer to Ptuj and Dobrovnik. In most calibrated part of the model – in Slovenia, the differences in scenarios are only a few degrees, which is almost negligible regarding the depth of layers and known heterogeneity of deltaic sediments. In Hungary, the difference can be up to 22 degrees Celsius.

We do not see a noticeable effect of the Ljutomer Fault zone on the temperature distribution at the bottom of the transboundary Mura Fm. geothermal aquifer but it is most dependent on its depth.

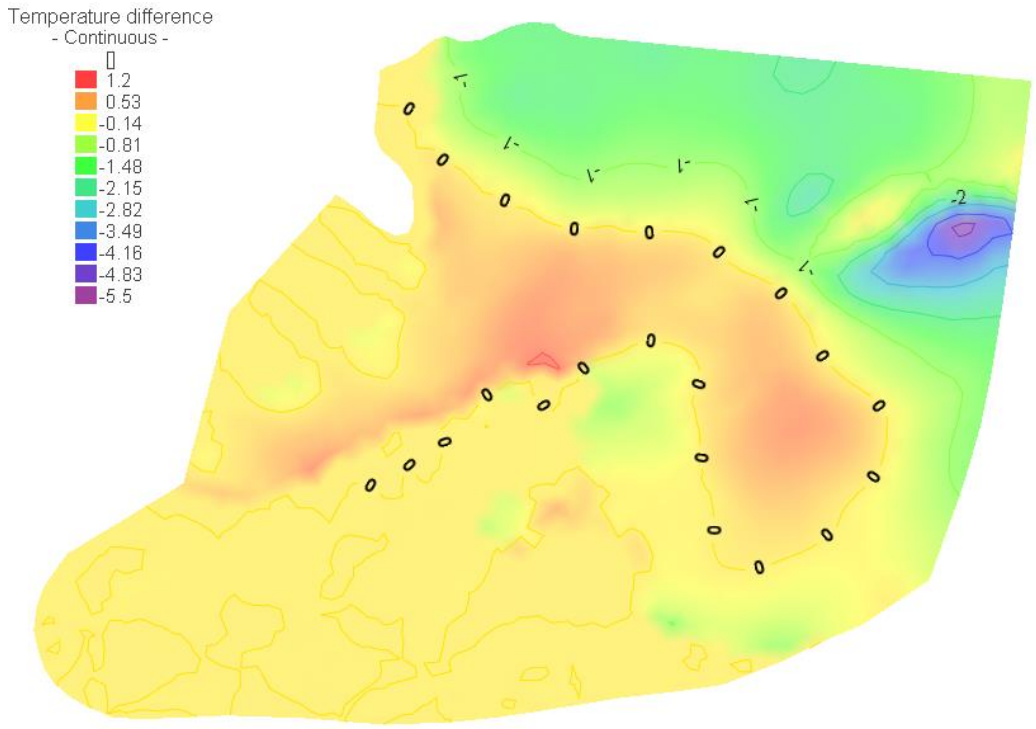

Figure 42: Temperature difference between Scenarios 1 and 2 at the bottom of the Mura Fm.

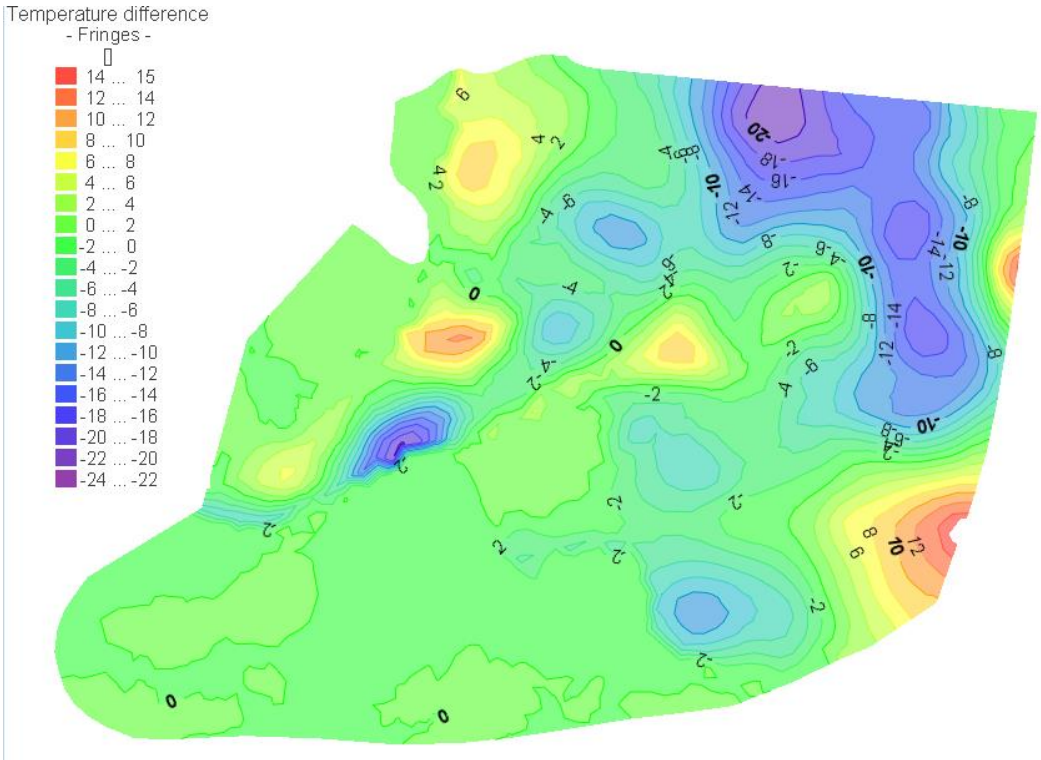

Figure 43: Temperature difference between Scenarios 4 and 1 for the bottom of Mura Fm.

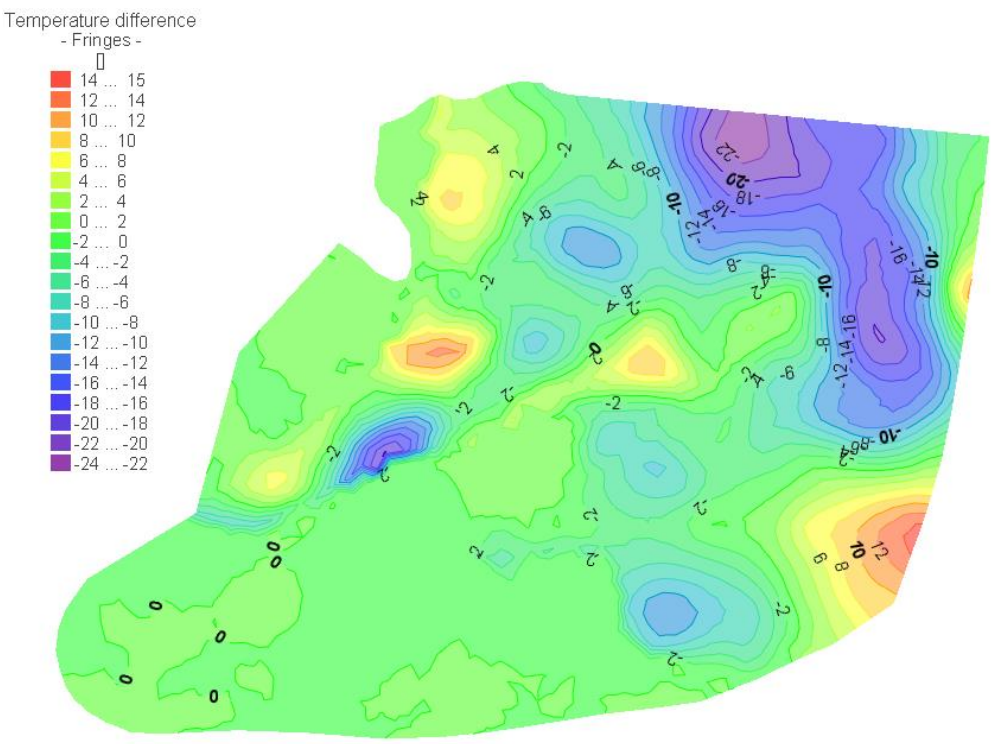

Figure 44:Temperature difference between Scenarios 4 and 1 at the bottom of the Mura Fm.

Regarding the temperatures at the top of Pre-Neogene basement rocks, differences in temperatures between scenarios are larger here than for previous Mura Fm (Figure 45, Figure 46, Figure 47). The difference between Scenarios 1 and 2 (Figure 45) clearly shows effects along the Ljutomer fault zone which in Scenario 2 has anisotropy with higher vertical permeability. This causes some convection zones, as hotter and colder differences are close-by. At their shallowest part in Croatia, where we had no calibration data, the models differ the least, for few degrees only and where Scenario 4 is the coldest. Scenario 4 is also much colder in NE part of the model, in Hungary, in comparison to others, as differences are now up to 30 degrees. This is a higher difference than simulated in shallower Neogene layers.

It is evident that at the elevated Murska Sobota extensional block in NW part of the model, in Slovenia, the Scenario 4 gives regionally higher temperatures than the homogeneous models. What we also noticed is that a big difference occurs in SE part of the model, where Scenario 4 showed locally almost 50 degrees more than the other ones. This does not occur in the Ljutomer Fault zone area but in the southernmost deepest part of the Basin.

Along the Ljutomer fault zone, Scenario 4 gave mostly lower temperature values than the other homogeneous layers, especially at its most north-eastern part. In general it ''divides'' NW and SW positioned areas where Scenario 4 gave higher values than other models (Figure 46, Figure 47).

From the simulated temperatures (Figure 34, Figure 37, Figure 40) we may interpret the effect of the Ljutomer fault zone in Slovenia as such:.

Temperature distribution at top of basement mostly follows the topography (basin deepening). But, as this is a recharge zone for deep layers in Slovenia, we see that at the SW part od the model, for example near Ptuj, the temperature fringes in the Ljutomer fault zone are narrower than expected by topography. This means that cold water, which infiltrates within the shallower parts of the Ljutomer fault zone, moves along the regional flow path faster in the fault zone and, therefore, locally cools down the west part of the model. On the opposite side, the heated outflow plume is evident in NE part of the model, in Hungary, in all scenarios.

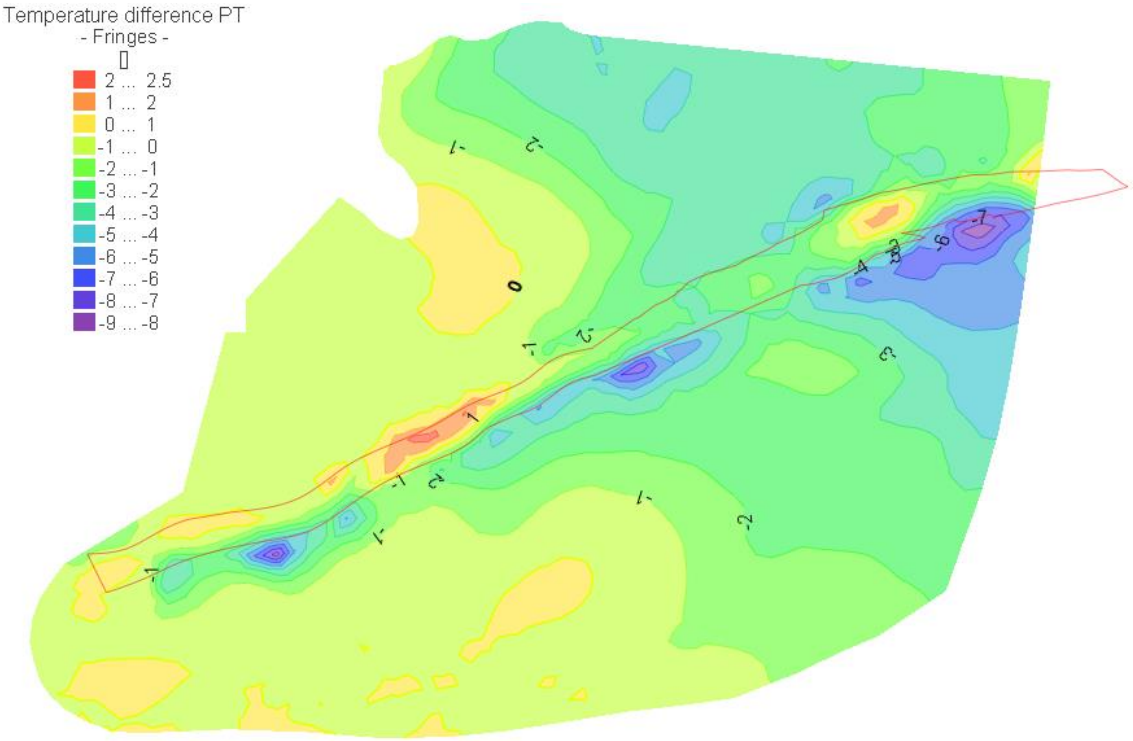

Figure 45: Temperature difference between Scenarios 1 and 2 at the top of Pre-Neogene basement

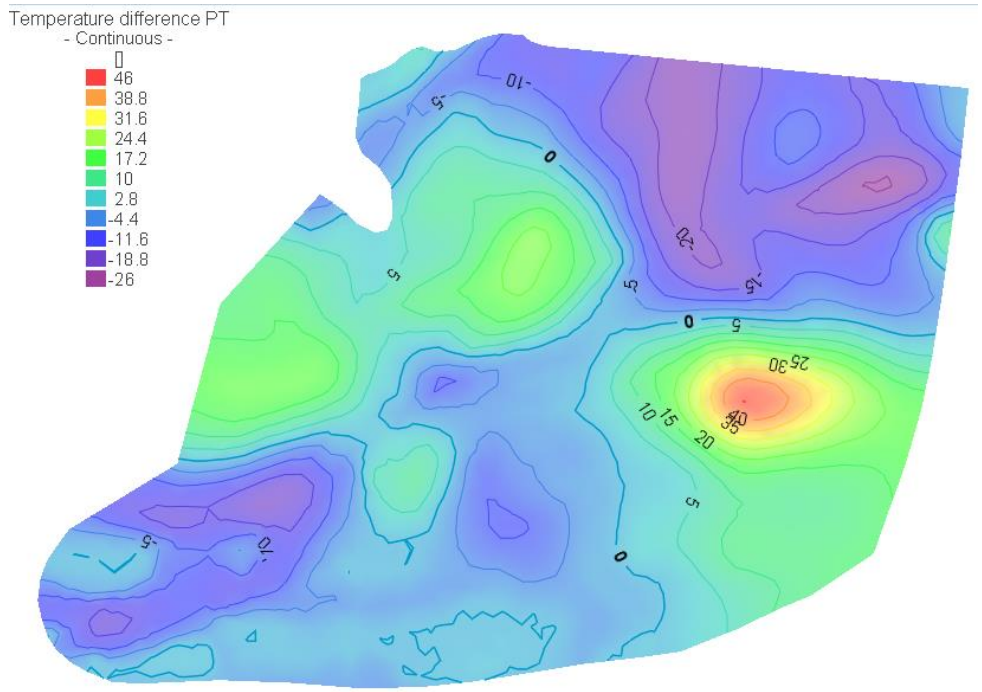

Figure 46: Temperature difference between Scenarios 4 and 1 at the top of Pre-Neogene basement

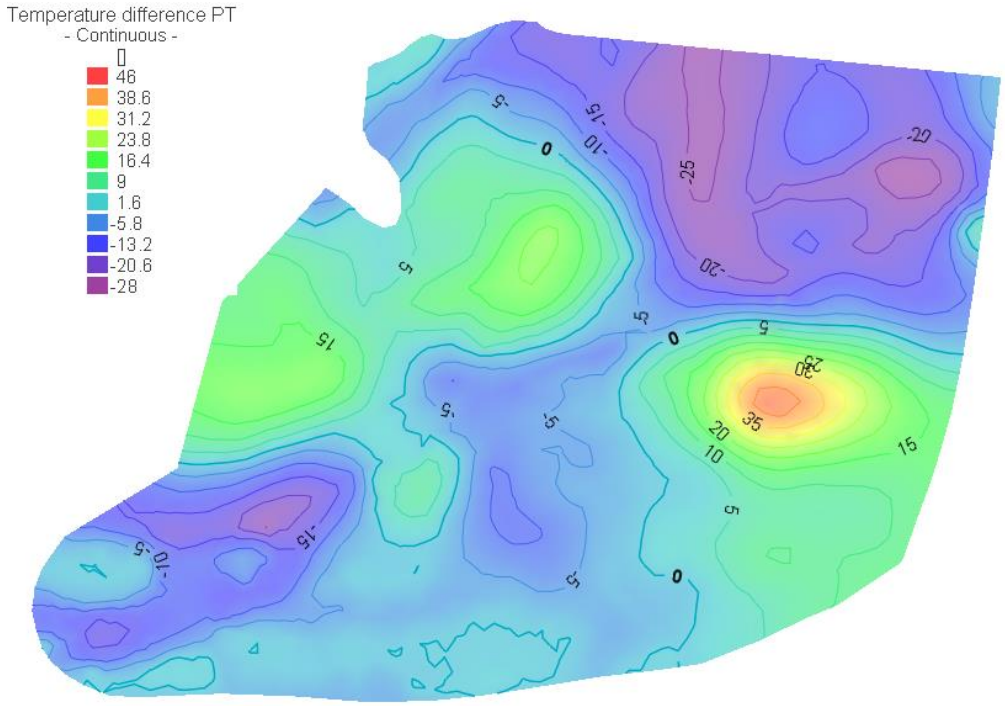

Figure 47: Temperature difference between Scenarios 4 and 2 at the top of Pre-Neogene basement

Therefore, it is inferred that some convection cells evolve in the Pre-Neogene basement rocks. They affect temperatures in the basement (Figure 50), however, they do not noticeably effect

on the temperature distribution in the shallower layers, the regional and transboundary geothermal aquifer in the Neogene Mura Fm. Where very conductive, horizontal temperature distribution is simulated. The Scenarios 2 and 4 give slightly different prognosis, the best fitted Scenario 4 implies heat sweeping in the Ljutomer Fault zone, and its transfer to more southern areas.

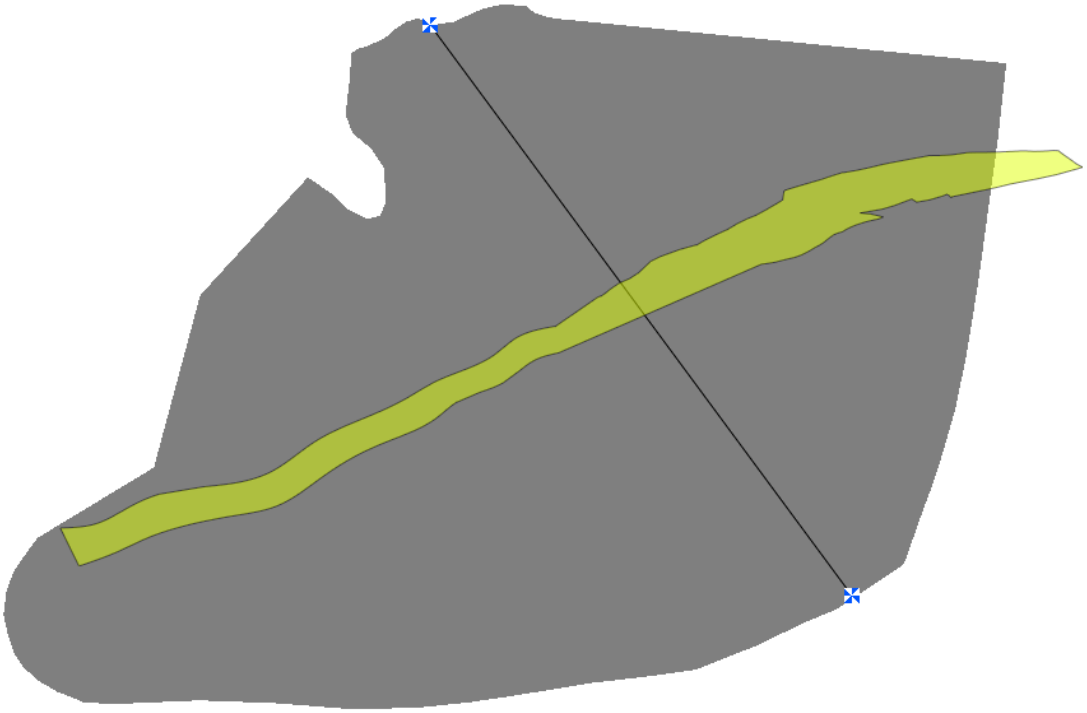

Figure 48: Flow and temperature cross-section line in NW-SE direction (black line), crossing the two sub-basins and the Ljutomer Fault zone (yellow)

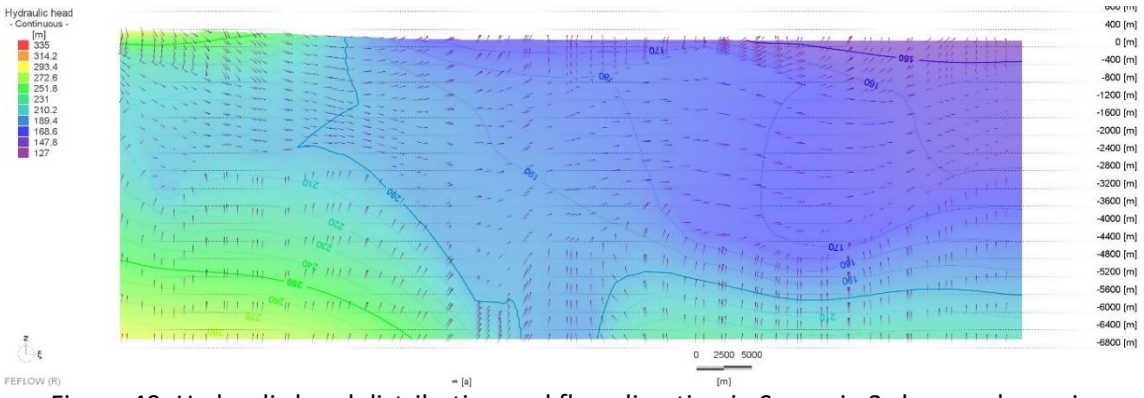

Figure 49: Hydraulic head distribution and flow direction in Scenario 2 show recharge in Goričko area and outflow in flatlands and southern parts. Lower heads occur in the Ljutomer fault zone.

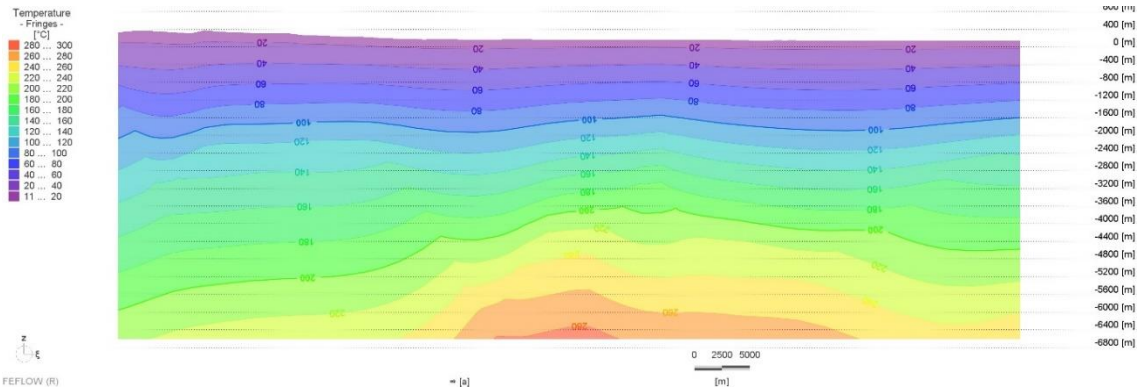

Figure 50: Temperature cross-section from Goričko to Croatia in Scenario 2 shows heat upwelling in the Ljutomer fault zone.

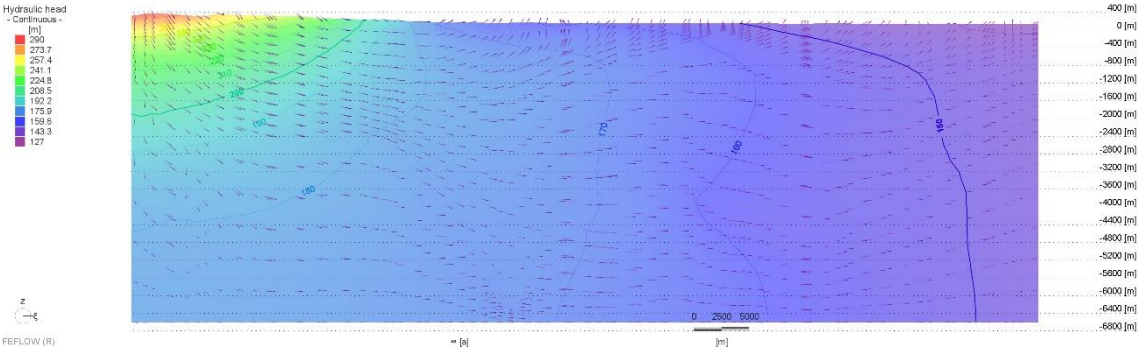

Figure 51: Hydraulic head distribution and flow direction in best fitted Scenario 4 show different heads than in Scenario 2. In Sc. 4, the flow in basement in the central part of the model is more horizontal – it represents the intermittent point of regional flow lines. The same is that recharge is in Goričko Hills area and outflow in flatlands on the southern parts. Heads are the same (very little vertical gradient) in the Ljutomer fault zone.

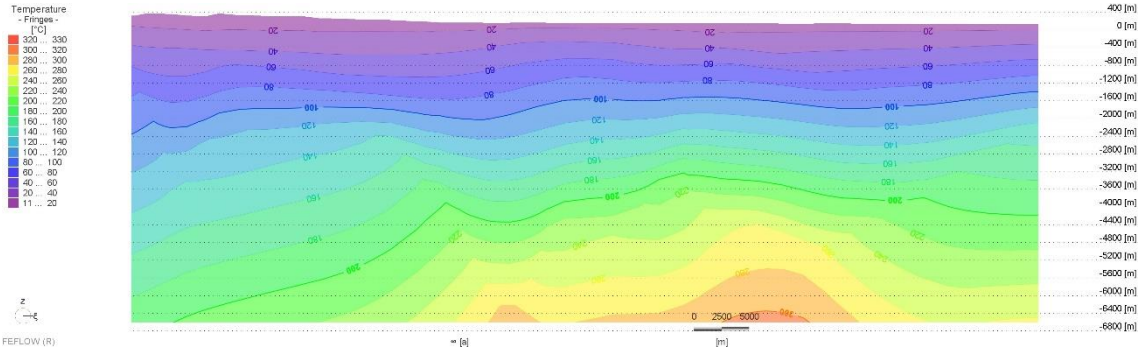

Figure 52: Temperature cross-section from Goričko to Croatia in best fitted Scenario 4 shows less heat upwelling in the Ljutomer fault zone but rather larger area of heat upwelling south of the Ljutomer fault zone.

3.2 Groundwater

We collected data on mineral and thermal waters as geomanifestations from national databases and projects T-JAM, TRANSENERGY, DARLINGe and HOOVER. Below, we listed definitions as they

differ among the countries and altogether 53 identified water geomanifestations (Table 2). Most (36) items are reported in Slovenia, 11 in Hungary and 6 in Croatia. Most abundant are thermal waters (22), followed by thermomineral waters (17) and then there are 6 mineral and 8 natural mineral waters reported. The latter only in Slovenia. It is also worth noticing that in Slovenia we did not list individual geothermal or mineral water springs and wells but we have selected only one point per a location instead, due to a regional scale of the investigation.

Table 2: List of geomanifestations linked to waters

Country and type of geomanifestation	No.
Croatia	**6**
thermal water	5
thermomineral_water	1
Hungary	**11**
mineral water	1
thermal water	10
Slovenia	**36**
mineral water	5
natural mineral water	8
thermal water	7
thermomineral_water	16
SUM	**53**

3.2.1 Mineral water

Mineral water in **Slovenia** is defined in the Water Act (Official Gazzette of Rep. Of Slovenia No. 67/02, 2/04 – ZZdrI-A, 41/04 – ZVO-1, 57/08, 57/12, 100/13, 40/14, 56/15). Row 5. of the article 7 defines the mineral water as a groundwater which fulfils the written criteria, and originates from a well, a spring or a capture. The issue is that the criteria are NOT listed anywhere. In practice, we use the term mineral water for mineralized waters containing more than 1 g/l of total dissolved solids, or enriched in free gases (>250 mg/l free CO_2), e.g. CO2, H2S,.. or some other component, e.g. iron. Beside this classification, we also use the natural mineral water approach, but for bottled waters only, which is defined in the Rules on natural mineral water, spring water and table water (Official Gazette of Rep. Of Slovenia No. 50/04, 75/05 in 45/08 – ZKme-1). Article 4 defines it as water which beside microbiological requirements from the 5th article also: has a source in a subsurface water source (is groundwater), protected from any possibility of contamination, and springs or is pumped at a spring from one or more natural outflows or wells; has properties which clearly distinguish it from drinking water and may be connected to content of dissolved solids, trace elements or other ingredients, and may have certain nutritional and physiological effects; has the same purity as at the source… and the deviation from the mean annual measured values for the main constituents specific to the individual natural mineral water, may not exceed ± 20%.

Natural mineral water rules apply in **Hungary** since 2004. Annex 2 to Regulation 65/2004. (IV. 27.) FVM-ESzCsM-GKM joint decree determines the characteristic properties of natural mineral water a) which have a beneficial effect on health, 1) geological and hydrogeological, 2) physical, chemical and physico-chemical, 3) microbiological, 4) if necessary, on the basis of

pharmacological, physiological and clinical considerations. (b) Annex II, Part II. according to the criteria listed in (c) be determined by scientific methods approved by the competent authorities. The tests provided for in point (a) (4) need not be carried out if the water has the characteristics on the basis of which it was recognized as a natural mineral water before the entry into force of this Regulation. This is particularly the case where the water in question contains at least 1000 mg of total dissolved solids or at least 250 mg of free carbon dioxide per kilogram, both at the point of abstraction and after bottling. 2. The composition, temperature and other essential characteristics of natural mineral water must be constant within the limits of natural fluctuations and must not be affected by any changes in the flow rate. The number of non-pathogenic living colonies of natural mineral water according to Section 5 (1) means the total number of colonies within acceptable limits, which has been tested at the water abstraction site and prior to any treatment and whose quality and quantity determined during water recognition are regularly checked. Annex 5 to Regulation 65/2004. (IV. 27.) FVM-ESzCsM-GKM joint decree claims and their conditions for natural mineral water. The mineral water / thermal water sorting for the project is based on a public database. www.vizeink.hu.

Traditional 'mineral water' in **Croatia** as mineralized water, enriched in free gases or some other component does not exist in Croatian legislation but is often used in professional papers. Natural mineral water is defined in the Guideline on natural mineral, natural spring and table waters (Official Gazette of Rep. of Croatia 85/19): 1) Natural mineral water is water that meets the microbiological criteria prescribed in Articles 13, 14 and 15 of this Guideline, originates from aquifers, and it is captured and filled from springs. (2) Natural mineral water differs from water for human consumption: a) by their natural properties which characterize the content and quantity of certain mineral substances, trace elements or other substances and, as the case may be, certain physiological effects, and b) by its original purity whereby both properties are preserved due to the underground origin of natural mineral water which is protected from all risks of pollution. (3) The properties referred to in paragraph 2 of this Article, which may give natural mineral water properties suitable for health, must be assessed: a) from the following points of view: 1. hydrogeological, 2. physical, chemical and physico-chemical, 3. microbiological and 4. as appropriate, pharmacological, physiological and clinical. b) in accordance with the requirements and criteria set out in Annex 1 to this Guideline, and c) in accordance with scientific methods approved by the competent authority. (4) The tests referred to in paragraph 3 (a) (4) of this Article shall not be compulsory if the water has such properties as regards its composition for which it was considered a natural mineral water in the Member State of origin before 17 July 1980. This is especially true when such water contains at least 1000 mg/kg of total dissolved solids or 250 mg/kg of free carbon dioxide both at the source and after filling into the packaging, ie on the market. (5) The composition, temperature and other essential properties of natural mineral water must remain stable within the limits of natural fluctuation, and they must not be affected by possible oscillations in the yield or water flow.

3.2.2 Thermal water

Thermal water in **Slovenia** is defined in the Water Act (Official Gazette of Rep. Of Slovenia No. 67/02, 2/04 – ZZdrI-A, 41/04 – ZVO-1, 57/08, 57/12, 100/13, 40/14, 56/15). Row 6. of the article 7 defines it as a groundwater from a well, spring or a capture which is heated in geothermal processes in Earth's crust and has the temperature at the spring or wellhead at least of 20 °C. Thermomineral water is defined in the Water Act (Official Gazette of Rep. Of Slovenia No. 67/02,

2/04 – ZZdrI-A, 41/04 – ZVO-1, 57/08, 57/12, 100/13, 40/14, 56/15). Row 7. of the article 7 defines it as the thermal water with properties of mineral water.

Thermal water in **Hungary** is defined in Annex 1 to the 1995 LVII. Law as being all groundwater (from the aquifer) with an outflow temperature (measured at the surface) of 30 ° C or higher. However, to show geomanifestations in the Mura-Zala basin we will show wells which are capable of producing water with temperature at and above 20 °C as this data was compiled within the TRANSENERGY project.

Thermal water in **Croatia** is recognized as groundwater with outflow temperature at above average annual air temperature of the spring or well recharge area (only scientific definition exists).

3.2.2.1 Chemical and isotopic composition of investigated waters and mofettes

We gathered recent analyses of waters and mofettes which had available information on chemical and isotopic composition, plus the noble gases (Appendix 1, metadata in Table 3).

Table 3: List of available analyses. We used following classification: mineral waters have EC above 1000 µS/cm, thermal waters temperature >20 °C, thermomineral waters both characteristics, and mofettes are classified as explained in this report. If several analyses were available for each object, they are counted for as one.

Country	No. of objects	No. of mineral waters	No. of mofettes	No. of thermal waters	No. of thermomineral waters	No. of chemical analyses	No. of stable isotope analyses	No. of noble gas analyses
Croatia	**6**	0	0	3	3	6	4	1
Hungary	**6**	0	0	2	6	6	6	4
Slovenia	**33**	13	4	4	12	29	24	19
SUM	**45**	**13**	**4**	**9**	**21**	**41**	**34**	**24**

Based on main ions, the prevalent water type is Na-HCO_3 occurring mainly in Neogene clastic aquifers and the second one Ca-Mg-HCO_3 in both, the Neogene as well as the dolomites. As Hungarian samples tap waters from Neogene stratified layers in the basin centre, the Na-HCO_3 type indicates evolved cation exchange (Figure 53). In Croatia and Slovenia also basement and carbonate rocks at the outskirts of the basin are producing water, therefore, this composition is much more diverse (Figure 53, Figure 54). Types with addition of sulphate or chloride are rarer (Table 5, Figure 55) but locally predominant. Sulphate either origins from dissolution of evaporites or oxidation of pyrite mainly while chloride ions in water from Neogene layers are linked to hydrocarbon accumulations.

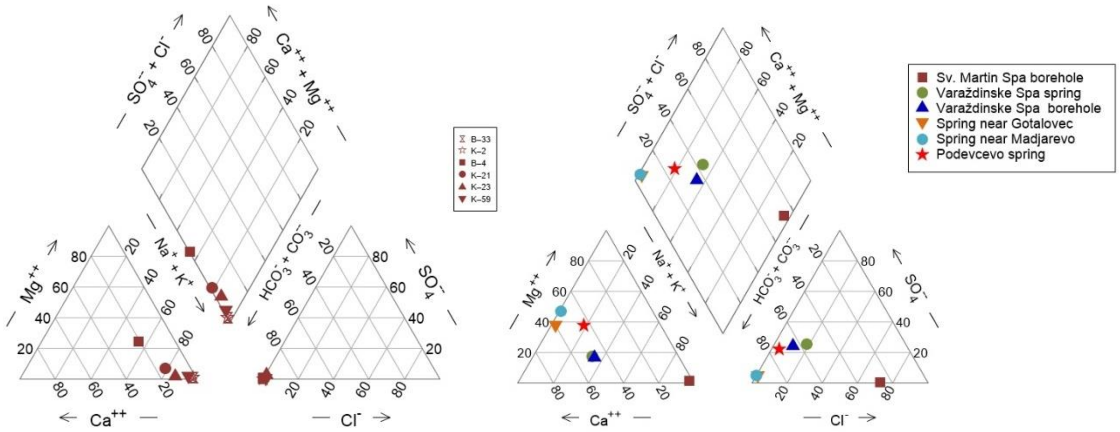

Figure 53: Piper plot of Hungarian (left) and Croatian (right) samples

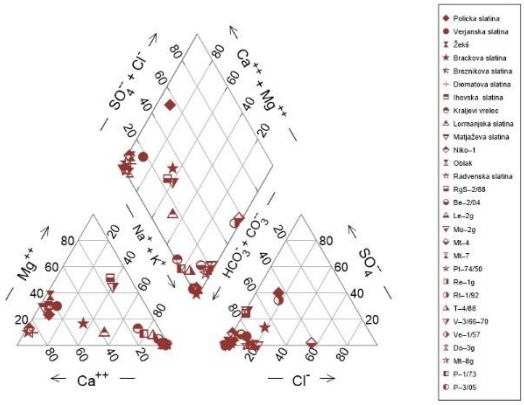

Figure 54: Piper plot of Slovenian samples

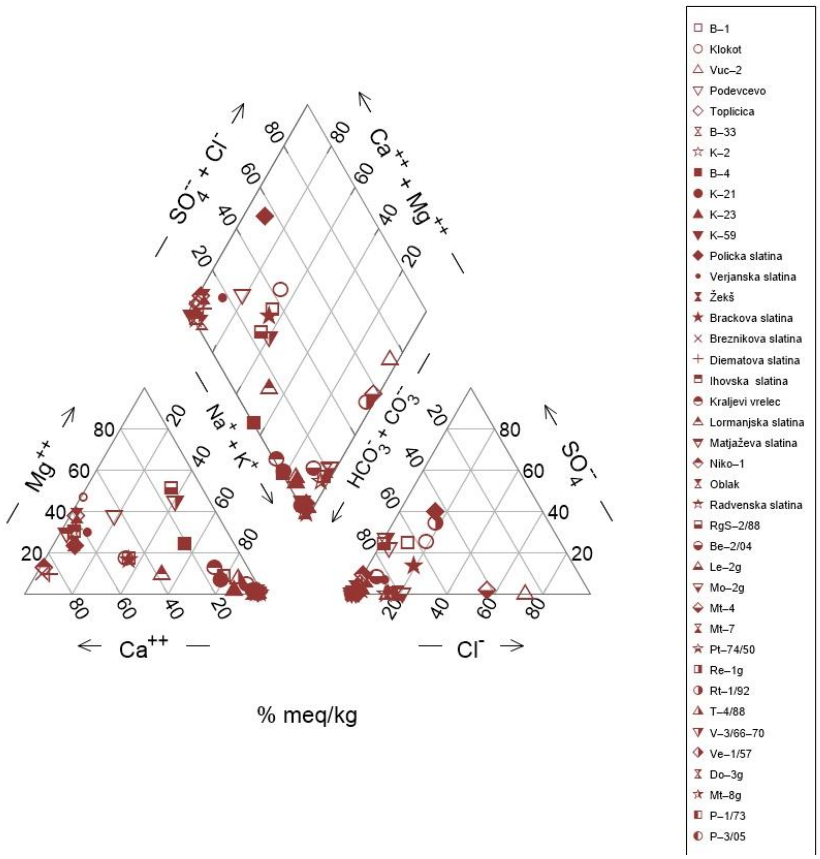

Figure 55: Piper plot of samples from all three countries

Table 4: Basic statistics of main ions by aquifers and deuterium excess

Parameter	**EC (uS/cm)**			**Na+ (mg/l)**			**Ca2+ (mg/l)**			**Mg2+ (mg/l)**			**HCO3- (mg/l)**			**SO42- (mg/l)**			**Cl- (mg/l)**			***d*-excess**		
Aquifer type	Min	Max	Aver	Min	Max	Aver	Min	Max	Aver	Min	Max	Aver	Min	Max	Aver	Min	Max	Aver	Min	Max	Aver	Min	Max	Aver
Neogene clastic rocks	70	16880	2674	0,7	4270	468	4,2	499	115	0,6	129	29	6,1	7870	1346	0,2	168	24	0,3	3880	284	-3,3	25,0	10,4
Oligocene andesitic tuff	10280	11080	10700	1470	1530	1500	461	480	471	894,0	1120	1007	7810	8300	8055	2120,0	2240	2180	68,0	99	84	20,0	21,8	20,9
Paleozoic metamorphic rocks	1384	8000	5488	31,8	1750	891	80,2	219	150	47,8	50	49	988	4660	2824	22,2	344	183	0,2	207	104	10,7	11,2	11,0
Triassic cl. and volcanoclastics	5730	5730	5730	1600	1600	1600	29,0	29	29	10,0	10	10	1949	1949	1949	1100,0	1100	1100	430,0	430	430	12,5	12,5	12,5
Triassic dolomite	437	1176	801	1,5	98	40	56,6	127	87	23,7	36	29	338	510	405	13,8	156	83	1,3	87	31	10,1	11,7	10,8
All analyses	**70**	**16880**	**3345**	**0,7**	**4270**	**512**	**4,2**	**499**	**128**	**0,6**	**1120**	**75**	**6,1**	**8300**	**1631**	**0,2**	**2240**	**167**	**0,2**	**3880**	**236**	**-3,3**	**25,0**	**11,1**

Table 5: Water types by aquifers. Above 20 meq% was taken as a threshold value.

Aquifer type	Ca-HCO3	Ca-Mg-HCO3	Ca-Mg-HCO3-SO4	Ca-Na-HCO3	Ca-Na-HCO3-SO4	Na-Ca-HCO3	Na-HCO3	Na-HCO3-SO4	Na-Cl-HCO3	Na-Mg-Ca-HCO3	Mg-Na-HCO3-SO4
Neogene clastic rocks	3	6	1	1		2	16		3	1	
Oligocene andesitic tuff											2
Paleozoic metamorphic rocks		1					1				
Triassic clastics and volcanoclastics								1			
Triassic dolomite		2			3						
All analyses	**3**	**9**	**1**	**1**	**3**	**2**	**17**	**1**	**3**	**1**	**2**

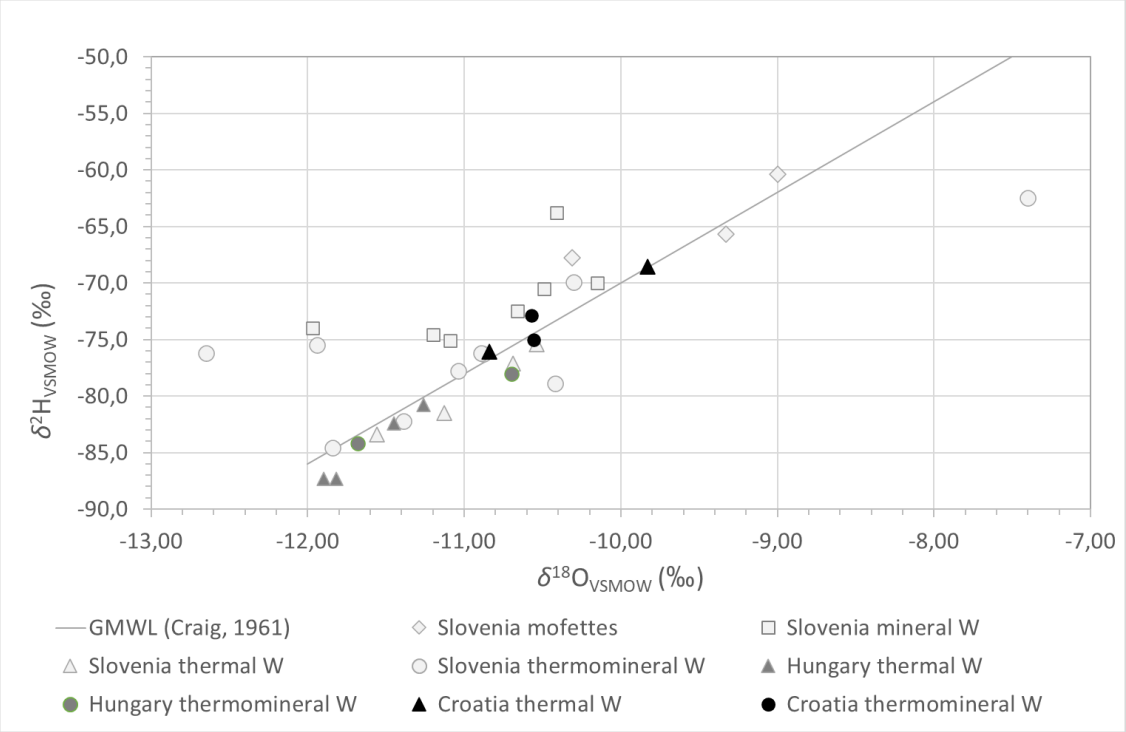

Figure 56: Stable isotope plot of oxygen and deuterium in investigated waters

Isotopic composition of waters is diverse. Stable isotopes of waters show large range of values: $\delta^{18}O$ is between -12.65 and -7.50 ‰ and deuterium between -87.3 and -60.4 ‰ (Figure 56). It is evident that most waters origin from precipitation, however, in Slovenian waters other processes are also evident. Large oxygen shift towards lighter isotopes is measured for mineral and thermomineral waters in Radenci and Rogaška Slatina area in Slovenia and attributed to CO_2 exhalation. Trček & Leis (2017) already reported it for the latter site while in Radenci we made new analyses showing this. On the opposite, two Slovenian waters show oxygen enrichment which is attributed to presence of hydrocarbons in the aquifer. This was noticed already by Pezdič et al. (1995) and even waters today still exhibit such strong mixing with hydrocarbon waters. Hungarian waters obviously tap deeper aquifers, recharged in colder periods as their isotopic composition shows depletion with heavier isotopes, and this water is isotopically very similar to the Slovenian, situated close-by. On the opposite, the Croatian waters contain enriched meteoric waters which are quite similar to annual averaged recent precipitation. The heaviest waters as a group are represented by mofettes, which also show rather diverse range of values, which we explain as originating from very recent, active precipitation.

The average deuterium excess differentiates among aquifer lithologies (Table 4). It is the lowest in Hungarian and Slovenian Neogene clastic rocks (10,4 ‰) and Croatian Triassic dolomite (10,8 ‰) but also Slovenian Paleozoic metamorphic rocks are quite similar (11,0 ‰). There is some distinction of waters from the deepest well in Rogaška Slatina in Slovenia tapping the Triassic clastites and volcanoclastics (12,5 ‰) and this location also holds waters with extreme d-exceess of 20,9 ‰. Both due to mantle CO_2 exhalations (Brauer et al. 2016).

Tritium activity is not negligible only in mofettes and most mineral waters (being the highest 8.6 TU in 2014) in Slovenia, showing either recent precipitation or mixing of it with mineral water.

There is no information for Croatia, while thermal and thermomineral waters in Hungary and Slovenia, mostly abstracted from few-hundred-meters deep wells, show <0.5 TU.

The calculated noble gas temperatures are available for Neogene geothermal aquifers. Data is mostly available for Upper Pannonian loose sandstone as older layer with hydrocarbon waters show degassing and NGTs cannot be calculated. They are between 3.6-6.4 ± 0.8 °C in Slovenia and 5.5-7.5 ± 0.8 °C in Hungary. They slightly rise along the flow path as the regional flow is assumed from west to east. Therefore, we interpret this aquifer as having an active regional flow, so no major faults which would restrict groundwater flow are assumed in this part f the Neogene sequence. The temperatures are much below the current average annual air temperatures of the region, of approximately 10-11 °C, so the water origin is attributed to infiltration of precipitation during interglacial periods of the Pleistocene.

3.3 Mantle helium gas seeps

We interpret a clear connection of noble gas composition to the regional structural framework. Degassing of helium from the mantle and to it connected geogenic CO_2 in occurs in vicinity of deep regional faults, which was noticed already by Szocs et al. (2013) and Brauer et al. (2016), among others. It also depends which reference value is taken as a mantle helium threshold value, and we used R/Ra = 6,5 for calculations.

Altogether, we identified 17 sites with more than 5% of mantle helium, of which only one each were in Croatia and Hungary, and the rest in Slovenia (Figure 15). Ten of them have >70% (Table 6). From few repeated analyses we noticed that percentage slightly varies among sampling campaigns, but still values are extreme even worldwide: Radenci (71-88%), Benedikt (77%), Ščavnica valley (79-87%) and Nuskova (95%) are connected to the Raba fault system while Rogaška Slatina (73-97%) to the active Šoštanj and Labot fault zones.

Table 6: List of geomanifestations linked to mantle helium exhalation

Site	Country	Max share of mantle helium (%)
B-1	Croatia	6
Le-2g	Slovenia	8
K-59	Hungary	9
Mt-8g	Slovenia	13
Re-1g	Slovenia	14
Mt-6	Slovenia	14
Rt-1/92	Slovenia	16
V-M	Slovenia	71
Kraljevi vrelec	Slovenia	73
Be-2/04	Slovenia	77
Slepice	Slovenia	79
RgS-2/88	Slovenia	84
Matjaževa slatina	Slovenia	87
T-4/88	Slovenia	88
Nu-9	Slovenia	92
Niko-1	Slovenia	95

Site	Country	Max share of mantle helium (%)
V-3/66-70	Slovenia	97

Sites producing thermal and thermomineral water from the Upper Pannonian sedimentary basin aquifer in Hungary and Slovenia, and Triassic clastic and volcanoclastic aquifer in Rogaška Slatina in Slovenia show little mantle helium contribution (4-14%), indicating some permeable zones in this partly consolidated siliciclastic sandstone and siltstone. Some mantle gas component is evident also in the Triassic dolomites in Varaždinske Toplice in Croatia (6%), despite having rather fast groundwater circulation in comparison to other geothermal sites. The sealing capacity of clayey Neogene clastic rocks and lack of active open faults is evident in Ptuj in Slovenia, where only 1.5% of mantle helium was measured.

3.4 CO_2 gas seeps

Natural CO_2 springs or mofettes are only known to exist in the Slovenian part of the pilot area where 8 sites are reported (Table 7, Figure 15): Ivanjševska slatina, Lokavska slatina, Polička slatina, Rihtarovci, Žekš, Strmec, Slepice and Verjanska slatina. They are linked to existence of deep open fault zones. Their location is reported also in the Geological Atlas of Slovenia (many of its maps are freely available at portal eGeologija: http://peridot.geo-zs.si/geonetwork/srv/eng/catalog.search#/home).

Table 7: List of geomanifestations linked to CO_2 gas seeps

Country and type of geomanifestation	**No.**
Croatian mofettes	**0**
Hungarian mofettes	**0**
Slovenian mofettes	**8**

Wet mofettes constantly emit cold CO_2, hold acid surface or meteoric water in a pond, and have bare soil or changed vegetation possibly present around degassing centres. We classified Ivanjševska slatina, Polička slatina, Verjanska slatina and Slepice as wet mofettes. In this case and due to very strong natural discharge of gasses we also assigned Žeks as a wet mofette, even though mineral water with more than 1 g/l of total dissolved solids springs out at this site. We found no connection between the depth of the springs and the intensity of gas emissions.

As dry mofettes we classified Rihtarovci, Strmec, and a mofette at Lokavska slatina (Figure 57).

An extensive fieldwork was performed in 2014–2015 (Gabor & Rman, 2016) when distinction among wet and dry mofettes, and mineral waters was done. The later research of Brauer et al. (2016) shown that several sites between towns Lenart-Benedikt-Radenci-Nuskova in NE Slovenia have lots of geogene gas. It is predominately very pure CO_2, but methane may also present locally. The isotope signatures of gases indicate an origin of helium and CO_2 predominantly (>75%) in the subcontinental mantle. The measured $^3He/^4He$ ratios range from 4.62 to 5.97 Ra and include the highest ones recorded in the whole Pannonian Basin system, while the gaseous $\delta^{13}C$ is between -5.1 to -3.5 ‰.

In May 2019, we found additional smaller gas vents at two sites – few ten meters away in a forest at mofette Žekš near Benedikt and several meters from the main went of Polička slatina near the Ščavnica River valley.

Figure 57: Dry mofette at Lokavska slatina (left) and wet mofette Slepice (right)

Figure 58: New local vents which are evident only after rain period and when vegetation is small

3.5 Seismicity

Seismic activity data revealed 910 events where the largest share (74%) appertains to Slovenia. The least events are reported for Hungarian part of the pilot area (Table 8).

Table 8: List of geomanifestations linked to seizmicity

Magnitude	Croatia	Hungary	Slovenia	Total No.
<1	4	2	260	
1-2	27	10	310	
2-3	133	6	62	
3-4	40	3	10	
4-5	9	1	3	

Magnitude	Croatia	Hungary	Slovenia	Total No.
5-6	3	0		
no data	1		26	
SUM	**217**	**22**	**671**	**910**

Different datasets were available for the three countries and this is probably one of the reasons for some variability of datasets. For all countries SHEEC 1000-1899 © 2013 database (https://www.emidius.eu/SHEEC/sheec_1000_1899.html; Stucchi et al., 2012), SHEEC 1900-2006 database (https://www.gfz-potsdam.de/sheec/, Grünthal et al. 2013) and data from Graczer Zoltan et al. (2002-2018) were used. For Croatia and Slovenia data from Herak et al. (1996) were also available and even more datasets only for Slovenia, that is data from Živčić (2021).

The structure reflects a rich tectonic history since the middle Mesozoic. Buried under thick Neogene marine and terrestrial sediments of Paratethyan origin, the underlying basement is as complex as anything encountered at the Alpine-Dinaric junction to the west. The complex structure of both, the Neogene sediments and the pre-Neogene basement, controlled the evolution of the area through Neogene and Quaternary. The Pannonian domain, which includes NE Slovenia in its northwest part, consists of several structural blocks, mainly the ALCAPA and TISZA crustal blocks/mega-units, that underwent thinning due to crustal extension and thermal collapse of the Pannonian basin (e.g. Handy at al., 2014; Horváth et al., 2015).

The northeast part of Slovenia is part of the ALCAPA mega-unit, divided from the Southern Alps by the Periadriatic fault system. The ALCAPA mega-unit comprises the Austroalpine unit of the Alps (Schmid et al., 2020 and references therein). The structure and activity in the eastern part of Slovenia are mostly controlled by the interaction between the ALCAPA and TISZA mega-units. TISZA is an accreted tectonic block/mega-unit composed of composite terranes of Eurasian origin formed in the Mesozoic and final emplacement present-day configuration in Paleogene-Miocene (Csontos et al., 1998; Handy et al., 2014; Schmid et al., 2020). The boundary between the ALCAPA and TISZA mega-units is the Miocene-formed Mid-Hungarian Zone (MHZ). The northern edge of the MHZ, also referred to as the Balaton fault/line is the eastward continuation of the Periadriatic fault system. The MHZ is zone of repeated tectonic inversions (Csontos et al., 1998), currently a sinistral strike-slip zone resulting from the TISZA eastward motion outpacing the eastward motion of ALCAPA (Serpelloni et al., 2016).

There are two fault systems in the GeoConnect³d project area in northeast Slovenia: the Raba fault system and the Balaton fault system (Figure 59), which itself is part of the MHZ zone. The lower Neogene rifting phase produced a multiple systems of normal faults with general WSW-ESE strikes and northerly and southerly dips. Two deep basins formed in NE Slovenia: the Radgona-Vas sub-basin in the north, with the Burgenland swell its north and the Haloze-Ljutomer-Budafa sub-basin in the south, separated by the Murska Sobota extensional block. The Radgona-Vas sub-basin formed along the Raba fault system normal faults, it is approximately 50 km long and 10 km wide and up to approximately 3000 m deep. The Haloze-Ljutomer-Budafa basin is an extremely deep basin, with maximum depths >6000 m, was formed along another system of normal faults, which was inverted in late Neogene as reverse faults (Fodor et al., 2002). These faults now form the Ljutomer fault and associated smaller faults. The Ljutomer fault zone is part of the Balaton line (c.f. Schmid et al., 2020), the northernmost part of the Mid-

Hungarian Zone, the contact zone between the TISZA and ALCAPA mega units. The segments that make up the Ljutomer fault zone initially formed as normal faults, undergoing later inversion and reverse, likely transpressive movement.

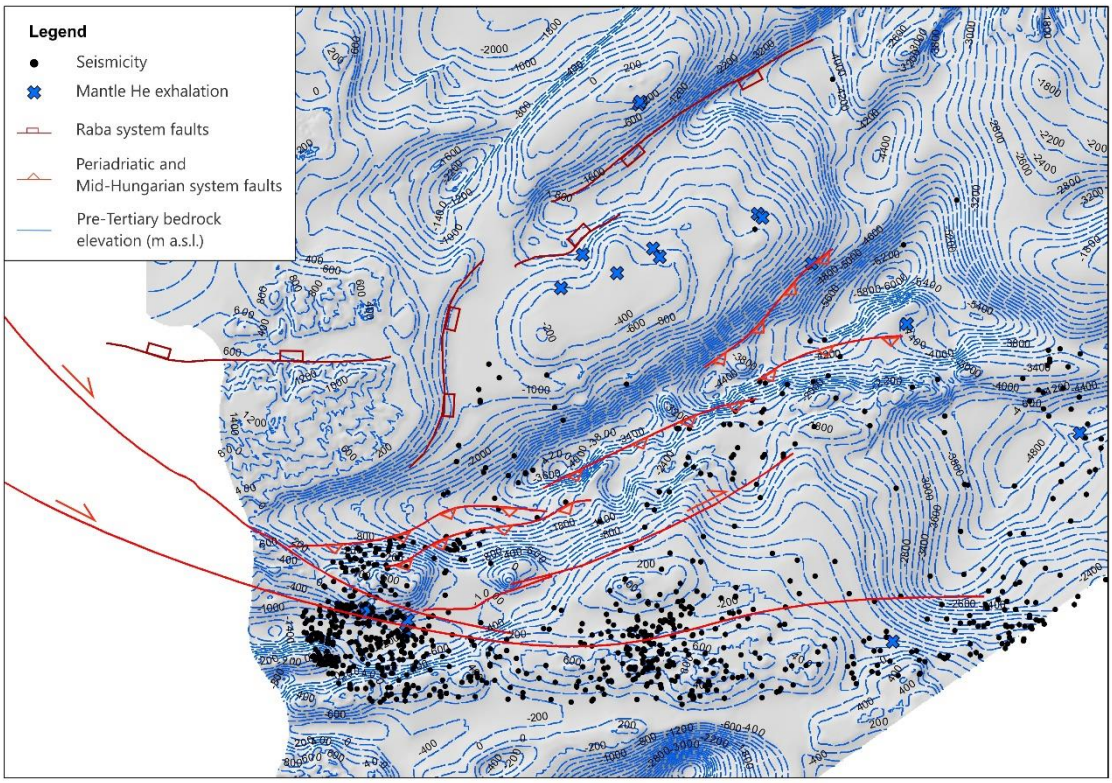

Figure 59: Generalized map of structures in northeast Slovenia with structural elements from the text. Fault traces at pre-Neogene basement level are approximate and generalized. Dark red indicates (probably) inactive faults, bright red active and probably active faults. For general use only.

Seismicity is strongly concentrated in the southern part of the project area (Figure 60). This data includes instrumental microseismicity recorded by the Slovenian national network of between January 1990 and July 2020. Here elevated activity is expected as this is part of the tectonically active Mid-Hungarian Zone. Two local seismicity clusters stand out. One diffuse seismicity cluster appears to be related to the Ljutomer fault; epicenters are located to the south of the fault tip surface projection, consistent with the southward dip of the fault. This may be interpreted as indications of the activity of the fault, however, more precise relocation of hypocenters will be required. The second cluster is located at the extreme SW end of the project area. In this part, the faults of the MHZ and two major faults of the Periadriatic fault system (PAL) – the Šoštanj and the Labot faults – converge. Locally very strong long-term transpression and uplift is evidenced by the Boč mountain. Elsewhere in the project area there is little seismicity. This is expected, as the area encompasses the Raba fault system, which is considered likely inactive or of very low activity.

Seismicity reflects the known active and inactive fault systems well and in general confirms their respective activities. A significant anomaly is also present and currently not yet explained. A diffuse, but significant concentration of seismicity is present along the western edge of the project area. Where no faults currently recognized as active are present. This seismicity generally correlates with the Maribor fault, a presumably inactive normal fault, the SW-most extension of the Raba fault system, that runs along the S and E flanks of the Pohorje mountains.

Reanalysis and relocation of hypocenters will be required to further investigate this potential link, however, this seismicity is considered anomalous.

3.6 Mineral occurrences

Mineral occurrences may represent mineralised hydrothermal fluid flows in some time in past. Based on database from Mintell4EU database, available only for Slovenia, there are 2 sites with gold, one with iron and one with lead reported in Slovenia. No other data was available.

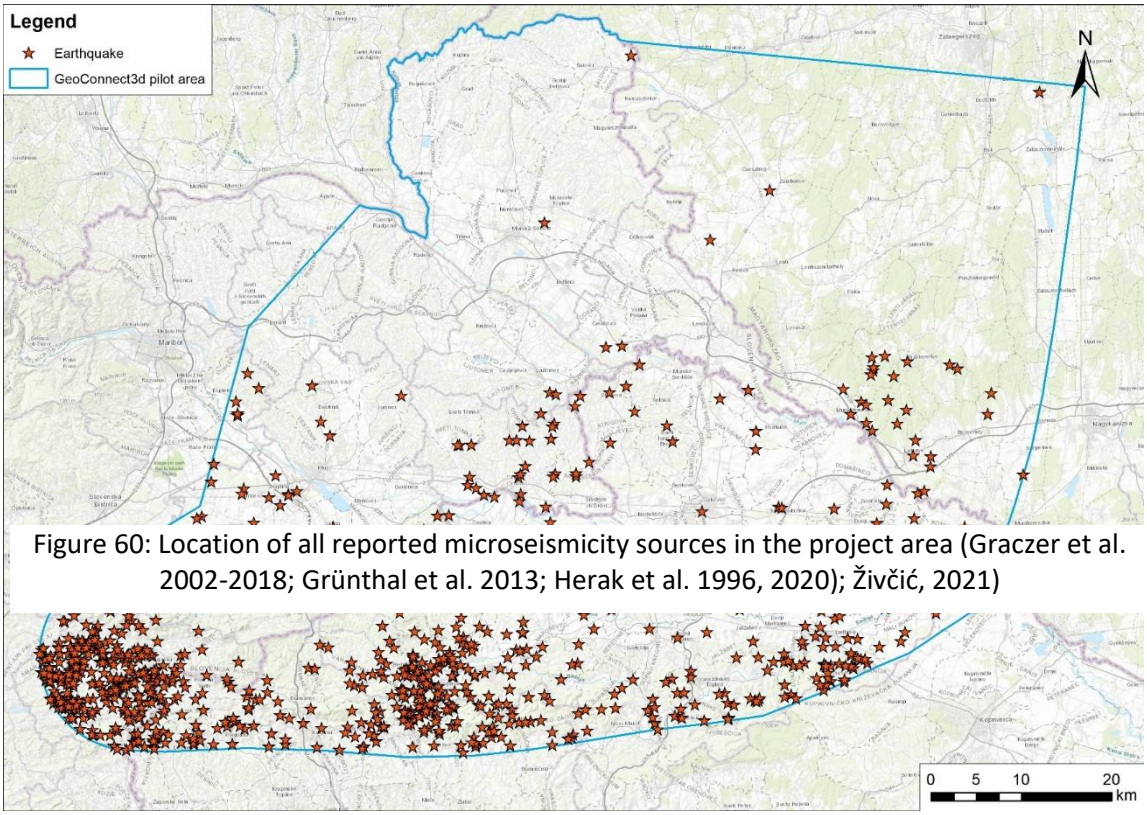

Figure 60: Location of all reported microseismicity sources in the project area (Graczer et al. 2002-2018; Grünthal et al. 2013; Herak et al. 1996, 2020); Živčić, 2021)

3.7 Organic matter occurrences

Hungary has no reported coal outcrops or oil and gas natural springs in the pilot area but lots of hydrocarbon accumulations: 15 oil and gas fields and 4 solely gas fields. Slovenia has 38 sites where coal was identified or mined and two hydrocarbon accumulations (oil and gas fields). Croatia has 40 coal outcrops, an oil spring in Peklenica, 6 oil and 1 gas field (Table 9).

Table 9: List of geomanifestations linked to oil and natural gas fields

Country and type of geomanifestation	No.
Croatia	**48**
coal	40
oil spring	1
gas field	1
oil field	6
Hungary	**19**
coal	0
gas field	4
oil and gas field	15
Slovenia	**40**
coal	38
oil and gas field	2
SUM	**107**

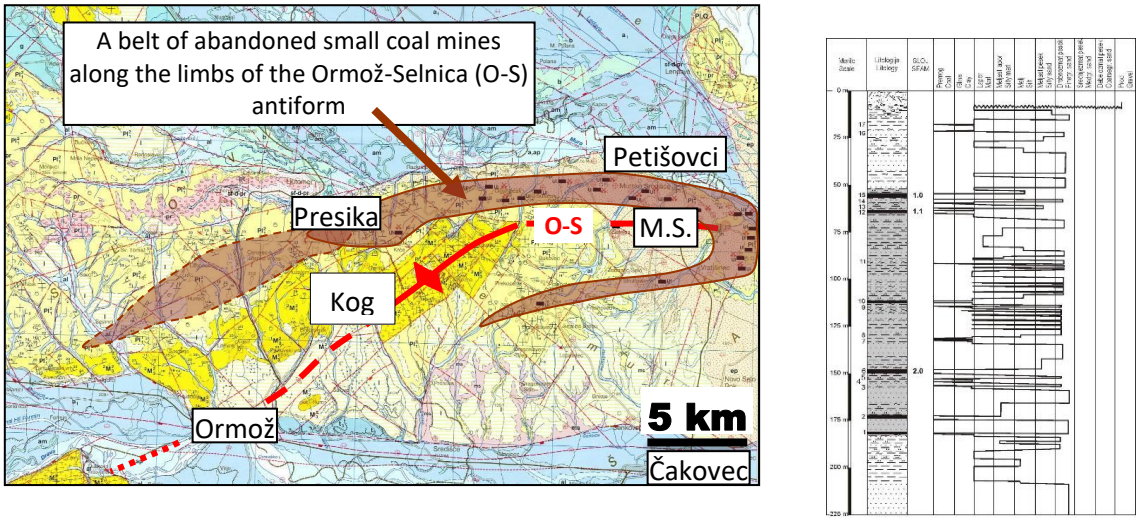

Figure 61: Left: A belt of coal occurrences along the limbs of the Ormož-Selnica Antiform (O-S). M.S. – Mursko Središće was the largest coal mine in the region. Right: Coal-bearing Pontian (Upper Miocene) strata in Petišovci (Mura Fm in SLO; Ujfalu Fm in H., Ivanić Grad ? in CRO). Among ca. 17 coal beds only three are up to 2 m thick.

In the Mura-Zala sub-Basin, along the Mura river, between Mursko Središće (Croatia) and Petišovci (Slovenia), numerous thin beds of outcropping brown coal (lignite) occur (Takšić, 1967; Markič et al., 2011; Figure 61). In the late 19th century, tens of coal beds were recovered at the surface and then mined not deeply underground. Sporadic water inrushes, low thickness, primitive excavation, and low consumption were the reasons to close most of the coal operations already between the Wars. The last coal mine in this area was Mursko Središće, closed in 1972. Coal exploration in the wider area of Slovenia and Croatia flourished again in the 1980s after an "oil crisis" in the 1970s but was stopped already before 1990. One outstanding feature of coals in the Mura-Zala sub-Basin is their high arsenic (As) content (Markič, 2017).

Apart of coal outcrops, some oil and gas seeps were known in the “NE-Slovenia – NW Croatia” area as well (Pleničar, 1954), whereas underground accumulations of hydrocarbons of economic value exist in all three countries – Hungary, Croatia, and Slovenia. One of most known oil springs is known from the Peklenica district at Mursko Središće (Figure 62). Surface seepages of oil were historically known at several sites but after hydrocarbon fields of Petišovci, Lovászy, Selnica, Peklenica and some others were exploited since the second half of the 19th century, most have ceased. In the last ten years, the Petišovci field in Slovenia, connected with the Lovászy field in Hungary, was also an area of new exploration by deep reflection seismic survey and drilling of two wells, 3500 m deep. In 2011, several shallow water ponds on the Ormož-Selnica Antiform in the Kog area in Slovenia were investigated (Markič & Toman, 2011) if some oils are naturally discharging. They are in a swampy land, up to 4 m wide and 30 m long. On the surface, there was very thin layer of decaying organic matter and an “oily” appearance. Visible was also bubbling of gas which we attributed to a decay of organic matter at the bottom of the ponds. There was no smell initiating the presence of hydrocarbons. Analysis of polycyclic aromatic HCs (PAH) showed concentration 0.005 µg/l and below (limit for potable water is 0.1 µg/l). Concentration of mineral oils (MOs) was below 0.1 mg/l, while the limit for the surface waters by Slovenian legislation is 0.05 mg/l. It is interpreted that these MOs were of “anthropogenic” origin and are not a true geomanifestation, unfortunately for us.

Figure 62: Field museum in Peklenica near Mursko Središće (Croatia). Left: historical view with wooden three-rigs. Right: oil in a well – geomanifestation at the surface. (Photo: Markič and Marković, 2018)

Kercmar, 2018). Both consist of alternating 10-40 m thick impermeable marls and porous oil- and/or-gas-bearing sandstones of low porosity – below 15 %, decreasing with depth to ca. 7% only. The Petišovci hydrocarbons are therefore characterized as the tight gas and oil. The shallow »conventional« reservoirs occur in 4 main horizons in a depth interval from ca. 1200 to 1800 m. They were exploited in the 1950s (mostly oil) and 1960s (mostly gas). Nowadays, they are depleted – offering a possibility for e.g., storage of CO_2. The deep reservoirs occur below a depth of ca 2.2 km down to a depth of 3.5 km (deepest wells) or even more? A similar situation is in the neighbouring hydrocarbons fields, of which some were reactivated recently (e.g. Vučkovec, Vukanovec, Zebanec in CRO).

A basic structure for both hydrocarbons and coals in the Mura-Zala sub-Basin is the Ormož-Selnica Antiform formed between two regional reverse faults – the Ljutomer Fault and the Donat fault (Djurasek, 1988; Gosar, 1994/95; Hasenhüttel et al. 2001; Kerčmar, 2018).

Due to regional compressive tectonics, generation of an antiform fissure system, deeply generated hydrocarbons moved upwards to less impermeable strata (seals) and were trapped there as hydrocarbons concentrations (fields).

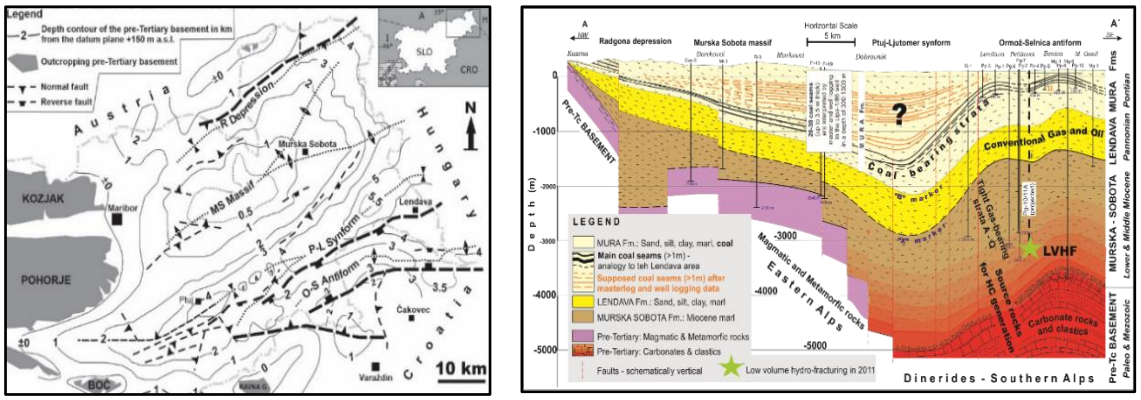

Figure 63: *Structural map of the Mura-Zala sub-Basin by depth contours of the pre-Tertiary basement (simplified after Djurasek, 1988; and Gosar, 1994/95). Right: NW-SE Cross-section – note the Ormož-Selnica antiform, coals, hydrocarbons, and low volume hydrofracturing (LVHF) in 2012 for enhanced gas recovery.*

More about the Mura-Zala geomanifestations can be read at blog posts of the Geoconnect3d project:

Tectonics and seismicity in NE Slovenia, https://geoera.eu/blog/tectonics-seismicity-ne-slovenia/

Oil and Gas geomanifestations in the Mura-Zala Basin (Petišovci-Dolina; NE Slovenia), https://geoera.eu/blog/oil-and-gas-geomanifestations-mura-zala/

Natural carbon dioxide emissions as mofettes in Slovenia, https://geoera.eu/blog/mofettes-in-slovenia/

A survey of presumably hydrocarbons-containing water ponds in the Kog hills (Pannonian Basin, NE Slovenia), https://geoera.eu/blog/a-survey-of-presumably-hydrocarbons-containing-water-ponds-in-the-kog-hills-pannonian-basin-ne-slovenia/

Geomanifestations in North East Slovenia, https://geoera.eu/blog/geomanifestations-in-north-east-slovenia/

Croatian earthquakes – Discovery of the Mohorovičić (Moho) discontinuity, https://geoera.eu/blog/croatian-earthquakes-moho/

The story of medical oil – Naphtalan, https://geoera.eu/blog/the-story-of-medical-oil-naphtalan/

Meet the Scientist #6 – Tomislav Kurečić, https://geoera.eu/blog/meet-the-scientist-6/

Meet the scientist #4 – Dejan Šram, https://geoera.eu/blog/meet-the-scientist-4/

Meet the scientist #3 – Nina Rman, https://geoera.eu/blog/meet-the-scientist-3/

4 GEOMANIFESTATIONS IN THE BATTONYA HIGH

4.1 Geology and tectonics

The pilot area is situated in the Tisza Mega-unit, southeast of the Mid-Hungarian deformation zone represented by the Balaton-, Tóalmás-, Kapos-line (Figure 64). This territory is far from the borders of the geological units but is in the middle of the most intensively rifted and depressed area of the Pannonian Basin. The metamorphic core complex in the centre of the pilot area surrounded by two very deep sub-basins had a various depression and emerging history. At the time of the un-burial of the initiation of the core complex system we find it on the surface in the Early Miocene, then it suffered a considerable sink to about the Pliocene to more than two thousand meters depth, then from about the Pleistocene it has been in a slight emerging phase again.

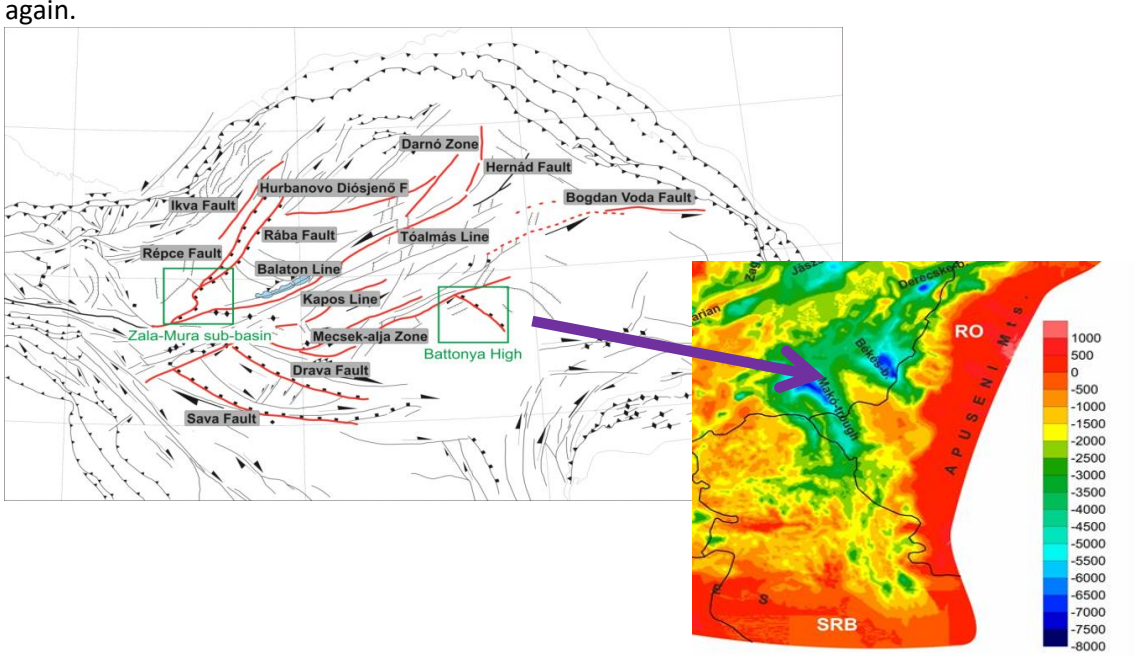

Figure 64: Main tectonic lines of the Pannonian Basin and the topography of the pre-Cenozoic basement [m.a.s.l.]

The buried Battonya–Pusztaföldvár High (basement ridge) is built up of nappe structures, in which the material of a metamorphic basement nappe overthrusted to the Palaeo-Mesozoic sequence by northern, north-western direction. The area belongs to the Tisza Mega-unit with the greatest part associated with the nappe-imbricated structure Békés–Codru Unit. Only the north-western corner of the area stretches over to the Villány–Bihor Unit. The formation of the nappe system is predominantly the result of the Cretaceous (Austrian) compressional tectonics. The strike of the nappe is of NE–SW direction; and Cenozoic transverse faults of NW–SE strike can also be observed (Figure 65).

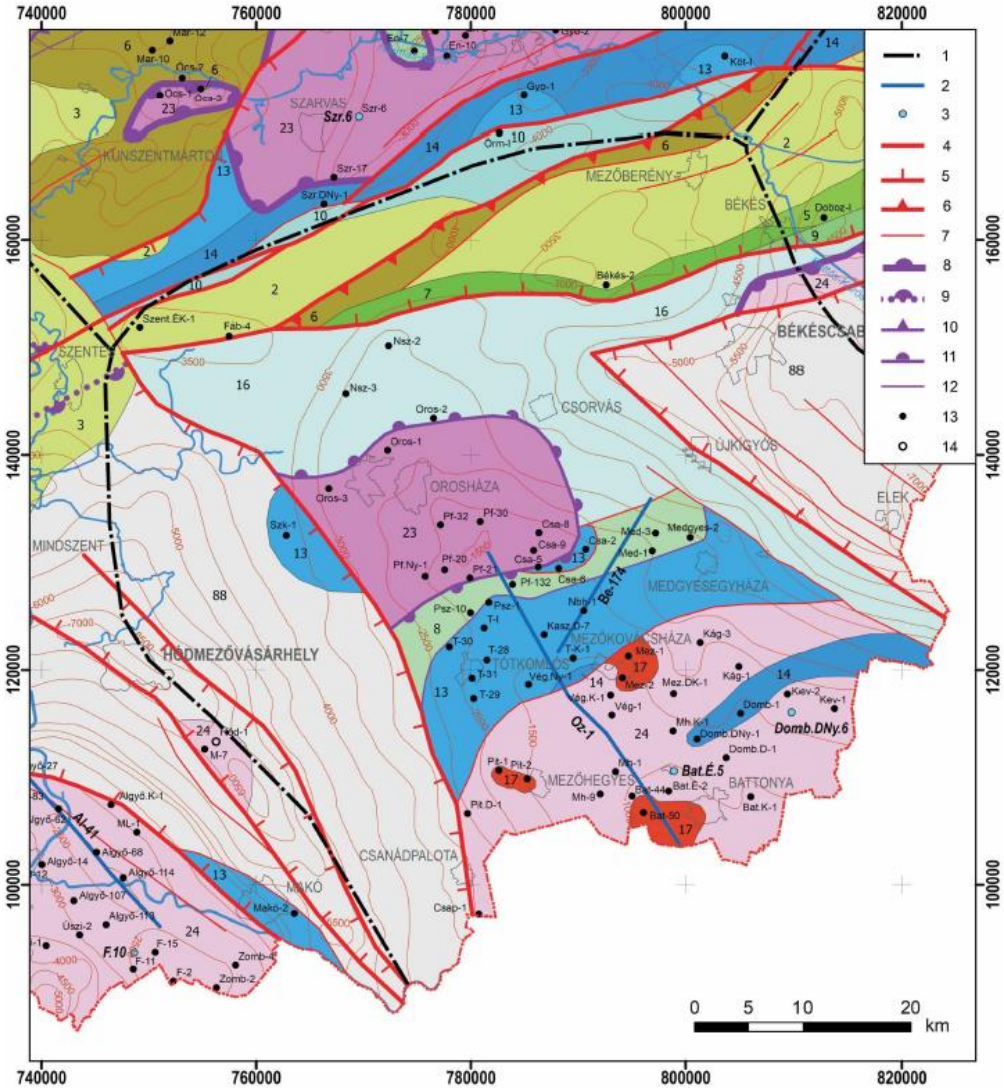

Figure 65: Pre-Cenozoic geological map of the Battonya High area (Haas et al. 2010). Elements of legend: 1. boundary line of the Battonya High area, 2. trace line of the sample 2D seismic profiles in this chapter, 3. location of wells including sample geophysical logs on the figures in this chapter,, 4. second-order Cenozoic tectonic line, 5. second-order Cenozoic normal fault, 6. second-order Cenozoic overthrust, 7. third-order Cenozoic tectonic line, 8. first-order Mesozoic nappe boundary, 9. first-order Mesozoic nappe boundary, covered, 10. second-order Mesozoic overthrust, 11. second-order Mesozoic nappe, 12. third-order Mesozoic tectonic line, 13. wells hit the basement, 14. wells stopped above the pre-Cenozoic basement Legend for geological formations: 2. Senonian flysch, 3. Senonian continental, shallow- and deep-marine (bathyal) formations, 5. Lower Cretaceous limestone of platform facies, 6. Lower Cretaceous basic volcanics and their redeposited marine sediments, 7. Lower Cretaceous pelagic marls, limestones, 8. Jurassic–Lower Cretaceous pelagic limestones, marls, 9. Middle Jurassic – Lower Cretaceous pelagic limestones, cherty limestones, 10. Lower–Middle Jurassic pelagic, fine siliciclastic formations, 13. Middle Triassic shallow-marine siliciclastic and carbonate formations, 14. Lower Triassic siliciclastic formations of fluvial and delta facies, 15. low- grade metamorphic Mesozoic formations, 16. Mesozoic formations without subdivision, 17. Permian

rhyolite, 23. Variscan metamorphite formations (gneiss, mica, amphibolite), 24. Variscan crystalline rocks without subdivision, 88. inadequately evaluable or unknown basement

The basement rock masses sliped down along detachment faults gravitationally from the Battonya High in the syn-rift phase of the development of the Pannonian Basin — during the large-scale extension and now forms the basement of the Makó and Békés basins (Horváth, Rumpler 1984, Nemcok et al. 2006, Tari et al. 1999). The relatively emerged rock mass fragment constitutes the Battonya–Pusztaföldvár High, to the NE and SW of which the two deepest Neogene basement depressions of Hungary are situated: the Békés Basin and the Makó Trough (Figure 65). The basins are of halfgraben structure, thus the tectonic lines bounded the basins on one side consist of a main fault with low number of planes and several small faults on the other side (Posgay et al. 1996, Hajnal et al. 1996). This arrangement influences the structure of the ridges between the depressions as well, thus the south-western side of the Battonya–Pusztaföldvár High slid down most probably with a series of lesser normal faults toward the Makó Trough (Figure 66).

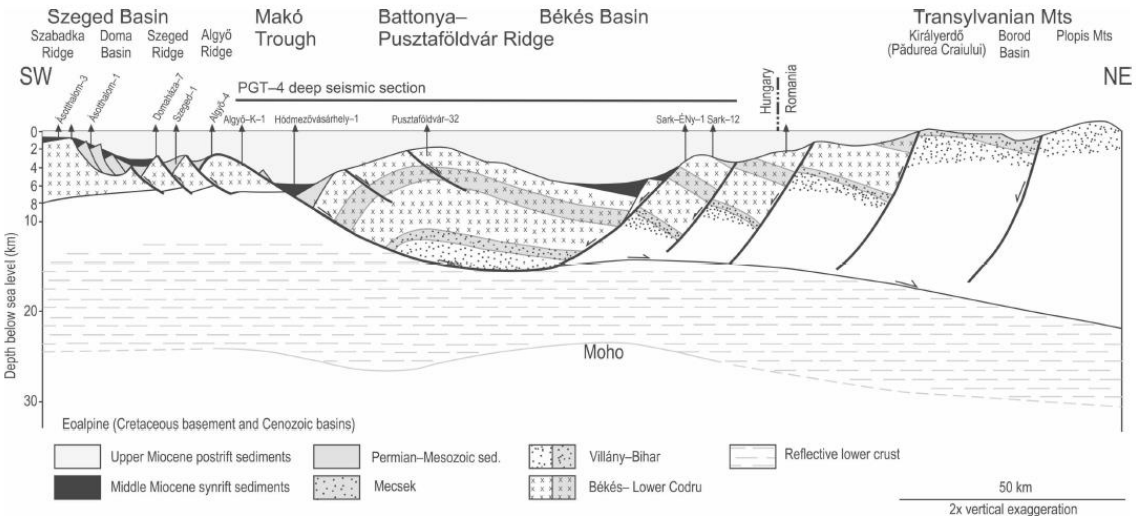

Figure 66: Regional geological profile in the south-eastern part of the Pannonian Basin (adapted from Tari et al. 1999)

The Neogene sequence rests on the basement with a considerable unconformity. During the Neogene new, primarily extensional tectonic phases commenced. The pre-Pannonian Cenozoic formations are made up predominantly of Miocene continental and shallow marine clastic sedimentary formations occurring in patches and characterised by varying thicknesses.

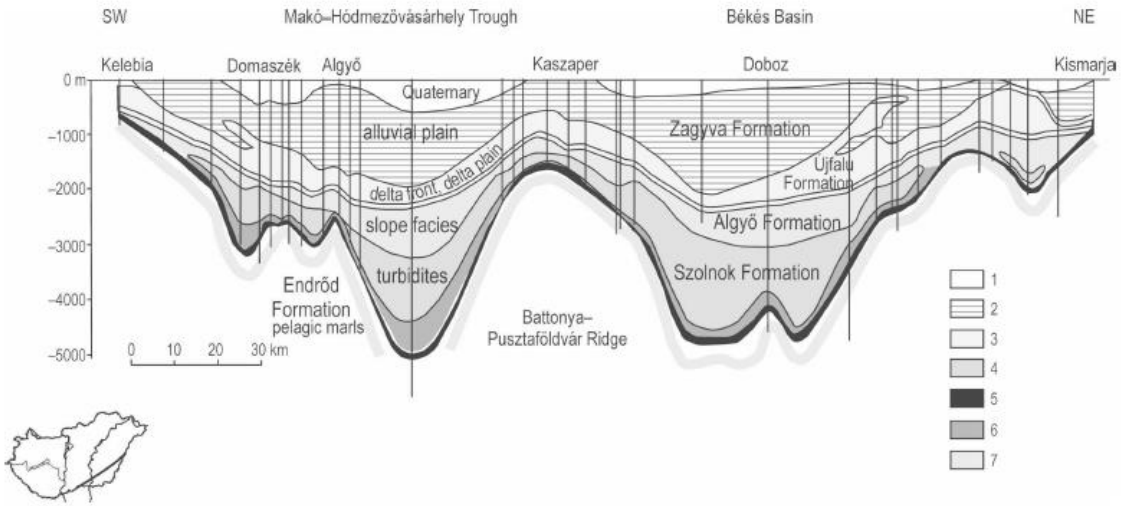

Figure 67: The schematic stratigraphic–sedimentological profile of Pannonian formations in the southern part of the Great Hungarian Plain (Juhász 1989). Legend: 1. fine-grained sandstone; 2. medium-grained sandstone; 3. siltstone; 4. argillaceous marl; 5. calcareous marl; 6. conglomerate; 7. Neogene basement

The Pannonian formations (Figure 67) are transgressed at some places directly over the Palaeozoic–Mesozoic basement complex. Elsewhere they overlie the sporadically occurring older Miocene formations; the thickness of the pre-Pannonian Miocene formations reaches several thousand metres.

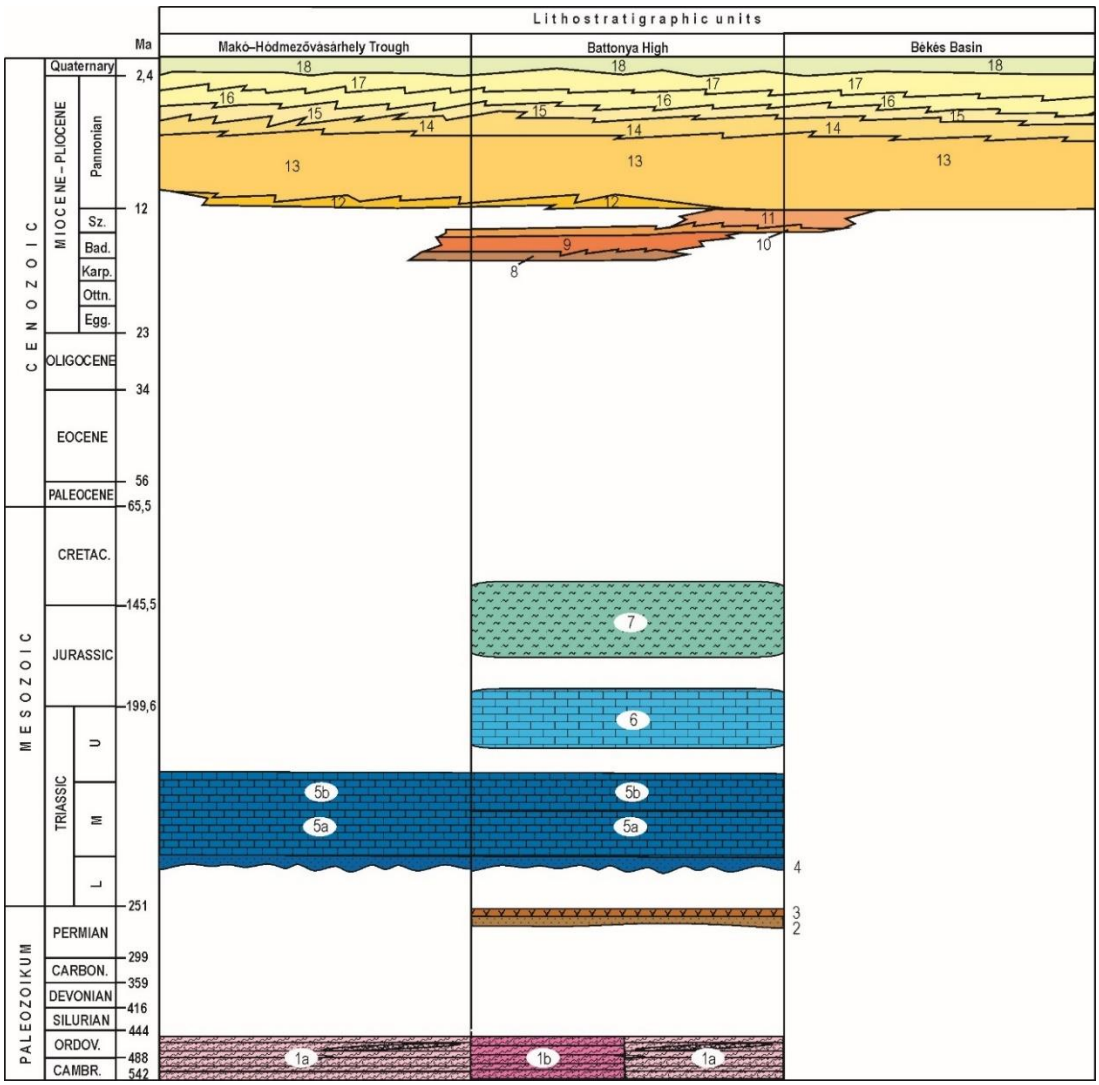

Figure 68: Lithostratigraphic column of the Makó Trough, Battonya–Pusztaföldvár High and the Békés Basin (after Haas & Budai 2014, modified by Selmeczi, Piros, Kun). Legend: V V V – traces of volcanic activity. Formations seen in the profile: 1a. Variscan medium-grained granitoids (quartz monzonodiorite, granodiorite, monzogranite); 1b. Variscan medium-grade metamorphic (mica schist, paragneiss, amphibolite);2. Permian continental clastic formations; 3. Permian rhyolite; 4. Lower Triassic siliciclastic formations of fluvial and delta facies; 5 a, 5 b. Middle Triassic shallow-marine, siliciclastic and carbonate formations; 6. Jurassic shallow-marine and condensed pelagic limestone formations; 7. Jurassic – Lower Cretaceous pelagic limestones, marls; 8. Lower Badenian breccia-conglomerate; 9. Badenian shallow-marine biogenic limestones; 10. Sarmatian basal debris; 11. Sarmatian shallow-marine carbonate and siliciclastic beds; 12. Pannonian littoral conglomerates, sandstones; 13. Pannonian open-lake calcareous marls, marls, argillaceous marls; 14. Pannonian deep-water succession of turbidite origin; 15. Pannonian sediments of delta-slope facies; 16. Pannonian siliciclastic succession of littoral facies; 17. Pannonian siliciclastic succession of fluvial and lacustrine facies; 18. Quaternary sediments

4.2 Geomanifestations

The Battonya High and its region topographically is a very flat area in great extent due to thick, porous sediments as coverage, but beneath the surface very dramatic Paleozoic/Mesozoic basement relief can be found. Accordingly, the geomanifestations are not directly observed at the surface, but anomalies are detected in deep drilling well data. The basement high approaches the surface at around 1000 m, while in the boundary trenches the basement is several thousand metres deeper (even over 7000 m).

Known geomanifestations in the Battonya High pilot area:

- Thermal water reservoirs
- Oil and gas fields (more than 700 drills were completed, hydrocarbon traps: morphology of the Paleo-Mesozoic basement, base of Pannonian, sealing or closing effect impacts of faults, tectonic elements, capillary pressure condition flow regime)
- Seismicity
- Over-pressured zones
- Density driven flow system: Groundwater density varies due to spatial or temporal differences in temperature and concentration of dissolved solids. These differences in density can lead to interesting and sometimes unexpected flow patterns.

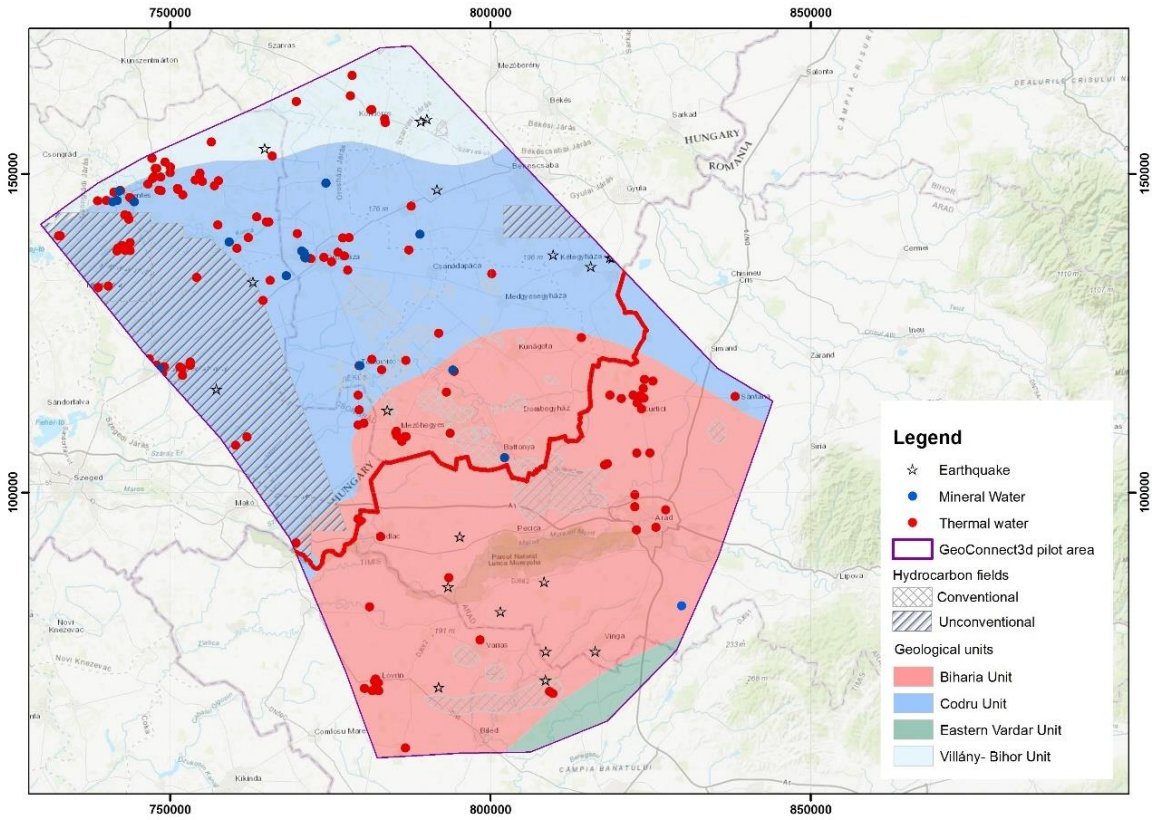

Figure 69: Example of geomanifestations in the Battonya High region, transboundary HU-RO area, in the eastern part of the Pannonian Basin

4.2.1 Geothermal anomalies

The average geothermal gradient in Hungary is approx. 4–5 K/100 m, which is about one and a half times the world average. This is because the Pannonian Basin, which includes Hungary, has a thinner crust than the world average. At only 24-26 km thick, it is about 10 km thinner than in neighbouring areas.

Thus, hot magma is closer to the surface and good insulating sediments (clays, sands) fill the basin. The high geothermal gradient is the result of the mantle diapir that formed either as the upwelling mantle material melted back much of the crust or due to the crust thinning after the roll-back extension of it.

In the Battonya High pilot area, a significant amount of heat can be derived from the upward fluid flow through the loosened/faulted zone of the graben (and possibly also through the fracture system of the crystalline / metamorphic blocks), i.e. also by convective heat transport. The Pannonian Basin is well-known of its good geothermal potential (Dövényi & Horváth 1988; Lenkey et al. 2002; Szanyi et al. 2009; Horváth et al., 2015) due to its favourable geological conditions, being rich in thermal waters. The Pannonian Basin is characterized by a positive geothermal anomaly, with heat flow density ranging from 50 to 130 mW/m2 with a mean value of 90-100 mW/m2 (Hurtel & Hanel 2002; Lenkey et al. 2002; Horváth et al. 2015) (Figure 72) and geothermal gradient of about 45 °C/km (Dövényi & Horváth, 1988). The wide range of the HFD values is explained by the presence of recharge areas and the cooling effect of the infiltrating meteoric waters. The overall positive geothermal character of the Pannonian Basin is related to the Early-Middle Miocene crustal extension when deep basins originated.

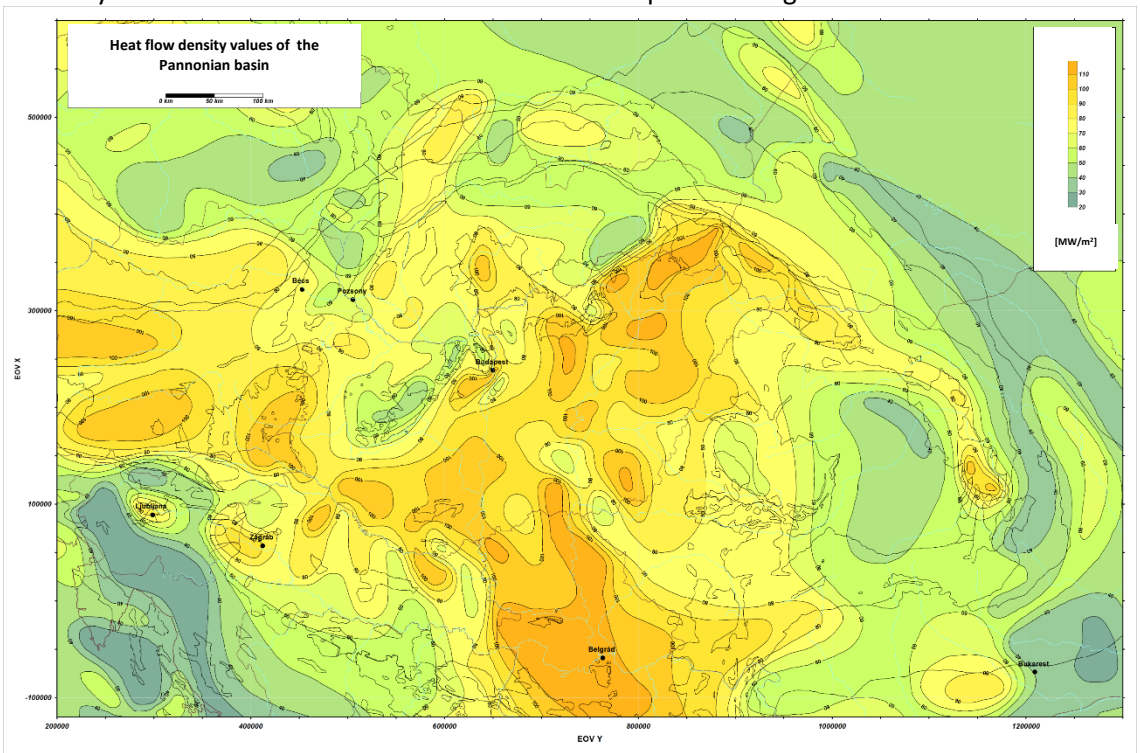

Figure 70: Heat flow map of the Pannonian Basin (Lenkey et al. 2002)

In the frame of DARLINGe project analytical model was set to indicate perspectives areas.

The estimated temperature is the result of a conductive geothermal model, but in most of the cases convection is the prior process in basement formations (especially in karst formations) and in the case of convection, calculated data can differ from the real values significantly. Nevertheless, the comparison of the calculated values of the conductive model to the measured temperature values in the basement formation is very important from geothermal potential point of view, because anomalies indicate the regions of intensive thermal convection (Figure 71).

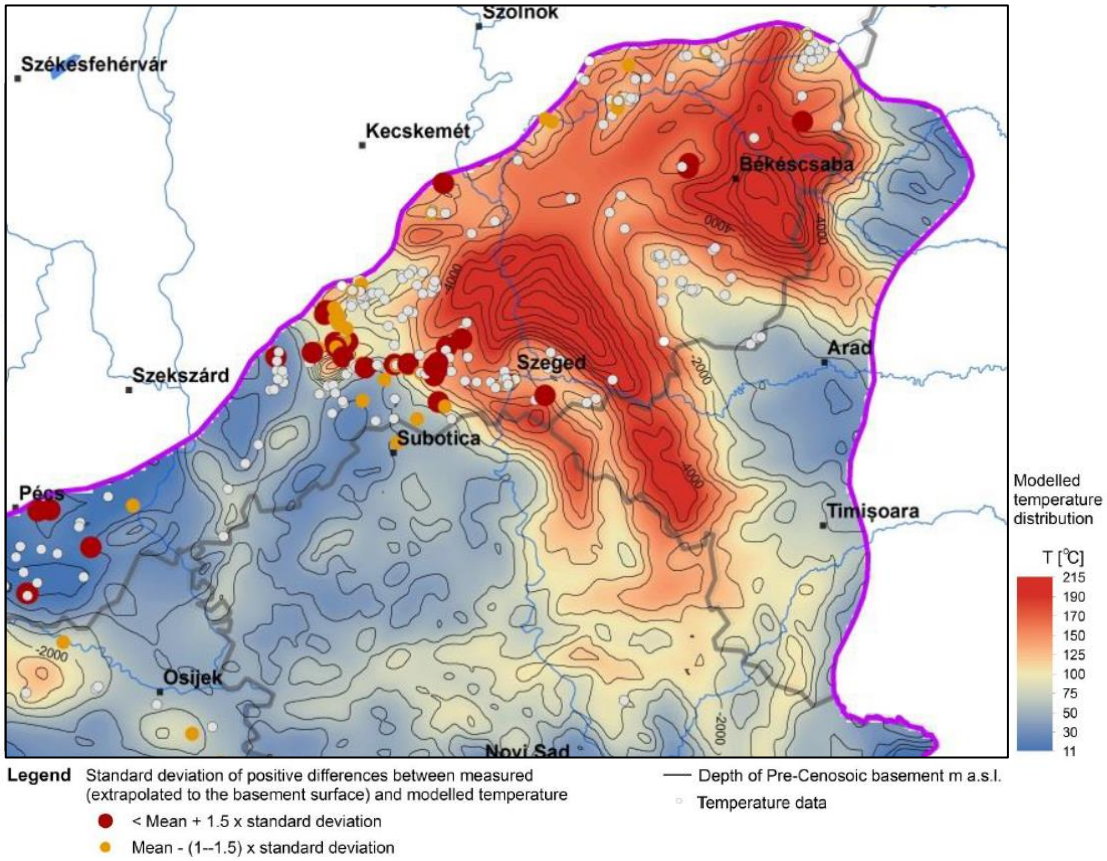

Figure 71: Geothermal potential map of the basement reservoirs. Comparison of the temperature estimated (by the conductive model) at the top of the basement to the measured temperature values which was extrapolated to the top of the basement/ – result of DARLINGe project: zoomed in on the pilot area (Rotár et al. 2018)

In the pilot area, a large number of temperature measurements have been taken in boreholes at a wide range of depths over the past 30-40 years. Summarized on one graph (Figure 72), the area average is approximately 43.9 Celsius/100 m. It can be seen that at greater depths the gradient is smaller, while at some depth intervals a convective component causes a positive thermal anomaly.

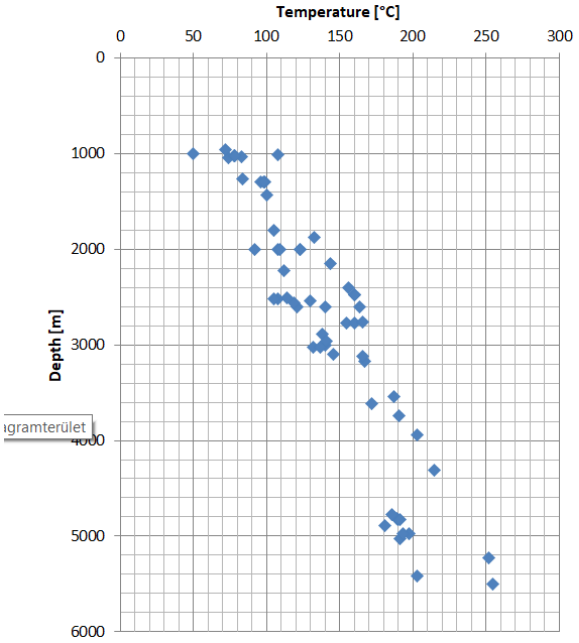

Figure 72: Temperature-depth profile of the boreholes of Battonya High pilot area (24 objects; 62 measurements)

4.2.2 HC reservoirs

The hydrocarbon accumulation zone in the area is associated with the relatively flat, 10–15 km wide and approximately 100 km long, tectonically divided palaeo-geomorphological ridge of the pre-Neogene basement with NW–SE strike, elevating in south-eastern direction and the limbs thereof. Occurrences with the largest area and resources are in the axial line of the ridge.
The most important reservoirs rocks in the pilot area (HC industry data) (Tatár et al. 1999, Szentgyörgyi et al. 2010), which are considered as aquifers for HC utilization, are:

- The upper, fractured zone and fragmented, weathered surface of the Palaeozoic basement rocks, Palaeozoic metamorphic granites (Battonya Complex), Permian rhyolite, rhyolite tuff (Gyűrűfű Rhyolite Formation);
- Lower Triassic fractured sandstones (Jakabhegy Sandstone Formation), Middle Triassic fractured, brecciated dolomites (Szeged and Csanádapáca Dolomite Formations);
- Middle–Upper Miocene, Badenian and Sarmatian conglomerates, sandstones, biogenic limestones (Abony, Ebes Formations);
- Pannonian basal conglomerates and sandstones (Békés Formation);
- Pannonian fractured basal calcareous marls, argillaceous marls (Endrőd Formation, Tótkomlós Calcareous Marl Member);
- Pannonian delta foreground facies, turbiditic sandstones (Szolnok Formation);
- Pannonian delta plain facies, various types of point bar and river bed sandstone successions, poorly consolidated sands (Újfalu Formation).

Hydrocarbon reservoirs in the Pannonian layers store natural gas, and these reservoirs are generally independent of each other. These layers are mostly characterised by hydrostatic or slightly lower pressure conditions.

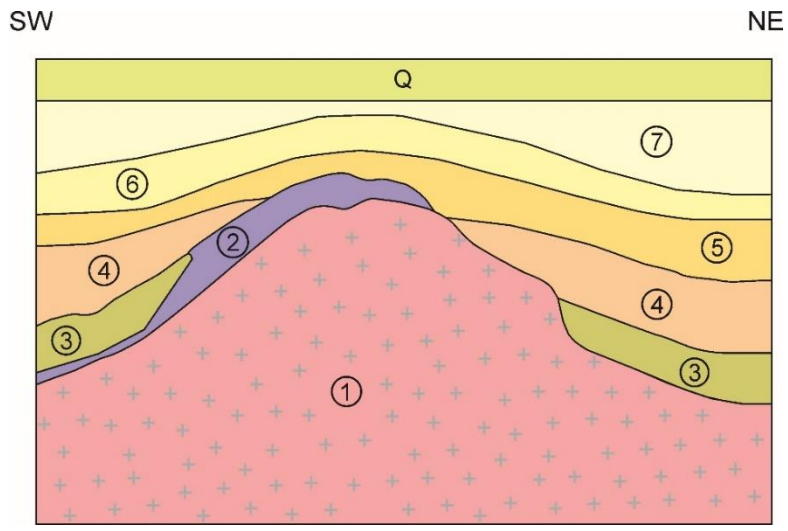

Figure 73: Potential reservoirs of the Battonya High

As illustrated in Figure 74, hydrocarbon fields are numerous in the pilot area in a national comparison, which highlights the potential for migration and trapping given by the structure. Petroleum reservoirs are broadly classified as conventional and unconventional reservoirs. In conventional reservoirs, the naturally occurring hydrocarbons, such as crude oil or natural gas, are trapped by overlying rock formations with lower permeability, while in unconventional reservoirs; the rocks have high porosity and low permeability, which keeps the hydrocarbons trapped in place, therefore not requiring a cap rock.

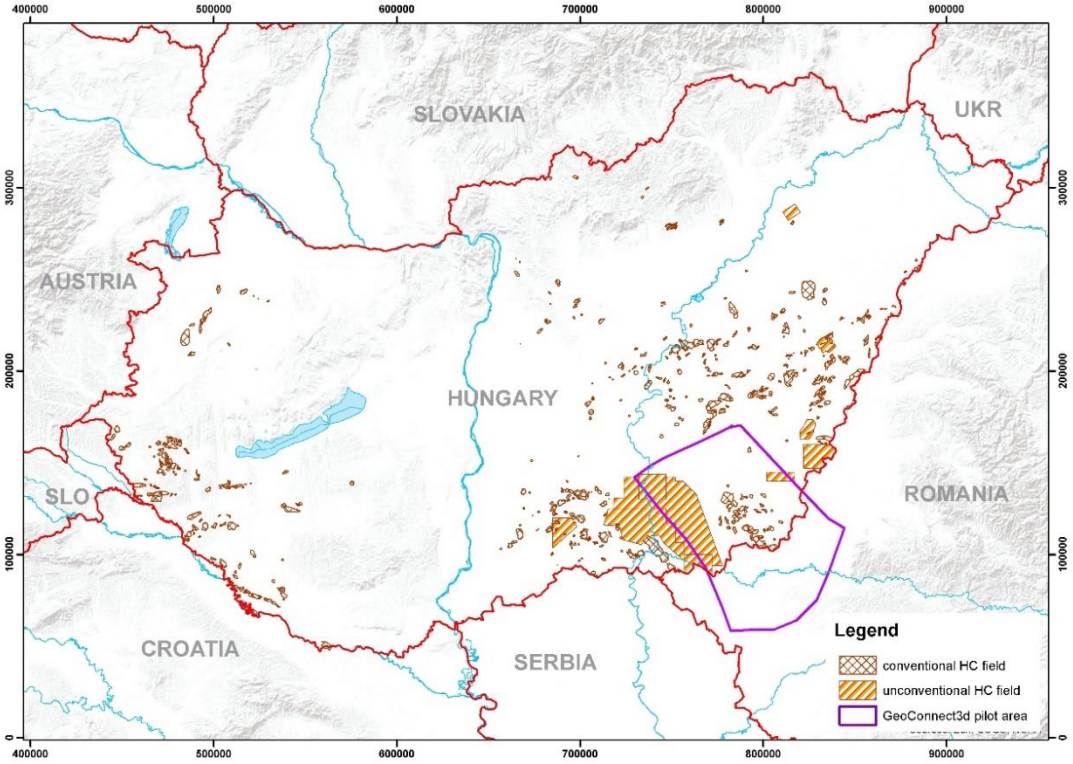

Figure 74: HC fields in the Hungarian parts of Pannonian basin

4.2.3 *Overpressured zone*

Three main pressure types have been applied to describe subsurface pressure conditions: the hydrostatic, the pore, and the lithostatic pressure. The hydrostatic pressure is the pressure of the water column, while the lithostatic is the pressure of the overburden rock mass at a given depth. Finally, the pore pressure means a pressure value that is measurable in the pore fluids. The hydrostatic pressure regime is present when the pore pressure is equal with the hydrostatic pressure. An abnormal pressure regime occurs when the pore pressure is smaller or higher than the hydrostatic pressure. Underpressure is the condition, when the pore pressure is lower the hydrostatic; this is the less frequent situation. However, overpressure is present when the pore pressure exceeds the hydrostatic conditions; it is known from several young sedimentary basins (Nagy et al 2021). In the Great Hungarian Plain, a major operational accident occurred (1985) during the exploration of a deep, high-temperature, high-pressure geothermal reservoir, with significant environmental damage.

The water steam blowout at the Fábiánsebestyén-4 well occurred under unique natural conditions, and its recovery was made possible by the exemplary cooperation of Hungarian and US oil industry experts. Tóth et al. (2003) composed a pressure anomaly map.

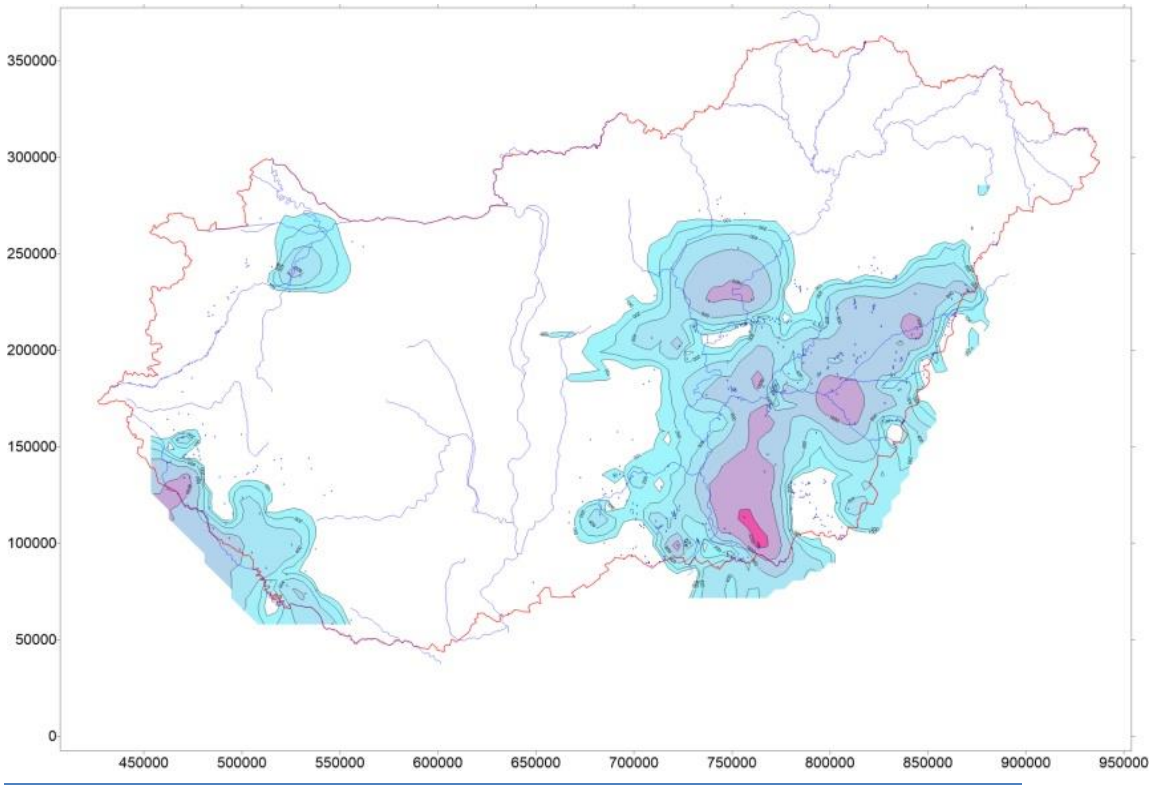

Figure 75: Overpressure map extrapolated from measured pressure values (Tóth et al. 2003)

4.2.4 *Hydrogeology, conditions of flow regime*

So-called groundwater bodies were delineated in the framework of the national water management plan. For example all together 185 different groundwater bodies are distinguished in Hungary. In this groundwater body system, there are seven different types concerning the

groundwater resources. We can speak about shallow porous, porous, porous thermal, shallow mountainous, mountainous, karst and thermal karst water bodies.

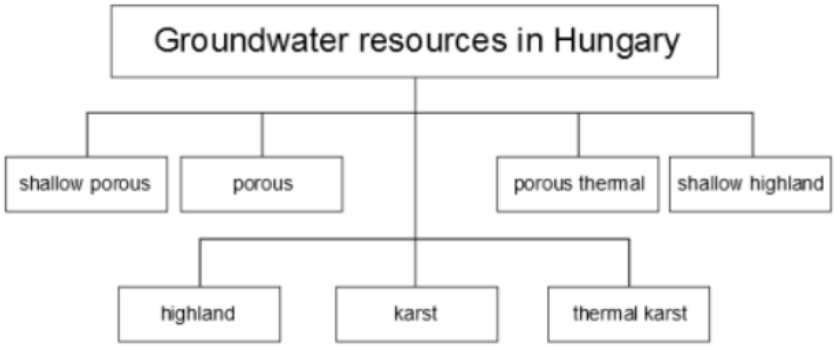

Figure 76: Classification the groundwater bodies by their aquifer type

The aquifers in the area were formed in the sandy and infusional loess layers of the Holocene and Upper Pleistocene aquifers. The thickness of the aquifers is estimated to be a few metres, sometimes a few tens of metres. The groundwater table follows the surface topography, with a depth of 3-4 m below the surface.

The regionally distributed cold and thermal aquifers are composed of river and floodplain sediments, which gradually increase in thickness from the back to the basins. Most of the water wells in the municipalities are located mainly in the sandier, relatively shallow layers of the upper 100-200 m thick sediment, which are easily accessible by shallow wells and have a good water quality. This is closely related to the underlying aquifer of the late Pannonian-age alluvial plain assemblage (Zagyva and Újfalu Formations), which is 600-800 m thick on the main terrain of the hinterland and up to 1200-1500 m thick towards the Makó Trough and the Békés Basin.

In the Zagyva Formation, we can delimit the intermediate flow system formed in the porous sediments of the basin. The sand bodies in the parts of the assemblage deeper than 400-500 m may already provide thermal water warmer than 30 °C. The most important regional aquifer for the supply of thermal water is the Újfalu Formation, including its sandier deltaic sediments.
The fracturing of the basement formations plays a role not only in the flow of stored water, but also in the migration and trapping of hydrocarbons occurring in the area. Deeper carbonates with low organic matter content can become carbon dioxide gas reservoirs under suitable thermal conditions. The migration of the gas generated here is mainly due to the fracture network of the rock, its tectonisation (vertical migration) and the erosional surface of the bedrock (horizontal migration), which may lead to the gas reaching the upper zones of shallow carbonate formations or the vicinity of the Pannonian bedrock. The pressure of the deposits formed at this level is generally lower than the hydrostatic pressure. (Kovács, 2018)

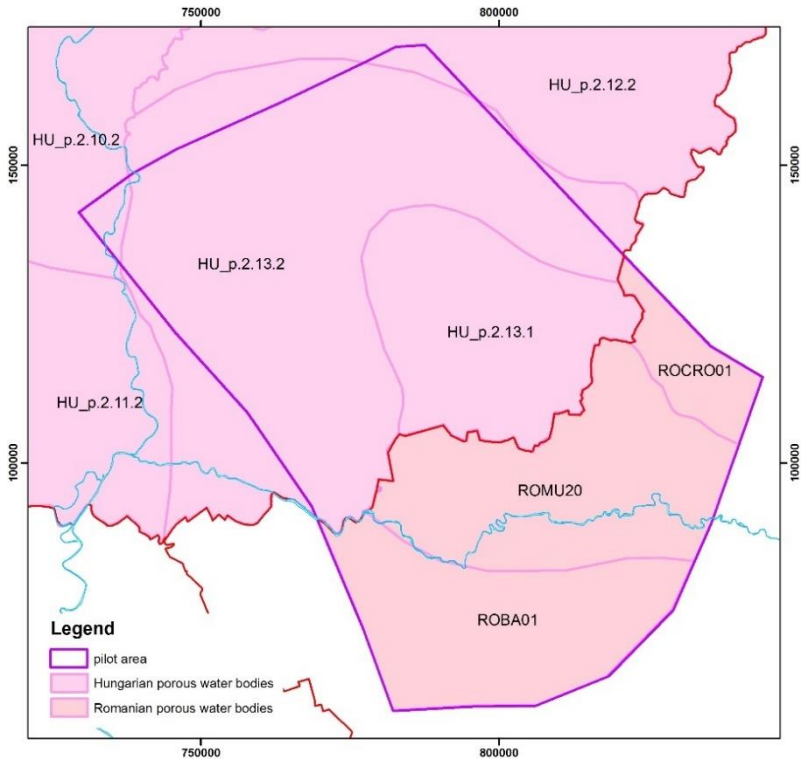

Figure 77: Porous deep groundwater waterbodies of the pilot area

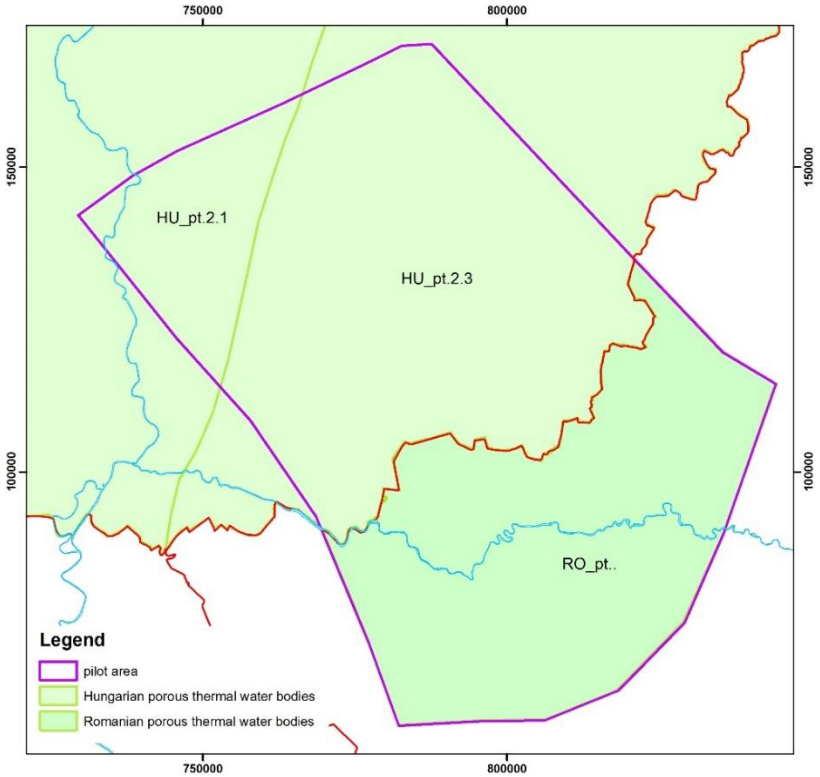

Figure 78: Porous thermal waterbodies of the pilot area

The public well data of the Water Framework Directive (2015) is maintained by the OVF (General Directorate of Water Management of Hungary). This data provides the statistics for the pilot area (Table 10).

Table 10: List of geomanifestations linked to groundwater wells

Country and type of geomanifestation	No of wells
Hungary	**130**
mineral water	16
thermal water	124
Romania	**40**
mineral water	1
thermal water	39
SUM	**170**

The geologically derived flow forcing paths fundamentally determine the composition and age of the fluids and in many cases the transport of saline water from deeper regions to shallower levels. The significant structural processes in the area may have had a significant impact on horizontal and vertical hydraulic permeability of the layers of the thermal aquifers and the hydro-geochemical characteristics.

4.2.5 Seismicity

The most active areas of the Pannonian basin are the Southern Alps, the North-West Dinarides and the Vrancea zone. Seismicity is remarkable at the Mur-Mürz-zone running from Mura valley to the western Carpathians; significant seismic activity can be seen in the eastern Carpathians (mainly in Maramureş region) and in Banat, that can be found in the southern part of the Carpathian basin. (http://www.seismology.hu/index.php/en/seismicity/seismicity-and-seismic-hazard)

Seismicity of the Hungarian part of Pannonian Basin on the whole, can be characterized as moderate (Figure 79, Table 11). Distribution of the earthquakes, however, is not homogeneous: there are significant differences between the seismic activity of the surrounding mountain areas and of the inner part of the Pannonian Basin.

The permeability of faults and fracture systems is influenced by numerous conditions, and seismic movements can contribute significantly in a positive (increasing) direction. In this way, seismic activity can be an indicator of the potential for deep vertical flow along faults. Since the hypocentres of the earthquakes are below the observable part of the basin by geophysics or boreholes, their direct connection to the fault zones is questionable.

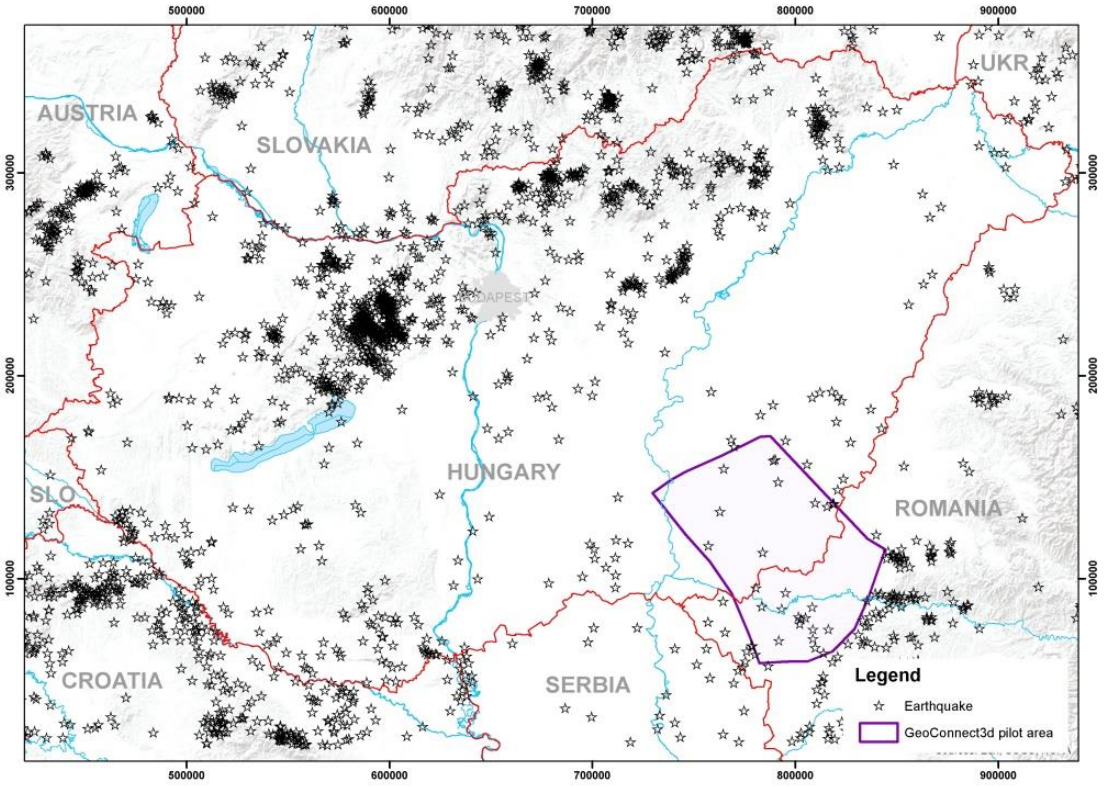

Figure 79: Seismic points (Earthquakes) of the Pannonian basin

Table 11: List of geomanifestations linked to seismicity (2002-2018)

Magnitude	Hungary*	Romania	
<1			
1-2	3		
2-3	6		
3-4	2		
4-5			
5-6			
no data		8	
SUM	11	8	19

*HU: Data from Hungary (2002-2018) came from the Kövesligethy Radó Seismological Observatory, Geodetic and Geophysical Institute, Research Centre for Astronomy and Earth Sciences (H-1112 Budapest, Meredek u. 18). It is published in the Earthquake bulletins, Hungarian National Seismological Bulletin, HU ISSN 2063-8558

4.3 Model examinations on geothermal anomalies

4.3.1.1 Conceptual model

The aim of the modelling is to investigate the geothermal anomaly of the Battonya High pilot area starting with conceptualizing before numerical modelling.

The outline of the conceptual model is summarised in the figure below (Figure 80). The red streamlines in the figure have already been confirmed as a result of the model runs. It shows

that sediments and fractured basement formations, besides their own flow regime, have a crossing and interconnection potential through chemically and mechanically fractured, weathered and probably highly fractured zone.

The weathered zone, as a conveyor belt, brings fluids with higher temperature and mineral composition at greater depths into shallower positions. In this flow path, both thermal water flow and hydrocarbon migration can occur on an accelerated timescale.

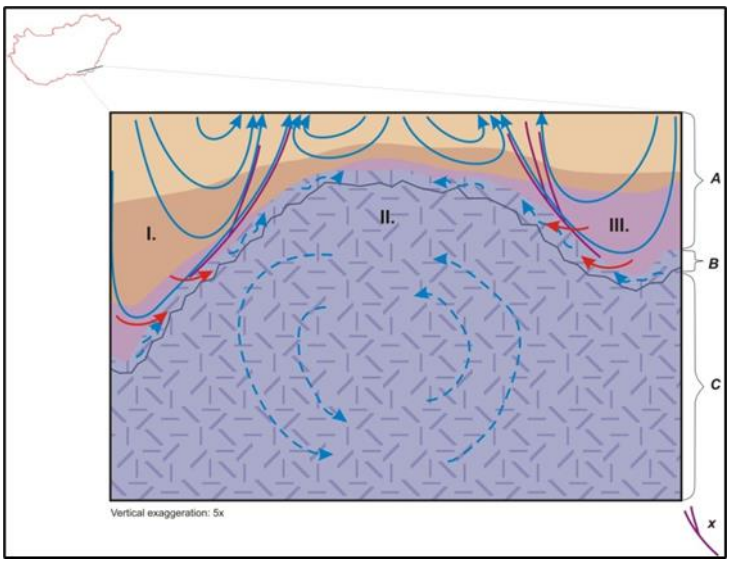

Figure 80: Theoretical flow scheme of the Battonya High and its troughs as the part of conceptualisation. Legend: I .: Makó Trough, II .: Battonya-Pusztaföldvár High, III .: Békés Basin; A: basin-filling sediment series, B: Weathered zone of basement high, C: Mesozoic, Paleozoic basement, x: hypothetical fault, red arrow: flowlines entering the crystalline basement.

In the model study, the flow regime and the interaction between two systems with markedly different hydrodynamic parameters (porous sediments and basement) were investigated.

When delimiting the area of the Battonya hydrodynamic model, we aimed to minimize water flow at the borders and to keep a sufficient distance from the study area (minimizing the border effect). The model boundary was drawn along the axes of the deep ditches surrounding the central ridge on both sides, to the east and west, along the major structural line in the north, while in the Romanian part of the area the boundary was drawn sufficiently far from the modelled area, somewhat arbitrarily. The relatively large model area of about 107 x 67 km (7 160.08 km^2, Figure 81) delimited was also advantageous for simulating the large depth (10 km) flows.

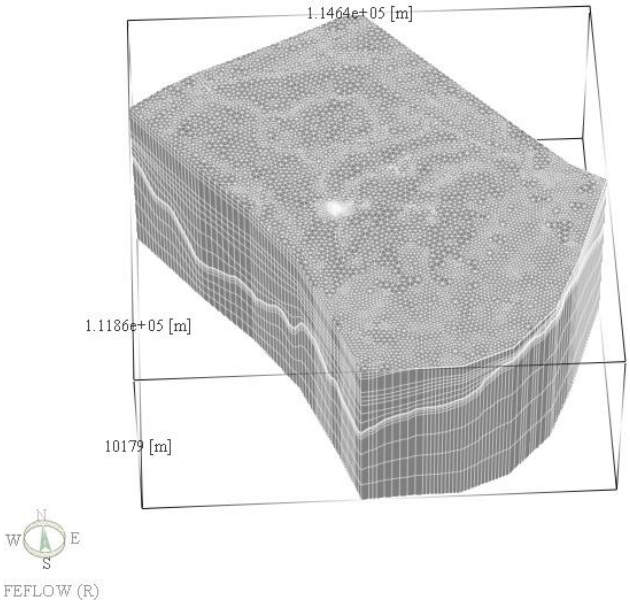

Figure 81: 3D view of the Battonya High pilot's model mesh

4.3.1.2 Geometry

The geometry of the model was created by separating the following master layers:

1. Surface
2. Quarter
3. Upper part of Pannonian
4. Lower part of Pannonian
5. pre-Cenozoic basement

The results of the 3D geological model (3D voxel model of the Pannonian Basin – Geoconnect^{3}d 4.1) were directly used to develop the model geometry. The upper part of the Pannonian is the top level of the slope, while the lower level is the Algyő Formation (the bottom level of the slope).

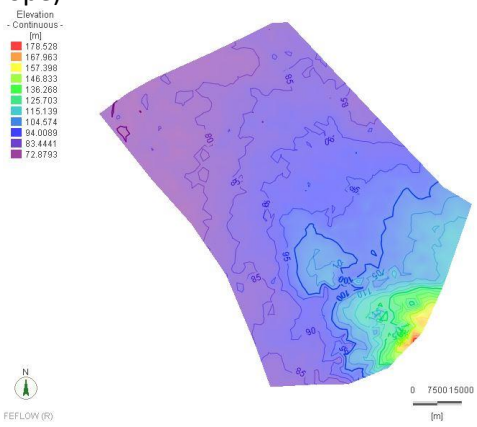

Figure 82: Surface elevation [m.a.s.l.]

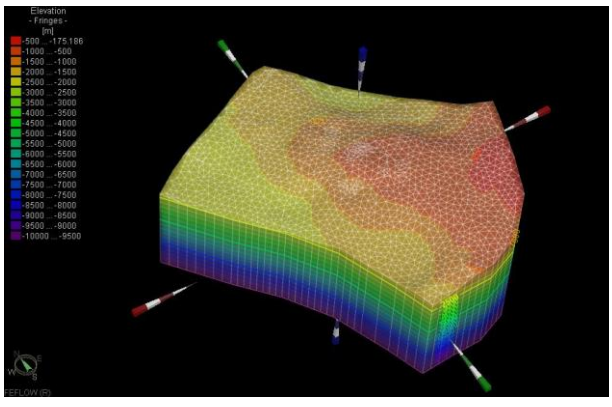

Figure 83: Elevation of the upper part of the Pannonian elevation [m.a.s.l.]

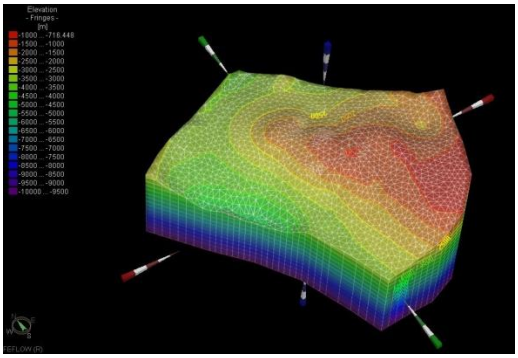

Figure 84: Elevation of the lower part of the Pannonian [m.a.s.l.]

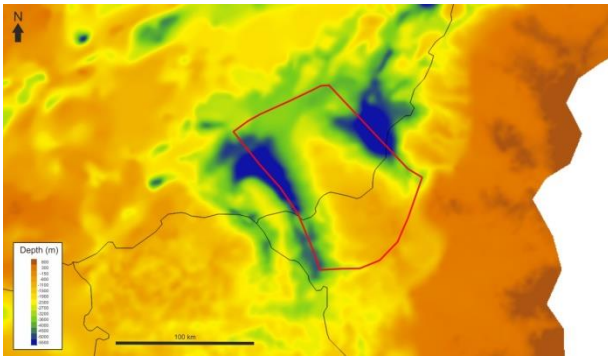

Figure 85: Pre-Cenozoic basement elevation [m.a.s.l.]

4.3.1.3 Hydrodynamic and heat transport parameters

The values of the hydraulic conductivity of the domain are in a wide range of about 5 orders of magnitude. The maximum values are represented in the sedimentary system by gravel, coarse sandy formations, and in the basement by fractured, karstic areas.

Table 12: Range of hydraulic conductivity values applied in the model

Layers	Geological background	Hydraulic conductivity (range, magnitude)
1-10. layer	Downwards fining mainly sand, sandy loam, clay	$K_{xx} = K_{yy}=1,0\times E^{-4} – 1,0\times E^{-9}$ m/s $K_{zz} = 1,0\times E^{-6} – 1,0\times E^{-10}$ m/s
11-18. layer	Crystalline, siliciclastic and carbonate rocks of various fractures	$K_{xx} = K_{yy}= K_{zz} = 1,6\times E^{-7} – 1,0\times E^{-10}$ m/s

The coupled heat flow mechanism in FEFLOW® software can be implemented in several ways. Now, in our model study, we have chosen the heat transfer without density dependence. To simulate geothermal processes, we need to know the thermal conductivity of the rocks, the porosity relevant for heat flow, the heat flux density distribution, the initial temperature distribution, etc.

The value range of thermal conductivity is quite narrow, and can be determined largely from literature data, and to a lesser extent fine-tuned in the calibration phase, based on previous model studies. The thermal conductivity of a water-saturated rock depends on the thermal conductivity of the rock matrix and the porosity.

The thermal conductivity of water is significantly lower than that of the rock matrix, so for water-saturated rocks of the same material, the thermal conductivity of rocks with higher porosity is lower.

In structural trenches and deep basins, the porosity of sediments decreases due to compaction, so the thermal conductivity of water-saturated rock increases with depth. The change in thermal conductivity due to the decrease in porosity could be significant in deep trenches, but the "efficiency" of conductive heat flow is far below that of convective heat transfer, i.e. heat transfer due to fluid flow.

Further trends in thermal conductivity values can be observed: the thermal conductivity of pelitic rocks is lower than that of pseudo-silicic rocks.

The range of values and spatial distribution of the thermal conductivity used in the model is illustrated in Figure 86. Table 12 shows the values and ranges of the parameters used in the model.

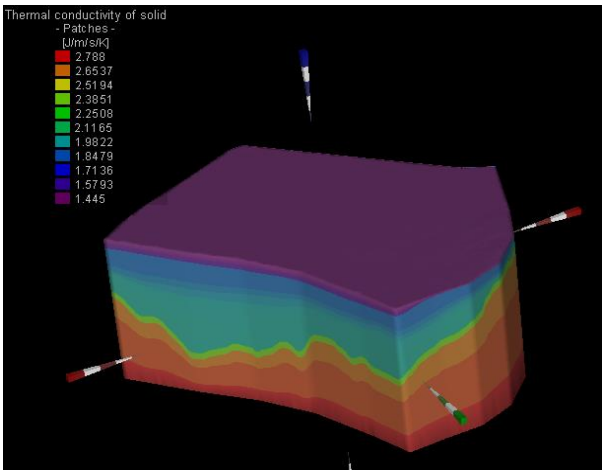

Figure 86: Initial temperature distribution in the model domain

Table 13 Heat transfer modelling Input parameters of the heat transfer modelling

Initial temperature distribution (for each	11.5-420 ºC
Porosity:	0.005-0.3
Specific heat per unit volume of fluid	4.2 MJ/m^{3}K
Volumetric specific heat of rock matrix:	2.52 MJ/m^{3}K
Thermal conductivity of flowing fluid:	0.65 J/m/s/K
Thermal conductivity of rock matrix:	1.8 – 3.48 J/m/s/K
Longitudinal dispersivity:	5 m
Transverse dispersivity:	0.5 m
Temperature boundary condition: Temperature (Type 1) - surface: Temperature (type 1) – bottom of the model	 11.5 ºC 400 ºC / 90 mW/m^2

4.3.1.4 Results

The results confirmed that positive thermal anomaly of the high is caused by the deep fluid flowing through the loose weathered zone, i.e. it is of convective origin (Figure 87). The zone with the better hydraulic conductivity causes flattening at the top of the high (Figure 88).
The model is a good representation of the long-term natural process. Further refined versions of the model will have potential to describe local variations and effects of productions.

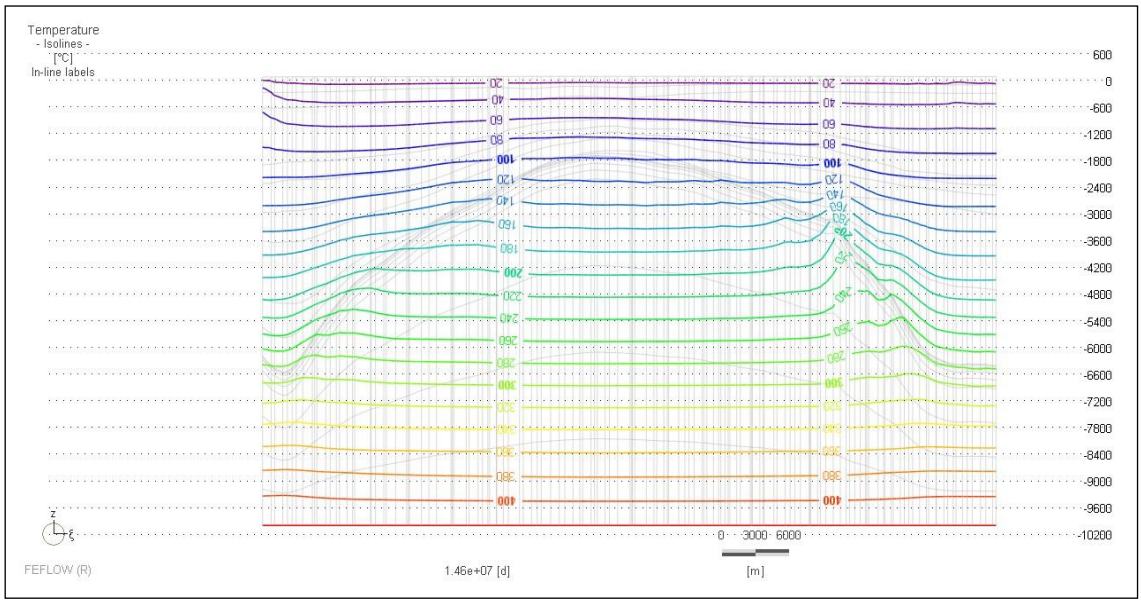

Figure 87: Modelled isotherm distribution (40 thousand years of run, no production) on vertical section [°C]

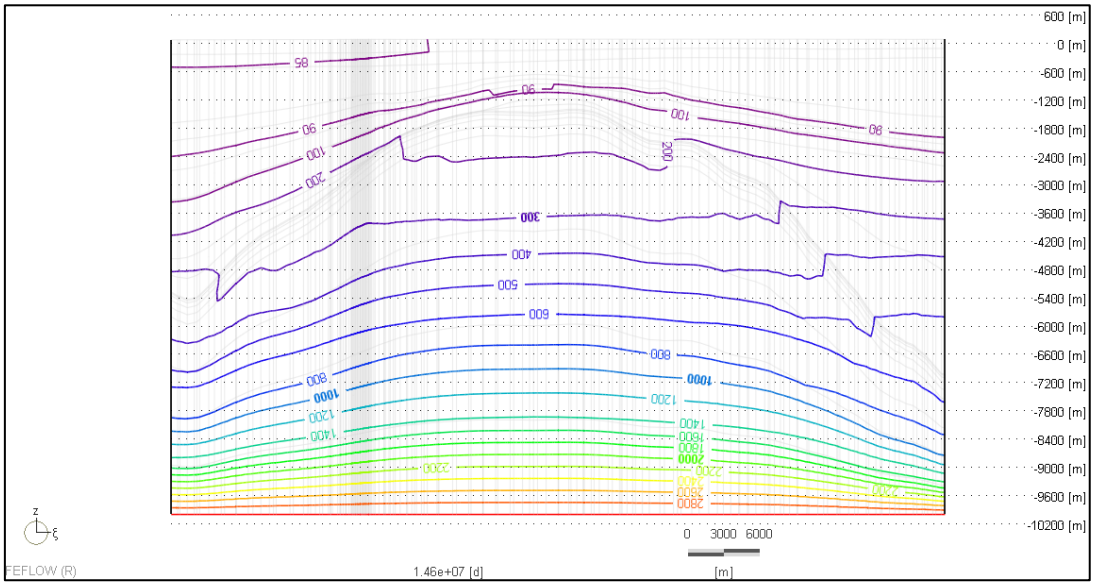

Figure 88: Modelled water level distribution (40 thousand years of run, no production) on vertical section [m.a.s.l.]

More about Hungarian geomanifestations and datasets can be found in the blog posts of the Geoconnect3d project:

Hungary's first interactive geothermal information platform ("OGRe") is publicly available in English, https://geoera.eu/blog/hungary-ogre/
Thermal springs and Water Lily , https://geoera.eu/blog/thermal-springs-and-water-lily/

Global warming on the surface – local warming from plate tectonics: Pannonian Basin, https://geoera.eu/blog/heat-pannonian-basin/

The blood from depths of the SW part of Pannonian basin system, https://geoera.eu/blog/the-blood-from-depths/

Meet the Scientist #11 – Gyula Maros PhD, https://geoera.eu/blog/meet-the-scientist-11/

5 GEOMANIFESTATIONS IN THE PANNONIAN BASIN WITHIN THE BORDER OF BOSNIA AND HERZEGOVINA

Bosnia and Herzegovina (BiH) is located on the extreme southern edge of the Pannonian Basin and therefore has a very complex geological and tectonic structure that has led to the existence of numerous geomanifestations in this area, most often related to regional faults among which is the largest Spreča - Kozara fault.

The Pannonian Basin covers approximately 20% of the territory of BiH. There are several sub-basins within this regional basin; the biggest are Semberija, Posavina i Tuzla basin. Numerous mineral raw materials have been discovered and used in them such as rock salt deposits in the Tuzla basin (Tuzla and Tetima deposits), thermal waters in Semberija (73-75°C) and Posavina (85-96°C). Geothermal reservoirs with greatest yields are located in Semberija ($T_{2,3}$ limestones), less yields are in Posavina (Sarmatian, Badenan and Mesozoic carbonates) and the lowest productivity is in Tertiary sediments of Tuzla basin.

Figure 89: Geomanifestations in Bosnia and Herzegovina

The Spreča-Kozara fault zone is one of the most important tectonic zones in South-eastern Europe with regard to finding mineral, thermal and thermomineral waters what is proven by numerous drillholes (Figure 89). Along this fault vertical displacement up to 2000 m were registered (Hrvatović, 2006). In addition to the mineral, thermal and thermomineral waters and gases, the Spreča-Kozara fault is characterized by different types of mineralization (Cu, Pb, pyrite

and others), numerous deposits of drinking groundwater as well as seismic active zones from which is the well-known Banjaluka region.

5.1 Geomanifestations linked to waters

Important phenomena of geomanifestations - mineral, thermal and thermomineral waters in the Pannonian Basin and along the regional Spreča-Kozara fault zone which represents the border between the Pannonian Basin and the Dinaride Ophiolite Zone were treated within the GeoConnect3d project. A total of 41 geomanifestations were processed (Table 14).

Table 14: Types of geomanifestation linked to waters in Bosnia and Herzegovina

Type of geomanifestation	No.
Mineral water (M)	12
Thermal water (TH)	13
Thermomineral water (THM)	16
SUM	**41**

As a criterion for mineral, thermal and thermomineral waters, the definitions prescribed by the Rulebook on the classification, categorization and calculation of groundwater reserves and the flow of their monitoring (Official Gazette of Federation of B&H, no. 47/11) have been taken:
"Mineral water" is groundwater with a mineralisation greater than 1 g/l, as well as the water with a mineralisation less than 1 g/l containing trace elements that may have a pharmacodynamic effects on the human body. The temperature of mineral water is less than or equal to the average annual air temperature of the area in which this water is located. The pharmacodynamic effects of certain microelements on the human body must be proven by tests in a verified health institution;

"Thermal water" is every groundwater whose temperature is higher than the average annual air temperature of the area where these waters are located.

"Thermomineral water" is mineral water whose temperature is higher than the average annual air temperature of the area where these waters are located and mineral waters properties also apply.

A total of 41 geomanifestations were processed and presented in the GeoConnect3d project database. Some characteristics of processed geomanifestations are shown in Table 15: water type (M-mineral, TH-thermal and THM - thermomineral water), temperature and CO_2 content. In the concept column, the most dominant property of water is given. Each geomanifestation is followed by appropriate photo or fact sheet on the web portal.

Table 15: Main characteristics of geomanifestations in BiH

geometryID	conceptID	localName	Type of water	Concept	Average temperature (°C)	Average CO_2 (g/l)
FZZG_g001	FZZG_c001	Well SB-1 Lješljani	THM	Hyperalcaline water	30,5	0,024

geometryID	conceptID	localName	Type of water	Concept	Average temperature (°C)	Average CO_2 (g/l)
FZZG_g002	FZZG_c002	Thermal spring Laktaši	TH	Thermal water	31	0,27
FZZG_g003	FZZG_c003	Well SL-1 Slatina	THM	CO_2 water	44	1,6
FZZG_g004	FZZG_c004	Well Kokori	TH	Thermal water	21	
FZZG_g005	FZZG_c005	Well B-5 Kulaši spa	TH	Hyperalcaline water	29,5	0,033
FZZG_g006	FZZG_c006	Well PEB-4 Ćelahuša	THM	CO_2 water	37,7	
FZZG_g007	FZZG_c007	Well OB-1 Boljanić	THM	CO_2 water	24,5	1,5
FZZG_g008	FZZG_c008	Well BD-1 Ljenobud	TH	Thermal water	29	0,018
FZZG_g009	FZZG_c009	Kiseljak Srebrenik	M	CO_2 water	14,8	0,57
FZZG_g010	FZZG_c010	Kiseljak Zahirovići	M	CO_2 water	12,2	0,66
FZZG_g011	FZZG_c011	Kiseljak Dragunja	M	CO_2 water	17,2	
FZZG_g012	FZZG_c012	Artesian thermal well in Suvo Polje	TH	Thermal water	17,4	
FZZG_g013	FZZG_c013	Well BM-2 - Kiseljak-Tuzla	TH	Hyperalcaline water	20	
FZZG_g014	FZZG_c014	Well "Novi izvor" Kiseljak	M	CO_2 water	13,5	
FZZG_g015	FZZG_c015	Well IEB-1 Ljubače	M	CO_2 water	13,5	0,53
FZZG_g016	FZZG_c016	Well PBS-2 Barice	M	CO_2 water	12	1,4
FZZG_g017	FZZG_c017	Spting Toplica	TH	Thermal water	24	
FZZG_g018	FZZG_c018	Well SL-1 Slavinovići	THM	Thermal water	34	
FZZG_g019	FZZG_c019	Well Tr-167 Trnovac	THM	Brine – salt water	19	
FZZG_g020	FZZG_c020	Well IB-2 Tušanj	THM	Brine – salt water	16,5	
FZZG_g021	FZZG_c021	Well DS-7 Tetima	THM	Brine – salt water	15	
FZZG_g022	FZZG_c022	Well TD-23 Tetima	THM	Brine – salt water	18,1	
FZZG_g023	FZZG_c023	Spring "Kiseljak Dubnica"	M	CO_2 water	13,6	
FZZG_g024	FZZG_c024	Spring "Rasol"	THM	H_2S water	24	
FZZG_g025	FZZG_c025	Spring "Kiseljak Jasenica"	M	CO_2 water	12,8	1,7
FZZG_g026	FZZG_c026	Well B-2 Kozluk	M	CO_2 water	14	3,5
FZZG_g027	FZZG_c027	Well GD-2 Slobomir	TH	Thermal water	73	0,0
FZZG_g028	FZZG_c028	Well S-1 Dvorovi	TH	Thermal water	75	0,07
FZZG_g029	FZZG_c029	Well B-5 Gradačac Spa	THM	Thermal water	28,8	
FZZG_g030	FZZG_c030	Well EB-1 Gradačac	TH	Thermal water	30	
FZZG_g031	FZZG_c031	Old thermal well in Gradačac (RIS NAUTIC)	TH	Thermal water	19	
FZZG_g032	FZZG_c032	Well Do-3/B Domaljevac	THM	Geothermal energy, geothermal heat exchangers borehole	86	

geometryID	conceptID	localName	Type of water	Concept	Average temperature (°C)	Average CO_2 (g/l)
FZZG_g033	FZZG_c033	Well Do-1 Domaljevac	THM	Geothermal energy, geothermal heat exchangers borehole	96	0,18
FZZG_g034	FZZG_c034	Thermal well in Kadar-Odžak	TH	Thermal water	19,8	
FZZG_g035	FZZG_c035	Thermal well BV-1 - Odžak	TH	Thermal water	18	
FZZG_g036	FZZG_c036	Mineral spring and well of Mlječanica	M	H_2S water	13,1	
FZZG_g037	FZZG_c037	Springs and wells of Gornji Šeher	THM	CO_2 water	35	0,19
FZZG_g038	FZZG_c038	Spring and wells -Vrućica Spa-Teslić	THM	CO_2 water	38	1,4
FZZG_g039	FZZG_c039	Spring and wells in Dolac-Tešanj	THM	CO_2 water	22	2,8
FZZG_g040	FZZG_c040	Spring Kiseljak Crni vrh	M	CO_2 water	13	1,6
FZZG_g041	FZZG_c041	Kiseljak Orašje Planje	M	CO_2 water	12	3,68

5.2 Discussion

In general, hyperalkaline waters are accumulated in ophiolite rocks or have some contact with them, while thermal water aquifers are usually limestones and dolomites of Mesozoic age. Salt waters are accumulated in Miocene clastites (Tuzla Basin), while H_2S waters are formed in Tertiary clastites (Mlječanica and Rasol-Priboj). CO_2 waters occur in zones of deep faults and their springs are often arranged linearly in the space.

Some of the characteristics on the most important geomanifestations are:

- Well SB-1 Lješljani has the highest CH_4 concentration (2706 mM) and pH (12.8) ever reported so far in peridotite-hosted hyperalkaline waters (Etiope at al., 2017). The water of Lješljani deposit occurs on two springs and a drillhole SB-1 (672 m) with a total yield about Q≈7 l/s. This water is characterized by Cl-OH-Na type, high conductivity EC=3,98 – 5,18 mS/cm and pH=12,0 – 12,8, as well as CH_4 (with its higher homologues) and N_2 free gasses composition.

- The highest temperature of water in Bosnia and Herzegovina is on the well Do-1 (1275,4 m) in Domaljevac (96°C on wellhead with natural outflow Q=22,2 l/s); aquifer of water are Sarmatian, Badenian and Mesozoic carbonates. Well Do-3/B Domaljevac with total depth of 1500 m has wellhead water temperature t= 86 ° C and EC = 19.330 µS/cm.

- Deep geothermal aquifers of thermal waters with greatest yields without natural springs are located in Semberija (K_2 and $T_{2,3}$ limestones). This spacious and very water - bearing

aquifer was found by two productive wells S-1 and GD-2, which have water temperature 75°C and 73°C.

- The most productive aquifer of thermal waters in Pannonian Basin with natural springs are Triassic limestones at locations: Toplica Spreča and Laktaši. Total yield of springs and wells in Toplica-Spreča is 250 l/s (t=24°C) and in Laktaši about 100 l/s (t=31°C).

- Hydrocarbonate - sulphate thermomineral water in Ilidža – Gradačac (well B-5 Gradačac Spa) issue in the fault zone from Sarmatian and Tortonian sediments, and in the same sediments 300–1.000 meters farther were drilled thermal HCO_3 waters (wells Well EB-1 Gradačac and RIS NAUTIC), which are in interference with the first waters. Mineralization of thermomineral water is about 1,3 g/l, and thermal 0,5 g/l.

- The highest mineralization (up to 320 g /l) have salt waters (brines) of Tuzla (wells in Trnovac i Tušanj) and Tetima, which originate from rock salt formation formed in the Miocene; the temperature of these waters is up to 27 °C.

- The highest value of the convective heat flow in BiH is obtained at drillhole Sl-1-Slavinovići (134.9 mW/m^2 for depth of 540 m of measured temperature) - Miošić, 2003. Thermomineral water of well Sl-1 has high mineralization (7.2 g/l), temperature of 34°C and dominant methane free gas; natural outflow of the well is about 5 l/s.

- Thermomineral waters with CO_2 exist in Slatina, Teslić, Boljanić, Ćelahuša, Sočkovac and they are in the relation with Spreča - Kozara fault zone. All of these deposits have drillholes/wells with great capacities of waters with free CO_2, especially high capacity of artesian waters were obtained at deposit Ćelahuša - Sočkovac in more wells, which have mutual hydraulic interference. Before construction of wells were natural springs of these waters at all deposit.

- Mineral CO_2 waters are generally with low yield, most often below 5 l/s (Jasenica, Kozluk, Dragunja, Dubnica, Srebrenik, Zahirovići, Barice, Crni vrh, Oraš Planje dr.).

- Origin of sulphate water with H_2S is in relation with dissolution of Tertiary sulphate evaporites (Mlječanica, Rasol-Priboj).

More about these geomanifestations can be found in the blog posts of the Geoconnect3d project:
https://geoera.eu/blog/significant-geomanifestations-in-bosnia-and-herzegovina/

Meet the Scientist #9 – Natalija Samardžić, https://geoera.eu/blog/meet-the-scientist-9/

Land subsidence as a consequence of artificial uncontrolled leaching of salt layers and forming of lakes “Pannonica” in Tuzla, Bosnia and Herzegovina, https://geoera.eu/blog/land-subsidence-salt-layers/

Significant geomanifestations along the contact of South Pannonian Basin and Dinaride Ophiolite Zone in Bosnia and Herzegovina, https://geoera.eu/blog/significant-geomanifestations-in-bosnia-and-herzegovina/

6 CONCLUSIONS

We identified many geomanifestations and were able to connect them to the regional structures. It is worth noticing that classification of mineral and thermal waters is diverse among the countries. Thermomineral water is a combination of the two. So when using this data further, one has to check its definitions first (Table 16). We also tested two transboundary numerical models in FEFLOW to evaluate the structural effect on geothermal anomalies.

Table 16: Comparison of definitions of waters among countries

Country	Mineral water	Thermal water
Bosnia & Herzegovina	1 g/l TDS, elevated trace elements	T > average annual air temperature
Croatia	According to EC directive on natural mineral waters	
Hungary		> 30 °C
Romania	≥ 1 g/l TDS, elevated trace elements, ≥ 1 g/l free CO_2	> 20 °C
Slovenia	Not defined but in practice used as 1 g/l TDS, elevated trace elements, >250 g/l free CO_2	> 20 °C

All in all, we identified the following:

In the Mura-Zala basin between Croatia, Hungary and Slovenia, we listed 9 wells with convection cells, 8 mofettes, 8 natural mineral waters, 6 mineral waters, 22 thermal and 17 thermomineral waters. There are actually more objects (wells) existing, as in Slovenia we reported only one well site as a representative when several wells or springs tapped the same water/aquifers. Mineral occurrences are rare, only 4. Organic matter occurrences are abundant, 78 coal sites, 1 oil spring, 5 gas fields, 6 oil fields and 17 oil and gas fields. Mantle helium exhalation is evident at 17 sites.

Thermal waters occur at various systems. The ones linked to warm spring systems emerge along (regional or local) faults in carbonates at basin outskirts while most waters are tapped from stratified Neogene strata in the sedimentary basin.

Along the Ljutomer fault zone we interpreted: convection cells causing geothermal anomalies, seismic activity, and structural traps resulting in hydrocarbon accumulations.

Along the Raba fault zone we interpreted: convection cells causing geothermal anomalies, some seismic activity at its western part, mineral and thermomineral waters, and CO_2 and mantle helium exhalations.

Along the Periadriatic fault system, where the Labot and Šoštanj fault zones join, we identified seismic activity, mineral and thermomineral waters, and CO_2 and mantle helium exhalations.

At Battonya High between Hungary and Romania, we identified convection cells causing geothermal anomalies, hydrocarbon accumulations, over-pressured zones, density-driven flow

systems, 17 mineral and 163 thermal waters and 19 seismic events. Here, geomanifestations are linked to fault zones in the basement and weathered zone on top of it, mainly.

In north Bosnia and Herzegovina, we identified 12 mineral, 13 thermal and 16 thermomineral waters along the Spreča-Kozara fault zone, which represents the border between the Pannonian Basin and the Dinaride Ophiolite Zone.

7 REFERENCES FOR STRUCTURAL FRAMEWORK

Argand, E. 1924: Des Alpes et de l'Afrique. – Bullétin de la Societé Vaudoise des Science Naturelles 55 (214), pp. 233–236

Bada, G., Horváth, F., Dövényi, P., Szafián, P., Windhoffer, G., Cloetingh, S. 2007b: Present-day stress field and tectonic inversion in the Pannonian basin. – Global and Planetary Change 58 (1–4), pp. 165–180.

Balázs, A., L. Matenco, I. Magyar, F. Horváth, and S. Cloetingh (2016): The link between tectonics and sedimentation in back-arc basins: New genetic constraints from the analysis of the Pannonian Basin, Tectonics, 35, 1526–1559, doi:10.1002/2015TC004109

Báldi, T. 1986: Mid-Tertiary stratigraphy and paleogeographic evolutionof Hungary. – Akadémiai Kiadó, Budapest, 201 p.

Balla, Z. 1988: On the Origin of the structural pattern of Hungary. – Acta Geologica Hungarica 31 (1–2), pp. 53–63.

Balla, Z., 1984: The Carpathian loop and the Pannonian basin: a kinematic analysis. – Geophysical Transactions 30 (4), pp. 313–353.

Balla, Z., 1986: Paleotectonic reconstruction of the central Alpine–Mediterrancan belt for the Neogene. – Tectonophysics 127, pp. 213–243.

Barros, R., Piessens, K. 2020: Two-step Structural Framework- Geomanifestations methodology — D2.4 Report WP2, 26 p.

Bereczki, L., Markos, G., Gärtner, D., Friedl, Z., Musitz, B., Maros, Gy. 2017: Szerkezeti modellezések a Pannon-medence szinrift részmedencéiben. – Extended abstract, 8. Kőzettani és geokémiai vándorgyűlés, MFGI, Budapest, pp. 25–26.

Budai, T., Maros, Gy. 2018: Geology of Hungary – an introduction to the geology of the sub-basins In: Kovács Zs. (ed.) 2018: Hydrocarbons in Hungary — Hungarian Energy and Public Utility Regulatory Authority, Budapest, pp. 19-27.

Channell, J. E. T., Horváth, F. 1976: The African/Adriatic promontory as a paleogeographical premise for Alpine orogeny and plate movements in the Carpatho–Balkan region. – Tectonophysics 35, pp. 71–101.

Csontos, L., Nagymarosy, A. 1998: The Mid-Hungarian line: a zone of repeated tectonic inversions – Tectonophysics 297, pp. 51–71.

Csontos, L., Nagymarosy, A., Horváth, F., Kovác, M. 1992: Tertiary evolution of the Intra Carpathian area: a model. – Tectonophysics 208, pp. 221–241.

Csontos, L., Vörös, A. 2004: Mesozoic plate tectonic reconstruction of the Carpathian region. – Palaeogeography, Palaeoclimatology, Palaeoecology 210, pp. 1–56.

Dewey, J. F. 1980: Episodicity, sequence and style at convergent plate boundaries. –In: Strangway, D. W. (ed.): The Continental Crust and its Mineral Deposits. – Special Paper 20., Geol. Assoc. Canada, Waterloo, Ontario pp. 553–573.

Fodor L. 2010: Mezozoos–kainozoos feszültségmezők és törésrendszerek a Pannon-medence ÉNy-i részén – módszertan és szerkezeti elemzés. – Akadémiai doktori értekezés 167 p.

Fodor L., Csontos L., Bada G., Györfi I., Benkovics L. 1999: Tertiary tectonic evolution of the Pannonian Basin system and neighbouring orogens: a new synthesis of paleostress data. – In: Durand, B., Jolivet, L., Horváth, F., Séranne, M. (eds): The Mediterranean Basins: tertiary Extension within the Alpine Orogen. – Geological Society, London, Special Publications 156, pp. 295–334.

Fodor, L., Csontos, L., Bada, G., Győrfi, I., Benkovics, L. 1999: Cenozoic tectonic evolution of the Pannonian basin system and neighbouring orogens: a new synthesis of paleostress data. In: Durand, B., Jolivet, L., Horváth, F., Séranne, M. (Eds.): The Mediterranean basins: Cenozoic extension within the Alpine orogen. Geological Society, London, Special Publications 156, 295-334.

Fodor, L., Jelen, B., Márton, E., Skaberne, D., Čar, J., Vrabec, M. 1998: Miocene–Pliocene tectonic evolution of the Slovenian Periadriatic Line and surrounding area – implication for Alpine-Carpathian extrusion models. – Tectonics 17, pp. 690–709.

Froizheim, N., Plašienka, D., Schuster, R. 2008: Alpine tectonics of the Alps and Western Carpathians. – In: McCann, T. 2008: The Geology of Central Europe Vol. 2. The Geological Society, London, pp. 1141–1232.

Grenerczy, Gy., Sella, G. F., Stein, S., Kenyeres, A. 2005: Tectonic implications of the GPS velocity field in the northern Adriatic region. – Geophysical Research Letters 32, L16311.

Haas, J. (ed.), Hámor, G., Jámbor, Á., Kovács, S., Nagymarosy, A., Szederkényi, T. 2001: Geology of Hungary – Eötvös University Press, Budapest, 317 p.

Haas, J., Mioč. P., Pamić, B., Tomljenović, P., Árkai, P., Bérczi-Makk, A., Koroknai, B., Kovács, S., Rálisch-Felgenhauer, E. 2000: Complex structural pattern of the Alpine-Dinaridic-Pannonian tripple junction. – Int. Journal Earth Sci. 89, pp. 377–389.

Handy M. R. Ustaszewski K.·Kissling E 2014: Reconstructing the Alps–Carpathians–Dinarides as a key to understanding switches in subduction polarity, slab gaps and surface motion — Int J Earth Sci (Geol Rundsch) DOI 10.1007/s00531-014-1060-3

Handy, M. R., Ustaszewski, K., Kissling, E. 2014 Reconstructing the Alps–Carpathians–Dinarides as a to understanding switches in subduction polarity, keyslab gaps and surface motion.– International Journal of Earth Sciences (Geol. Rundsch.) DOI: 10.1007/s00531-014-1060-3 Published online

Horváth, F. 1995: Phases of compression during the evolution of the Pannonian basin and its bearing on hydrocarbon exploration. – Mar. Petr. Geol. 12, pp. 837–844.

Horváth, F. 2007: A Pannon-medence geodinamikája. – Akadémiai doktori értekezés 239 p.

Horváth, F., Bada, G., Szafián, P., Tari, G., Ádám, A. and Cloetingh, S., 2006: Formation and deformation of the Pannonian Basin: constraints from observational data. In: D.G. Gee and R.A. Stephenson (Editors), European Lithosphere Dynamics. Geological Society, London, Memoir 32: 191-206.

Horváth, F., Cloetingh, S. 1996: Stress-induced late stage subsidence anomalies in the Pannonian basin. – Tectonophysics 266, pp. 287–300.

Horváth, F., Musitz, B., Balázs, A., Végh, A., Uhrin, A., Nádor, A., Koroknai, B., Pap, N., Tóth T., Wórum G. 2015: Evolution of the Pannonian basin and its geothermal resources.– Geothermics 53, pp. 328–352.

Horváth, F., Rumpler, J. 1984: The Pannonian basement: extension and subsidence of an Alpine orogene. Acta Geologica Hungarica 27, pp. 147–154.

Kázmér, M., Kovács, S. 1985: Permian-Paleogene Paleogeography along the Eastern part of the Insubric-Periadriatic Lineament system: Evidence for continental escape of the Bakony-Drauzug Unit. – Acta Geologica Hungarica 28, pp. 71–84.

Kovács, I., Falus, Gy., Stuart, G., Hidas, K., Szabó, Cs., Flower, M. F. J., Hegedűs, E., Posgay, K., Zilahi-Sebess, L. 2012: Seismic anisotropy and deformation patterns in upper mantle xenoliths from the central Carpathian–Pannonian region: Asthenospheric flow as a driving force for Cenozoic extension and extrusion? – Tectonophysics 514–517, pp. 168–179.

Lenkey, L. 1999: Geothermics of the Pannonian basin and its bearing on the tectonics of basin evolution. – PhD thesis, Vrije Univ., Amsterdam, 215 p.

Magyar, I., Geary, D.H. & Müller, P. 1999: Paleogeographic evolution of the Late Miocene Lake Pannon in Central Europe. – Palaeogeogr. Palaeoclimatol. Palaeoecol. 147, 151–167.

Márton, E. 2001: Tectonic implications of Tertiary paleomagnetic results from the PANCARDI area (Hungarian contribution). – Acta Geologica Hungarica 44, pp. 135–144.

Márton, E., Fodor, L. 2003: Tertiary paleomagnetic results and structural analysis from the Transdanubian Range (Hungary): Rotational disintegration of the AlCaPa unit. – Tectonophysics 363 (3–4), pp. 201–224.

Márton, E., Tischler, M., Csontos, L., Fügenschuh, B., Schmid, S. 2007: The contact zone between the AlCaPa and Tisza–Dacia mega-tectonic units of Northern Romania in the light of new paleomagnetic data. – Swiss J. Geosci. 100, pp. 109–124.

Matenco, L., Radivojević, D. 2012: On the formation and evolution of the Pannonian Basin: Constraints derived from the structure of the junction area between the Carpathians and Dinarides. – Tectonics 31, TC6007, doi:10.1029/2012TC003206

McKenzie, D. 1978: Some remarks on the development of sedimentary basins. – Earth and Planet. Sci. Lett. 40, pp. 25–32.

Mioč, P. 2003: Outline of the geology of Slovenia — Acta Geologica Hungarica, Vol. 46/1. pp. 3-27.

Palotai, M. 2013: Oligocene−Miocene Tectonic Evolution of the Central Part of the Mid-Hungarian Shear Zone A Közép-Magyarországi Zóna középső részének oligocén−miocén szerkezetfejlődése — PhD thesis Eötvös Loránd University 148. p.

Ratschbacher, L., Frisch, W., Lintzer, H. G., Merle, O. 1991: Lateral extrusion in the Eastern Alps. Part 2. Structural analysis. – Tectonics 10 (2), pp. 257–271.

Royden, L. H., Horváth F. (eds) 1988: The Pannonian Basin. A study in basin evolution. – AAPG Memoir 45, 394 p.

Schmid, M.S., Bernoulli, D., Fügenschuh, B., Matenco, L., Schefer, S., Schuster, R., Tischler, M., Ustaszewski, K. 2008: The Alpine-Carpathian-Dinaridic orogenic system: correlation and evolution of tectonic units DOI 10.1007/s00015-008-1247-3 Birkhäuser Verlag, Basel, 2008

Schmid, S. M., Fügenschuh, B., Kissling, E., Schuster, R. 2004: Tectonic map and overall architecture of the Alpine orogen. – Eclogae Geol. Helvet. 97, pp. 93–117.

Sebe, K., Selmeczi I., Szuromi-Korecz A., Hably, L., Kovács, Á., Benkó, Zs. 2018: Miocene syn-rift lacustrine sediments in the Mecsek Mts. (SW Hungary). – Swiss Journal of Geosciences 112, pp. 83–100.

Stampfli, G. M., G. Borell, 2004: The TRANSMED transsects in space and time: constraints on the paleotectonic evolution of the Mediterranean domain. – In: Cavazza, W., Roure, F., Spackman, W., Stampfli, G. M., Ziegler, P. (eds): The TRANSMED Atlas. – Springer, Berlin, Heidelberg, New York, pp. 53–80.

Tari G., Báldi T., Báldi-Beke M. 1993: Paleogene retroarc flexural basin beneath the Neogene Pannonian Basin: a geodynamic model. — Tectonophysics 226, pp. 433−455.

Ustaszewski, K., S. Schmid, B. Fügenschuh, M. Tischler, E. Kissling, And W. Spakman 2008: A map-view restoration of the Alpine-Carpathian-Dinaridic system for the early Miocene, Swiss, J. Geosci. Prague, 101, 273–294, doi:10.1007/s00015-008-1288-7.

8 REFERENCES FOR MURA-ZALA BASIN

Alföldi, L., Gálfi, J., Liebe, P., 1985: Heat flow anomalies caused by water circulation. J. Geodyn. 4, 199-217.

Andrews, J.N., Burgess, W.G., Edmunds, W.M., Kay, R.L.F., Lee, D.J., 1982: The thermal spring of Bath. Nature, 298, 339-343.

Békési, E., Lenkey, L., Limberger, J., Porkoláb, K., Balázs, A., Bonté, D., Vrijlandt, M., Horváth, F., Cloetingh, S., Wees, J.D. 2018: Subsurface temperature model of the Hungarian part of the Pannonian Basin. Global and Planetary Change, 171, 48-64. DOI.org/10.1016/j.gloplacha.2017.09.020

Benoit, W.R., 1978: The use of shallow and deep temperature gradients in geothermal exploration in northwestern Nevada using the Desert Peak thermal anomaly as a model, Geothermal Resources Council Trans., 2, 45-46.

Blackwell, D.D., Morgan, P., 1976: Geological and geophysical exploration of the Marysville geothermal area, Montana, USA. In Proc. Second UN Symposium on the Development and Use of Geothermal Resources, San Francisco, 895-902.

Bräuer, K., Geissler, W., Kämpf, H., Niedermann, S., Rman, N., 2016. Helium and carbon isotope signatures of gas exhalations in the westernmost Pannonian Basin (SE Austria/ NE Slovenia): evidence for active litospheric mantle degassing. Chem. Geol. 422, 60–70.

Chapman, D.S., Howell, J., Sass, J.H., 1984: A note on drillhole depths required for reliable heat flow determinations. Tectonophysics, 103/1-4, Elsevier, 11-18.

Djurasek, S. 1988: Rezultati suvremenih geofizičkih istraživanja u SR Sloveniji (1985-1987). (Results of geophysical exploration in Slovenia (1985-1987)). Nafta, 39, 311-326.

Gabor, L., Rman, N. 2016: Mofettes in Slovenske gorice, Slovenia. Geologija 59/2, 155-177. DOI: 10.5474/geologija.2016.009

GeoZS, 2014: Programme Groundwaters and Geochemistry, 2004 – 2019. Funded by the Slovenian Research Agency.

Gosar, A. 1994/95: Modeliranje refleksijskih seizmičnih podatkov za podzemno skladiščenje plina v strukturah Pečarovci in Dankovci - Murska depresija. (Modelling of seismic reflection data for underground gas storage in the Pečarovci and Dankovci structure – Mura depression). Geologija, 37/38, 483-549.

Gosar, A. & Ravnik, D. 2007: Uporabna geofizika - univerzitetni učbenik za študente geologije, geotehnologije in rudarstva. Naravoslovnotehniška fakulteta, Oddelek za geotehnologijo in rudarstvo, Ljubljana, 218 p.

Gosar, M., Šajn, R., Miler, M., Burger, A. & Bavec, Š. (2020). Overview of existing information on important closed (or in closing phase) and abandoned mining waste sites and related mines in Slovenia. Geologija, 63: 221–250. https://doi.org/10.5474/geologija.2020.018

Goetzl, G., Zekiri, F. 2012: Summary report “Geothermal Models at Supra-Regional Scale”. Report for project Transenergy.

Graczer Z. et al, 2002-2018: Hungarian National Seismological Bulletin HU ISSN 2063-8558 avaiable on: http://www.seismology.hu/index.php/en/seismicity/earthquake-bulletins/31-hungarian-national-seismological-bulletin

Griesser, J.C., Rybach, L., 1989: Numerical thermohydraulic modeling of deep groundwater circulation in crystalline basement: an example of calibration. International Union of Geodesy and Geophysics and American Geophysical Union, 65-74.

Grünthal, G., Wahlström, R., Stromeyer, D. 2013: The SHARE European Earthquake Catalogue (SHEEC) for the time period 1900-2006 and its comparison to the European Mediterranean Earthquake Catalogue (EMEC). Journal of Seismology (submitted).

Hasenhüttl, C., Kraljić, M., Sachsenhofer, R.F., Jelen, B. & Rieger, R. 2001: Source rocks and hydrocarbon generation in Slovenia (Mura Depression, Pannonian Basin). Marine and Petroleum Geology, 18: 115-132, doi:10.1016/S0264-8172(00)00046-5.

Herak, M., Herak, D., and Markušic, S. 1996: Revision of the earthquake catalogue and seismicity of Croatia, 1908-1992. Terra Nova, 8, 86-94.

HGI-CGS, 2021: Croatian Research Agency financing.

Ionescu, A., Rman, N. 2021: Unpublished data on samples within a Deep Carbon Observatory project “Improving the estimation of the tectonic carbon flux”. University of Perugia and GeoZS

Ivanković, J., Nosan, A. 1973: Hydrogeology of Čatež Spa (in Slovene). Geologija 16, 353-361, http://www.geologija-revija.si/dokument.aspx?id=252

Jaffé, F.C., Rybach, L., Vuataz, F., 1976: Thermal springs in Switzerland and their relation to seismotectonic features. In: Proc. Int. Congr. On Thermal Waters, Geothermal Energy and Volcanology of the Mediterranean Area, Vol. I, Athens, 275-285.

Jurišić-Mitrović, V. 2001: Report on the results of chemical analyzes of water samples for the task "Monograph of thermal and mineral springs of the Republic of Croatia". HGI, Zagreb (in Croatian).

Kerčmar, J. 2018: Nahajališča zemeljskega plina na nafto-plinskem polju Petišovci. Geologija 61/2, 163-176, Ljubljana.

Kilty, K., Chapman, D.S., Mase, C.W., 1979: Forced convective heat transfer in the Monroe hot springs geothermal system. J. Volcanol. Geothermal Res. 6, 257-277.

Kruk, B., Kastmuller, Ž., Kruk, Lj., Miko, S. & Dedić, Ž. 2006: Resource of mineral raw materials in the area of Međimurje County. Unpl. Croatian Geological Survey, Zagreb (in Croatian)

Lapajne, J. 1975: Geophysical research in area of Čatež Spa (in Slovene). Geologija 18, 315-324 http://www.geologija-revija.si/dokument.aspx?id=332

Lapanje, A., Jelen, B., Rifelj, H., Mozetič, S., Rman, N., Ferjan, T., Rikanović, R., Matoz, T., 2008: Hydrogeological professional grounds for granting water rights for explotation of mineral water in Nuskova. Report in Slovenian in archives of GeoZS. Funded by the Rajska oaza d.o.o.

Lenkey, L., Dövényi, P., Horváth, F., Cloetingh, S., 2002: Geothermics of the Pannonian Basin and its bearing on the neotectonics. EGU Stephan Mueller Special Publication Series 3., 29–40.

Lenkey, L., Raáb, D., Goetzl, G., Lapanje, A., Nádor, A., Rajver, D., Rotár-Szalkai, A., Svasta, J., Zekiri, F., 2017: Lithospheric scale 3D thermal model of the Alpine-Pannonian transition zone. Acta Geod. Geophys., DOI 10.1007/s40328-017-0194-8

Markič, M. 2017: High arsenic (As) content in coals from Neogene deposits of the Pannonian Basin in Slovenia. Geologija 60/2, 173-180.

Markič, M., Toman, M. 2011: GeoZS Report Arch. No: C-II-30d/b1-1/44, 6p.

Markič, M., Turk, V., Kruk, B., Šolar, S.V., 2011: Coal in the Mura Formation (Pontian) between Lendava (Slovenia) and Mursko Središće (Croatia), and in the wider area of NE Slovenia (in Slovenian). Geologija, 54/1, 97-120, doi: 10.5474/geologija.2011.008.

Markič, M., Lapanje, A., Rajver, D., Rman, N., Šram, D., Kumelj, Š. 2016: Geological evaluation of potential unconventional oil and gas resources in Europe – Evaluation of the potential in Slovenia - H2020 call, B.2.9.: "Energy Policy support on unconventional gas and oil" from the European Commission, by JRC-IET, service contract no. 11411 between The European Union and GEUS and subcontracting agreement between GEUS and GeoZS. Geological Survey of Slovenia, 37 p.

Mintell4EU, 2020. https://geoera.eu/projects/mintell4eu7/

Mioč, P. & Marković, S. 1998: Basic geological map of Slovenia and Croatia – Čakovec 1:100.000 (in Slovene with Eng. Summary). Inštitut za geologijo, geotehniko in geofiziko, Ljubljana in Inštitut za geološka istraživanja, Zagreb.

Nador, A., Lapanje, A., Toth, G., Rman, N., Szocs, T., Prestor, J., Uhrin, A., Rrajver, D., Fodor, L., Murati, J., Szekely, E. 2012: Transboundary geothermal resources of the Mura-Zala basin: a need for joint thermal aquifer management of Slovenia and Hungary. Geologija 55/2, 209-224, doi:10.5474/geologija.2012.013

Nosan, A. 1959: Hydrogeology of Čatež Spa (in Slovene). Geologija 5, 63-79, http://www.geologija-revija.si/dokument.aspx?id=79

Novak, M., Rman, N., 2016. Geološki atlas Slovenije. Geološki zavod Slovenije, Ljubljana. 124 pp.

Pezdič, J., Dolenec, T., Pirc, S., Žižek, D. (1995). Hydrogeochemical properties and activity of the fluids in the Pomurje region of the Pannonian sedimentary basin. Acta Geologica Hungarica, 39, 319-340.

Pleničar, M., 1954: Obmurska naftna nahajališča. Geologija 2, 36-93.

Powell, W.G., Chapman, D.S., Balling, N., Beck, A.E., 1988: Continental heat flow density. In: R. Haenel, L. Rybach, L. Stegena (eds): Handbook of terrestrial heat-flow density determination. Kluwer Academic publishers, Dordrecht, 167-222.

Rajver, D., 2001: Geothermal characteristics of the Krško basin with emphasis on geophysical investigations. M. Sc. Thesis, University of Ljubljana, Ljubljana, Slovenia, 203 pp. (in Slovene, with English abstr.).

Rajver, D., Ravnik, D. 2002: Geothermal pattern of Slovenia-enlarged data base and improved geothermal maps (in Slovene). Geologija 45/2, 519-524, doi:10.5474/geologija.2002.058

Rman, N., Bălan, L.L., Bobovečki, I. et al. 2020: Geothermal sources and utilization practice in six countries along the southern part of the Pannonian basin. Environ Earth Sci 79, 1. https://doi.org/10.1007/s12665-019-8746-6

Rman, N., Szőcs, T., Palcsu, L., Lapanje, A. 2021: Chemical and isotopic composition of CO2 rich magnesium-sodium-bicarbonate-sulphate type mineral waters from volcanoclastic aquifer in Rogaška Slatina, Slovenia. Environmental Geochemistry and Health (in review process).

Rotár-Szalkai, Á., Maros, Gy., Bereczki, L., Markos, L., Babinszki, E., Zilahi-Sebess, L., Gulyás, Á., Kun, É., Szőcs, T., Kerékgyártó, T., Nádor, A., Rajver, D., Lapanje, A., Šram, D., Marković, T., Vranješ, A., Farnoaga, R., Samardžić, N., Hrvatović, H., Skopljak, F. & Jolović, B. 2018: D.5.1.1. Identification, ranking and characterization of potential geothermal reservoirs. Report of the DARLINGe project: 82 pp. Available at www.interreg-danube.eu/approved-projects/darlinge/outputs

Rybach, L., 1981: Geothermal systems, conductive heat flow, geothermal anomalies. In: L. Rybach and L.J.P. Muffler (eds): Geothermal systems: Principles and case histories. John Wiley and Sons, Chichester, 3-36.

Sachsenhofer, R. F., Jelen, B., Hasenhüttl C., Dunkl, I. & Rainer, T. 2001: Thermal history of Tertiary basins in Slovenia (Alpine-Dinaride-Pannonian junction). Tectonophysics, 334/2: 77-99.

Senekovič, M., 2011: Mineral waters of Lenart in the Slovenske gorice area, BSc Thesis (in Slovenian). Faculty of Natural Sciences and Engineering, University of Ljubljana.

Stucchi et al. 2012: The SHARE European Earthquake Catalogue (SHEEC) 1000–1899. Journal of Seismology, doi: 10.1007/s10950-012-9335-2.

Szőcs, T., Rman, N., Nador, A. et al. 2011: Results of project TRANSENERGY - Transboundary Geothermal Energy Resources of Slovenia, Austria, Hungary and Slovakia, 2010-2013. Implemented within the Central Europe Programme.

Szőcs, T., Rman, N., Süveges, M. et al. 2013: The application of isotope and chemical analyses in managing transboundary groundwater resources. Applied Geochemistry - Special Issue 32, 95-107. Doi: 10.1016/j.apgeochem.2012.10.006

Šram, D., Rman, N., Rižnar, I., Lapanje, A. 2015: The three-dimensional regional geological model of the Mura-Zala Basin, northeastern Slovenia. Geologija 58/2, 139-154, http://dx.doi.org/10.5474/geologija.2015.011

Takšić, A. 1967: Das Braunkohlenläger von Mursko Središće. Geološki vjesnik, 20, 303-315.

Trček, B., Leis, A. 2017: Overview of isotopic investigations of groundwaters in a fractured aquifer system near Rogaška Slatina, Slovenia. Geologija, 60 (1), 49-60.

Velić, J., Malvić, T., Cvetković, M., Vrbanac, B. 2012: Reservoir geology, hydrocarbon reserves and production in the Croatian part of the Pannonian Basin system. Geologia Croatica, 65/1, 91-101.

Živčić, M. 2021: Provided seismicity data in the project area in 1990-2021. Agencija RS za okolje, Urad za seizmologijo, Slovenia, Ljubljana.

9 REFERENCES FOR BATTONYA HIGH

Dövényi, P. & Horváth, F. 1988: A review of temperature; thermal conductivity; heat flow data from the Pannonian basin. — In: ROYDEN, L. H. & HORVÁTH, F. (eds): The Pannonian Basin, a Study in Basin Evolution. — American Association of Petroleum Geologists, Memoir 45, 195–223.

Haas J., Budai T., Csontos L., Fodor L., Konrád Gy. 2010: Magyarország pre-kainozoos földtani térképe, 1:500 000. (Pre-Cenozoic geological map of Hungary, 1:500 000.) — A Magyar Állami Földtani Intézet kiadványa, Budapest. (In Hungarian and in English)

Haas, J., Budai, T. (Eds.), 2014. Geology of the Pre-Cenozoic Basement of Hungary. Geological and Geophysical Institute of Hungary (Magyar Földtani és Geofizikai Intézet).

Hajnal, Z., Lucas, S., White, D., Lewry, J., Bezdan, S., Stauffer, M.R. & Thomas, M.D. (1996). Seismic reflection images of high-angle faults and linked detachments in the Trans-Hudson Orogen. Tectonics 15: doi: 10.1029/95TC02710. issn: 0278-7407.

Horváth, F. & Rumpler, J. 1984: The Pannonian basement: extension and subsidence of an Alpine orogene. — Acta Geologica Hungarica 27/3–4, 229–235

Horváth, F., Musitz, B., Balázs, A., Végh, A., Uhrin, A., Nádor, A., Koroknai, B., Pap, N., Tóth, T. & Wórum, G. 2015: Evolution of the Pannonian basin and its geothermal resources. — Geothermics 53, 328–352, http://doi.org/10.1016/j.geothermics.2014.07.009.

Hurter, S., Haenel, R. (Eds.), Atlas of geothermal resources in Europe, Office for Official Publications of the European Communities, Luxemburg (2002)

Juhász Gy., Molenaar, C. M., Bérczi, I., Révész, I., Kovács, A. & Szanyi, B. 1989: A Békési-medence pannóniai (s.l.) üledékösszletének rétegtani viszonyai. Stratigraphic framework of the Pannonian s. 1. sequence in the Békés basin. - Magyar Geofizika 30, 129-145 .

Kovács, Zs. (Ed.) 2018: Szénhidrogének Magyarországon. – Magyar Energetikai és Közmű-szabályozási Hivatal, Budapest 318 p.

Lenkey, L., Dövényi, P., Horváth, F. & Cloetingh, S. A. P. L. 2002: Geothermics of the Pannonian basin; its bearing on the neotectonics. — EGU Stephan Mueller Special Publication Series 3, 29–40. https://doi.org/10.5194/smsps-3-29-2002

Nagy, Zs., Baracza, M. K., Szabó, N. P. 2021: Magnitude Estimation of Overpressure Generation Mechanisms Using Quantitative Stochastic 2D Basin Models: A Case Study from the Danube-Tisza Interfluve Area in Hungary

Nemčok, M., Pogácsás, Gy., Pospíšil, L. 2006: Activity timing of the main tectonic systems in the Carpathian – Pannonian region in relation to the "roll-back destruction of the lithosphere "

(https://www.researchgate.net/publication/288193527_Activity_timing_of_the_main_tectonic_systems_in_the_CarpathianPannonian_region_in_relation_to_the_rollback_destruction_of_the_lithosphere [accessed May 10 2021].

Posgay K., Takács E., Szalai I., Bodoky T., Hegedűs E., Jánváriné K. I., Tímár Z., Varga G., Bérca I., Szalay Á., Nagy Z., Pápa A , Hajnal Z., Reilkoff B., Mueller St., Ansorge J., De Iaco R., Asudeh I. 1996: International deep reflection survey along the Hungarian Geotraverse. Geophys.Trans., 0, 1-2., 1-44

Rotár-Szalkai, Á, Maros, G. et al. D.5.4.1. Identification, ranking and characterization of potential geothermal reservoirs /DARLINGe project/. DARLINGe project: http://www.interreg-danube.eu/approved-projects/darlinge

Szanyi, J., Kovács, B. & Scharek, P. 2009: Geothermal Energy in Hungary: potentials and barriers. – European Geologist 27, 15–1

Szentgyörgyi K.-Né, Amran A., Árvai L., Balázs E.-Né, Belovai I.-Né., Berecz F., Eszes I.-Né, Gyergyói L., Kiss B., Kiss K., Magyar I., Mészáros Vince Cs., Milota K., Papp I., Pócsik M., Pusztai J., Spitzmüller Á., Sőreg V., Szabó I., Szalainé Bánlaki E., Szászfai J., Tatár A.-Né., Tóth D., Török J.-Né., Ujszászi K., Vargáné Tóth I., Verpecz A., Vincze M., Vinczéné Tóth M., Zahuczki P., Zsuppán Gy. 2010: Zárójelentés a 101. Battonya–Pusztaföldvár kutatási területen végzett szénhidrogén-kutatási tevékenységről I–V. — MOL Nyrt., Kézirat, MOL, MÁFGBA Budapest, SZBK.3406

Tari, G., Dövényi, P., Dunkl, I., Horváth, F., Lenkey, L., Stefanescu, M., Szafián, P. & Tóth, T. 1999: Lithospheric structure of the Pannonian basin derived from seismic, gravity and geothermal data. In: Durand, B., Jolivet, L., Horváth, F. & Séranne, M. (eds): The Mediterranean Basins: Tertiary extension within the Alpine Orogen. — Geological Society Special Publications 156, 215–250. https://doi.org/10.1144/gsl.sp.1999.156.01.12

Tatár A.-né, Balázs E.-né, Tirpák I., Gombos Cs., Nagy Gy.-né, Nagy L., Pusztai J., Szentgyörgyi K.-né, Török J.-né, Vadász Gy.-né, Tóth Z., Tóthné Medvei Zs., Vargáné Tóth I. 1999: Zárójelentés a 4. Battonya–pusztaföldvári gerinc K-i szárny területen végzett szénhidrogén-kutatási tevékenységről, I–II. – Mol Rt. – Kézirat, Magyar Állami Földtani, Geofizikai és Bányászati Adattár, Budapest, T.19938.

Tóth Gy., Rotárné Szalkai Á., Horváth I., 2003: A Kárpát-medence magyarországi részének hidrológiai modellezése. A Magyar Állami Földtani Intézet hozzájárulása a feladat megoldásához. Felszín alatti vizeink kutatása, feltárása, hasznosítása és védelme / A FELSZÍN ALATTI VIZEKÉRT ALAPÍTVÁNY által kiadott tanulmánykötetek 2003-ban felülvizsgált változatai
Liebe Pál (Eds)/ I., Szemelvények a kutatás és az oktatás munkáiból. X. FAVA Konferencia, Balatonfüred. pp. 1-15.

https://fava.hu/publikaciok/jubileumi_kiadvanyok/tanulmanyok_pdf/toth_mafi.pdf

Hungarian RBMP WFD - http://vizeink.hu/

10 REFERENCES FOR BIH

Đurić, N., 1988: Hydrogeological regionalization of the rock salt deposit Tetima near G. Tuzla, Proceedings of the Faculty of Mining and Geology, 17, University of Tuzla, Tuzla, 31-35.

Etiope G., Samardžić N., Grassa F., Hrvatović H., Miošić N., Skopljak F., 2017: Methane and hydrogen in hyperalkaline groundwaters of the serpentinized Dinaride ophiolite belt, Bosnia and Herzegovina, Applied Geochemistry, 84, 286-296.

Hadžihrustić I., Oruč E. et al., 2006: Supplementary mining project for stopping pumping of salt water at the Trnovac-Hukalo exploitation field, Unpublished document, Mining Institute, Tuzla.

Hrvatović, H., 2006: Geological guidebook through Bosnia and Herzegovina, Separate Monograph, Herald Geological, volume 25, Sarajevo.

Ivanković, B. and Begović, P., 2015: Report of drilling of exploration well IBK-1/15 on location Kokori, Municipality Prnjavor, Unpublished report, IBIS-Inženjering, Banja Luka.

Katzer F., 1919: To knowledge of mineral springs of Bosnia. State museum herald in Bosnia and Herzegovina, Sarajevo.

Milošević A., Cvijić R., Begović P., Ivanković B., 2019: Geologic field trip guide - II Congres of geologists of Bosne i Hercegovine, Association of Geologists of Bosnia and Herzegovina and the Faculty of Mining - University of Banja Luka.

Miošić N., 1977: Map of mineral, thermal and thermomineral waters of B&H, 1:200.000 with Explanation and Catalogue of occurrences. Geoinženjering, Sarajevo.

Miošić N., 1997: Thermomineral waters of Gračanica Municipality, Herald of Gračanica no. 4.
Miošić, N., 2003: Geothermal parameters and characteristics of hydrogeothermal regions of Bosnia and Herzegovina, Herald geological, 35, Sarajevo, 279 -307.

Miošić N., Samardžić N., 2015: Mineral, thermal and thermomineral waters of Bosnia and Herzegovina, Monograph-Mineral and Thermal waters of Southeastern Europe, edited by Petar Papić, Environmental Earth Sciences, Springer.

Miošić N., Samardžić N., Hrvatović H., 2015: The Current Status of Geothermal Energy Research and Use in Bosnia and Herzegovina, Proceedings World Geothermal Congress 2015, Melbourne, Australia, 19-25 April 2015

Miošić N., Skopljak F., Samardžić N., Saletović J., Begić S., 2010: Cadastre of mineral, thermal and thermomineral waters of Federation of Bosnia and Herzegovina (update status 31.12.2009.), Geological Survey of Federation of Bosnia and Herzegovina, Sarajevo.

Miošić N., Samardžić N., Hrvatović H., Skopljak F., 2019: Hyperalkaline thermomineral waters of Lješljani, Bosnia and Herzegovina, II Congress of geologists of Bosnia and Herzegovina, Laktaši, 2 - 4 October, 2019.

Samardžić N., 2007: Field trip notebook - recognition of terrain along Spreča fault zone, Unpublished material, Geological Survey of Federation of Bosnia and Herzegovina, Sarajevo.

Samardžić N., Hrvatović H., Miošić N., 2018: Significant geomanifestations along the contact of South Pannonian Basin and Dinaride Ophiolite Zone in Bosnia and Herzegovina, Blog post – GeoERA - GeoConnect3d project, https://geoera.eu/blog/significant-geomanifestations-in-bosnia-and-herzegovina/

Poljić M., 2018: Report on laboratory testing of water from thermal well Kadar, Institute for Chemical engineering, Tuzla.

Soklić I., 1982: Thermomineral water and oil gases of Slavinovići, Proceedings of the Faculty of Mining and Geology, University of Tuzla, No. 11, Tuzla.